Structural and Functional Analysis of Adenovirus Receptor Interaction

Dissertation zur Erlangung des akademischen Grades des Doktors der Naturwissenschaften (Dr. rer. nat.)

eingereicht im Fachbereich Biologie – Chemie – Pharmazie
der Freien Universität Berlin

vorgelegt von

Lars Pache
aus Bonn

Juni 2008

Erster Gutachter: Prof. Dr. Glen R. Nemerow

Zweiter Gutachter: Prof. Dr. Gerd Multhaup

Tag der Disputation: 5. September 2008

Acknowledgements

First of all, I would like to thank my advisor, Prof. Glen Nemerow for giving me the opportunity to work in his laboratory at The Scripps Research Institute. I am very grateful for his guidance, confidence and support.

I would like to extend my gratitude to Prof. Gerd Multhaup for being my advisor and the referee of this thesis on behalf of the Freie Universität Berlin.

I would also like to thank all members of the Nemerow Lab, especially Tina-Marie Mullen, Eugene Wu and Ronald Nepomuceno for their advice and expertise. Further, I would like to express my gratitude to Prof. Vijay Reddy of The Scripps Research Institute who offered his expertise in the determination of crystal structures.

Finally, I would like to thank my friends in San Diego and especially Olivier Harismendy as well as my parents for their support and confidence.

Table of contents

1. Introduction

1.1 General properties of adenovirus

The family of *Adenoviridae* consists of non-enveloped, icosahedral viruses with a double stranded DNA genome. It encompasses four established genera, with *Mastadenovirus* originating from mammals, *Aviadenovirus* from birds and the two smaller genera, *Atadenoviruses* and *Siadenovirus*, originating from a broad range of hosts (Davison et al., 2003). Currently, at least 51 strains of human adenovirus, belonging to the genus *Mastadenovirus*, have been identified. They are divided into six species, A to F, based on DNA homology and hemagglutination patterns (Table 1.1).

Table 1.1. **Classification of human adenoviruses** (adapted from Lukashok and Horwitz, 1998).

Species	Hemagglutination group		Serotypes	Tissue tropism
A	IV	(little or no agglutination)	12, 18, 31	Respiratory system
B	I	(complete agglutination of monkey erythrocytes)	(B1) 3, 7, 16, 21 (B2) 11, 14, 34, 35, 50	Respiratory system Kidney and urinary tract
C	III	(partial agglutination of rat erythrocytes)	1, 2, 5, 6	Respiratory system, liver
D	II	(complete agglutination of rat erythrocytes)	8-10, 13, 15, 17, 19, 20, 22-30, 32, 33, 36-39, 42-49, 51	Eye, genital tract
E	III	(partial agglutination of rat erythrocytes)	4	Respiratory system
F	III	(partial agglutination of rat erythrocytes)	40, 41	Gastrointestinal tract

Tissue specificity is commonly shared to a certain degree by the members of a particular adenovirus species, resulting in the association of specific Ad species with certain diseases (Shenk, 1996). Species C members Ad1, 2 and 5, for example, are frequently associated with respiratory infections, while most cases of Ad-related gastroenteritis are caused by species F adenoviruses Ad40 and 41. Ads 37, 19a and 8 of species D are predominantly responsible for causing a severe and highly infectious form of epidemic keratoconjunctivitis (EKC). The incubation period for primary Ad infections can range from 2 to 14 days. Common routes of infection are airborne and fecal-oral transmission or ocular conjunctival contact. Generally, Ad infections are self-limiting in immunocompetent patients. However, significant mortality has been observed upon infection of immunocompromised patients. Currently, there is no well-established antiviral therapy against adenovirus infection, although cidofovir, a cytosine nucleoside analogue, has been reported to be of some value in treating infections in stem cell transplant patients (Bordigoni et al., 2001).

Due to the ability to efficiently infect a variety of mammalian cell types independent of their cell cycle status, as well as the potential of this virus to accommodate large amounts of foreign DNA, adenovirus vectors are currently being exploited for gene transfer and vaccine delivery.

1.2 Adenovirus structure

The mature adenovirus particle is composed of an outer capsid and the inner, DNA-associated core (Shenk, 1996). The capsid is round with icosahedral symmetry (T = 25) and has a diameter between 800 and 1000 Å, not including the protruding fibers. It consists of three major proteins, hexon (protein II), penton base (pIII) and fiber (pIV) along with the four minor capsid proteins IIIa, VI, VIII and IX (Figure 1.1). The main structural component of the capsid is the hexon protein with 720 copies arranged in trimers. These hexon trimers represent 240 of the 252 capsomers and form the 20 capsid

facets, each of them consisting of 12 hexon homotrimers. The vertices of the icosahedral capsid are formed by one of the 12 penton capsomers that consist of five copies of the penton base protein with an attached trimer of the fiber protein. The fiber is a thin and elongated protein that ends in a C-terminal globular domain, called the fiber knob, giving it a head-to-tail morphology. It protrudes between 120 and 345 Å from the capsid, depending on the Ad serotype.

The minor capsid proteins likely have a scaffolding function, stabilizing the virus particle both from below the vertex and alongside the hexons, Other functions of the minor capsid proteins, in addition to their stabilizing capacities, have not been fully resolved. However, several viral functions have been assigned to protein VI (pVI). Besides its role as a shuttling adaptor, mediating hexon import into the nucleus (Wodrich et al., 2003), pVI has been shown to mediate disruption of the endosomal membrane, thus leading to the endosomal escape of the partially disassembled viral capsid (Wiethoff et al., 2005). Further, an 11 amino acid peptide derived from the C-terminus of pVI was found to serve as cofactor for the adenovirus cysteine protease p23 (Webster et al., 1993). Each virion is estimated to contain ~10 copies of this protease (Anderson, 1990) that is critically involved in the maturation of viral capsids by processing a number of viral proteins into their mature form. Upon release of progeny virions from the cell, the adenovirus protease is likely deactivated by the oxidizing conditions in the extracellular environment (Greber, 1998). During virus entry into the host cell, the protease would be reactivated and has been proposed to be involved in capsid disassembly. However, the precise role of the protease in the disassembly of the viral capsid is poorly understood to date.

Recent structural modeling of the adenovirus capsid by cryo electron microscopy (CryoEM) and image reconstruction have provided valuable insights into the likely locations of the minor capsid proteins (Fabry et al., 2005; Saban et al., 2006). Protein IX (pIX) has been located on the outside of

the capsid, at the interface of the hexon-hexon contact regions. Part of the density now assigned to pIX was previously thought to belong to protein IIIa (pIIIa). The newly assigned location of pIIIa is rather on the inner capsid surface, below the penton base. Due to its location and contacts with multiple other proteins in the vertex region it is thought to play a crucial role in the assembly and disassembly of the capsid, potentially as linchpin. This is in agreement with observations that pIIIa dissociates from the capsid at the same time as penton base and the peripentonal hexons (Wiethoff et al., 2005). Mass spectrometry studies suggest the presence of 60 copies of pIIIa in each virion (Lehmberg et al., 1999). This supports a model of five pIIIa copies, arranged in fivefold symmetry, binding to the penton base pentamer, thus covering most of the inner surface area of penton base. There, it makes contact with the density surrounding the inner capsid surface of the hexon trimers, that has been tentatively assigned to protein VIII. The cryoEM density tentatively assigned to pVI has been located within a cavity of the hexon trimer on the interior capsid surface. The model proposes three copies of pVI per hexon trimer with part of the protein bound inside the cavity, part folded over, onto the bottom of the hexons. However, mass spectrometric analysis of mature Ad particles suggests only partial occupancy of the potential pVI binding sites (Lehmberg et al., 1999).

Unlike the outer Ad capsid, the adenovirus core does not seem to have well-ordered symmetry, thus preventing suitable image reconstruction of this region. Each terminus of the double stranded, linear DNA genome contains an inverted terminal repeat (ITR) of 100-140 nucleotides that constitutes the viral origin of replication and is covalently linked to a copy of the terminal protein (TP). Three basic polypeptides, proteins V, VII and μ (also known as protein X) are associated with the DNA, forming a tightly packed nucleoprotein complex. The abundant, histone-like protein VII (pVII) is likely involved in the formation of nucleosome-like structures of the genome. Furthermore, pVII has been shown to contain nuclear localization signal

(NLS) sequences, indicating that it might serve as an adaptor that mediates nuclear import of the viral genome (Wodrich et al., 2006). Protein V (pV) is thought to function as a link between the nucleoprotein complex of the core and the outer capsid, likely by connecting the hexon-associated pVI with pVII and/or the DNA itself (Chatterjee et al., 1985; D. A. Matthews and Russell, 1998).

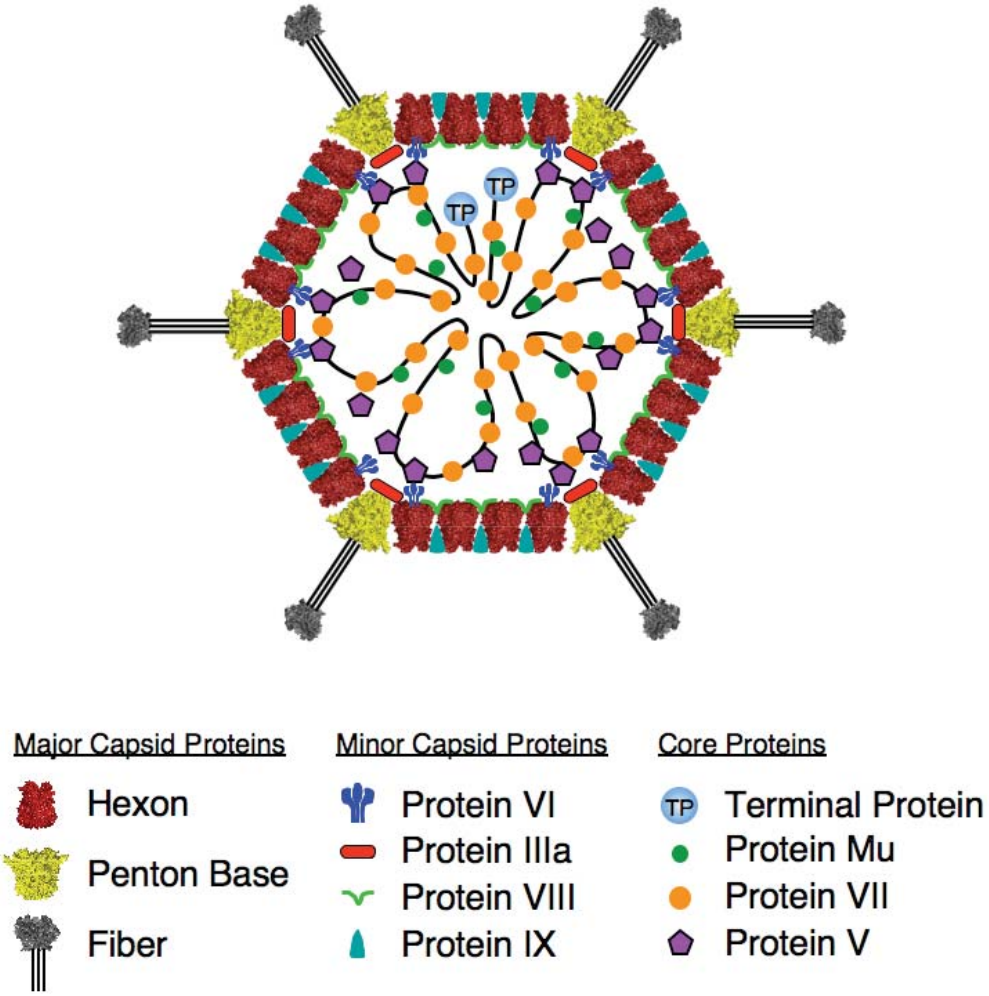

Figure 1.1. **Model of the adenovirus particle.**
The adenovirus capsid is composed of three major and four minor capsid proteins. The location of these proteins is based on a recent structural model generated by cryo-electron microscopy (Saban et al., 2006). The adenovirus core contains four proteins associated with the viral DNA. The Ad genome likely does not have an ordered structure and the precise locations of the core components have yet to be fully established.

1.3 Adenovirus infection

1.3.1 Virus entry

Initial Ad binding to the cell surface is mediated by the Ad fiber knob domain, which engages a primary attachment receptor such as the coxsackievirus and adenovirus receptor CAR or CD46 (Figure 1.2). Following initial attachment, a highly conserved Arg-Gly-Asp (RGD) motif located in an exposed loop of the penton base protein (Zubieta et al., 2005) binds to α_V integrins on the cell surface (Wickham et al., 1993). Integrin binding has been reported to result in the shedding of the fiber proteins from the adenovirus capsid, however it is not clear whether this happens at the cell surface or within the early endosome (Nakano et al., 2000). However, fiber release has been reported to occur independently of endosome acidification (Greber et al., 1993). Binding of the penton base to α_V integrins triggers a signaling cascade involving the activation of the phosphatidylinositol-3-OH kinase (PI3K) (E. Li et al., 1998b), which, in turn, activates Rac and CDC42, two members of the Rho family of GTPases (E. Li et al., 1998a). Activation of these proteins induces polymerization and reorganization of actin and leads to the dynamin-dependent endocytosis of the virus via clathrin-coated pits (Wang et al., 2007). Upon maturation of the virus-containing vesicle, endosomal acidification leads to conformational changes of the capsid (Greber et al., 1993), resulting in removal of the capsid vertices. Upon dissociation of penton base, protein IIIa and the peripentonal hexons from the capsid, multiple protein VI copies attached to central cavities of these hexons are likely released as well (Saban et al., 2006). The released protein VI, in turn, is thought to participate in the disruption of the endosomal membrane, thus allowing endosomal escape of the partially disassembled virion (Wiethoff et al., 2005). Following endosomal escape, the nucleocapsid is translocated towards the nucleus in a microtubule- and dynein-dependent manner (Dales and Chardonnet, 1973; Kelkar et al., 2004). After docking to the nuclear pore

complex (NPC) by direct interaction of NPC proteins with hexon (Trotman et al., 2001), the viral genome is imported into the nucleus, leading to viral replication (Greber et al., 1997; Greber et al., 1993). Following entry of the viral DNA into the nucleus, the primary transcription events are initiated from the E1 region of the viral genome. Adenovirus transcription can be divided into an early and a late phase with the onset of viral DNA replication defining the beginning of the late phase.

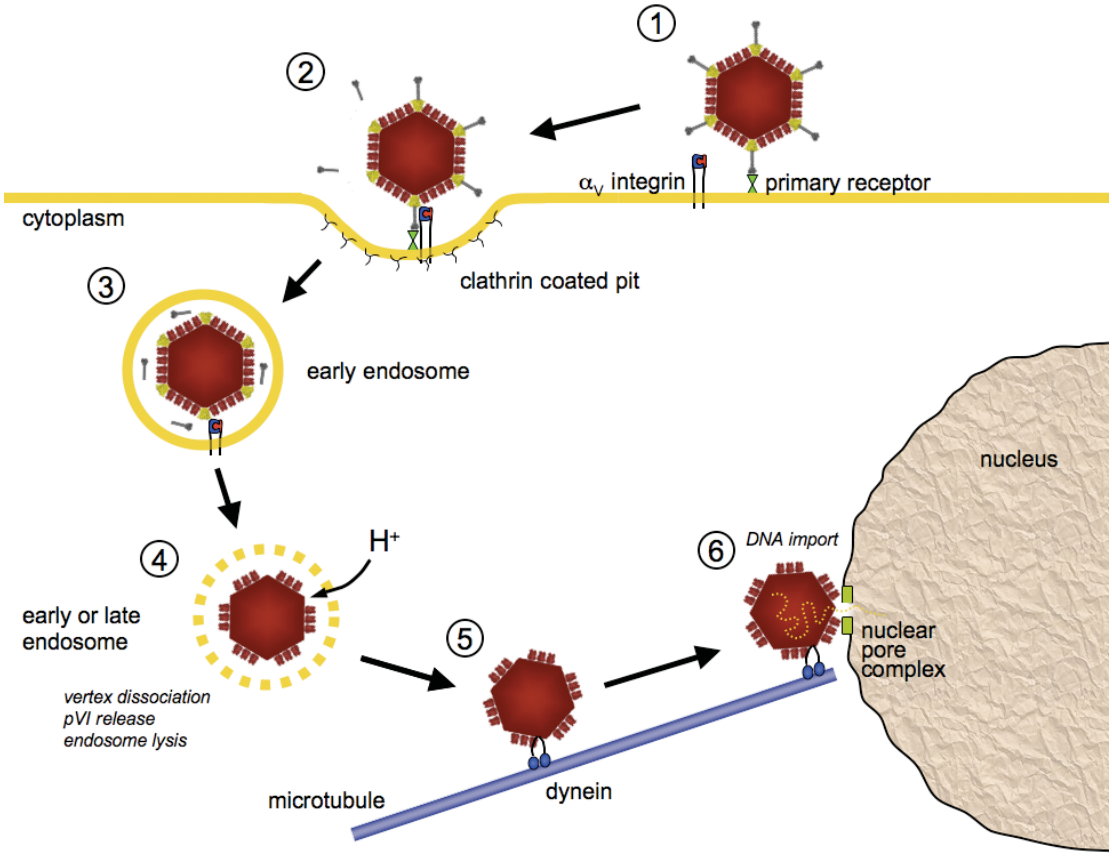

Figure 1.2. **Cell entry pathway of adenovirus.**
Adenovirus binds to a primary attachment receptor such as CAR or CD46 via the knob domain of its fiber protein (1). Following attachment to the cell surface, an exposed RGD motif in the Ad penton base binds to α_V integrins, which triggers receptor-mediated endocytosis by clathrin-coated vesicles (2). Early on during internalization, the virus loses its fiber protein. However, it is not clear whether this happens at the cell surface or within the early endosome (3). Upon acidification of the endosome, the virus capsid loses its vertices consisting of the penton base, protein IIIa, and the peripentonal hexons (4). Protein VI is thought to dissociate from hexon and mediate endosome lysis. The partially disassembled capsid then translocates towards the nucleus in a dynein- and microtubule-dependent way (5), where it docks to the nuclear pore complex, enabling nuclear DNA import (6).

1.3.2 Early phase of gene expression

The *E1A* encoded gene products of adenovirus are transcribed by cellular factors, instead of depending on the expression of newly synthesized viral factors, and is therefore termed “immediate early gene”. The primary function of *E1A* gene products is to facilitate virus replication by trans-activating the adenovirus early promoters of the other early gene cassettes (*E1B, E2, E3*, and *E4*) and by deregulating the cell cycle. *E1A* gene products stimulate cells to enter the S phase by binding to negative regulators of cell growth and interfering with their normal function (Ben-Israel and Kleinberger, 2002; Berk, 1986). The products of the *E1B* transcription units have anti-apoptotic functions to prevent cell death and allow virus production (Rao et al., 1992). Deregulation of the cell cycle by the E1A proteins leads to the accumulation of p53, a tumor repressor that can trigger cell-cycle arrest and apoptosis (Braithwaite et al., 1990; Lowe and Ruley, 1993). To prevent activation of the p53 pathway, products of the *E1B* and *E4* transcription units, the E1B-55K and the E4orf6 proteins, bind to and deactivate p53 (Querido et al., 2001; Sarnow et al., 1982).

Although replication of the adenovirus genome takes place in the nucleus, it depends on the expression of the adenovirus DNA polymerase, a DNA binding protein and a precursor terminal protein, which are encoded by the *E2* region. The products of the *E3* gene cassette are involved in the suppression of host cell immunity and therefore entirely dispensable for virus growth *in vitro*. The transcription unit *E4* encodes a number of proteins that have mainly anti-apoptotic functions. E4orf4 is an exception and stimulates apoptosis independent of the p53 pathway (Shtrichman et al., 1999), which is thought to play a role in the release of progeny virions during later steps of the infection

1.3.3 Late phase of gene expression

During the late phase of adenovirus replication, the cellular metabolism is shifted towards the assembly of new adenoviral particles. Transcription of cellular genes is not inhibited however the transport of cellular mRNAs to the cytoplasm is almost completely blocked. The gene products E1B-55K, E4orf3 and E4orf6 have been shown to modulate mRNA export from the nucleus to the cytoplasm, thus promoting selective export of viral mRNAs (Shenk, 1996).

While the expression of the early genes is initiated in different locations, the late genes are all under the control of a single promoter, the major late promoter (MLP). Transcription of the MLP controlled genes is activated by the products of the genes *IVa2* and *XI* that are expressed at high levels at the start of the DNA replication (Lutz and Kedinger, 1996; Lutz et al., 1997). Five families of late transcripts, termed L1-L5, are derived from a single primary transcript of the major late transcription unit (MLTU) that is processed by differential splicing and polyadenylation. All mRNAs transcribed from the MLTU contain an identical 5' noncoding sequence (Berget et al., 1977). This sequence, termed the tripartite leader (TPL), enables the preferential translation of viral mRNAs at the late stages of infection (Berkner and Sharp, 1985; Logan and Shenk, 1984). The transcripts of the late genes primarily encode structural proteins of the virus or proteins involved in virion assembly.

Assembly of the virions takes place in the nucleus (Shenk, 1996), therefore viral structural poteins must be imported into the nucleus, likely mediated by nuclear localization signals (NLS). However, trimerization of the hexon protein occurs in the cytoplasm with the help of the 100K chaperone protein, a product of the L4 transcription unit (Cepko and Sharp, 1983; Gambke and Deppert, 1983; Oosterom-Dragon and Ginsberg, 1981). The structural protein VI then mediates translocation of the hexon trimers into the nucleus (Wodrich et al., 2003), where they assemble together with penton and other components of the capsid. Details of the virion assembly remain

unclear and could involve insertion of the viral DNA into preformed empty capsids (D'Halluin et al., 1978a; D'Halluin et al., 1978b; Edvardsson et al., 1976) or, more likely, assembly of the virus capsid around the nucleoprotein core (W. Zhang and Imperiale, 2003). Following assembly and DNA encapsidation, a number of structural proteins (pIIIa, pVI, pVII, pVIII, TP and μ) are cleaved into their mature form by the adenovirus protease. Progeny virions are released from the cell by cell lysis. This process involves the adenovirus death protein (ADP), a gene product of the *E3* region that, unlike other E3 proteins, is transcribed from the MLP and therefore produced only during the late stages of infection (Tollefson et al., 1996a; Tollefson et al., 1996b).

1.4 Proteins involved in adenovirus-cell attachment

1.4.1 Fiber protein

Association with most primary attachment receptors is mediated by the adenovirus fiber protein that protrudes from the vertices of the Ad capsid (Shenk, 1996). With exception of the proposed binding of heparan sulfate glycosaminoglycan (HS-GAG) by a KKTK motif in the shaft domain (Dechecchi et al., 2001; Dechecchi et al., 2000), fiber adhesion to cell surface receptors is mediated by the C-terminal fiber knob domain. This high affinity attachment to a cellular receptor allows the virus to establish a subsequent, lower affinity binding to cell surface α_V integrins via the penton base protein, a step that triggers virus internalization (Wickham et al., 1993).

The structure of the fiber protein can be divided into three distinct domains: a N-terminal tail that binds to the penton base protein, a central shaft of variable length, consisting of repeating motifs, and a C-terminal globular knob domain that mediates attachment to cellular receptors. The sequence of the 44- to 52-residues long N-terminal tail is strongly conserved

among different human Ad serotypes (Chroboczek et al., 1995) and contains a basic nuclear localization signal, leading to its transportation into the nucleus, where the capsids of progeny virions are assembled (Hong and Engler, 1991). The tail domain is flexible and thus able to bend away from the axis of the fiber shaft, allowing a non-covalent attachment to the top surface of the penton base protein (Devaux et al., 1987). A universally conserved FNPVYPY motif in the tail of the fiber (Caillet-Boudin, 1989) mediates this association by binding to an equally conserved site located in a groove between two adjacent monomers of the penton base pentamer. The arrangement of the three tails extending towards the center of the penton base pentamer, followed by an outward bend, allows the formation of the trimeric fiber structure with the shaft emerging from the center of the complex (Zubieta et al., 2005). Remarkable is the trimeric-pentameric symmetry mismatch of the fiber association with the penton base pentamer, a situation that also exists in reovirus for the association of protein σ1 with the λ2 pentamer (Chappell et al., 2002).

The central shaft portion of the fiber protein is composed of a variable number of repeats (Table 1.2), ranging from 5.5 in Ad3 to 22.5 repeats in Ad12 (Chroboczek et al., 1995; Sarkioja et al., 2008). The repeating motif comprises 15 amino acids, forming an extended β-strand followed by a type 2 β-turn and another β-strand. Besides a conserved proline or glycine at position eight, the motif contains a number of conserved hydrophobic residues. The repeats are connected by variable loops and contribute an axial rise of ~13 Å per motif to the length of the fiber (Ruigrok et al., 1990; van Raaij et al., 1999). A clockwise displacement of about 50° between the repeating units causes a spiral staircase-like structure with about 7 repeats needed for a 360° turn. While most protein structures of other known fibrous proteins are based on α-helical coiled-coils, the collagen triple helix (Beck and Brodsky, 1998) or a β-helix (Steinbacher et al., 1994; Yoder et al., 1993), the

intertwined shaft structure of three polypeptide chains in the trimeric fiber complex constitute a unique fold, termed “triple-β-spiral” (van Raaij et al., 1999). The attachment protein σ1 of reovirus, that is closely related to the Ad fiber protein, was later shown to also contain a triple-β-spiral fold (Chappell et al., 2002). This structure is stabilized by a hydrophobic core of residues oriented towards the central axis, as well as a number of inter- and intra-chain hydrogen bonds involving main- and side-chains. This strongly crosslinked structure is responsible for the high rigidity of the fiber shaft. The hydrophobic core likely contributes to the ability of the fiber shaft to trimerize even in the absence of the knob domain. However, a minimum of approximately 7 shaft repeats, representing one 360° turn, is required for trimer formation of the shaft domain in the absence of the fiber knob (J. Li et al., 2006).

Table 1.2. **Number of repeats in known fiber shaft sequences** (adapted from Nicklin et al., 2005).

Species	Number of shaft repeats	Serotype(s)	Approx. length of fiber
A	20.5	31	320 Å
	22.5	12	340 Å
B1	5.5	3, 7d, 21	130 Å
	7.5	16	155 Å
B2	5.5	11, 14, 34, 35	130 Å
C	21.5	1, 2, 5	330 Å
D	7.5	8, 9, 15, 17, 19, 28, 30, 37	155 Å
E	11.5	4	220 Å
F	11.5/20.5†	40	220 Å/320† Å
	11.5/21.5†	41	220 Å/330† Å

† Species F Ads contain two fiber proteins, one long and one short.

Structural studies by negative-staining and electron microscopy revealed a bend in the fiber shaft of Ad2 that is located close to the penton base (Ruigrok et al., 1990). The location of this bend coincides with a sequence irregularity in the third repeat of the fiber shaft, that contains an insertion of four additional amino acids between the two β-strands of this repeat. These extra residues likely cannot be accommodated in the triple-β-spiral structure and are thought to mediate flexibility of the fiber shaft at this location. This derivation from the consensus motif along with an observed flexibility in the fiber shaft was found in the shaft portions of species A, C, E and F adenoviruses (Wu and Nemerow, 2004). A second tilt in the fiber has been observed at the interface between the shaft and the knob domains and is attributed to a linker sequence between the domains that causes flexibility (van Raaij et al., 1999).

Ad37, like all species D adenoviruses does not contain the irregular third repeat in the fiber shaft (Chroboczek et al., 1995). Cryo-electron microscopy studies confirmed that the fiber shaft of a virus from this species is indeed rigid and does not have a bend at the third shaft repeat (Chiu et al., 2001). Also, with 8 instead of 22 repeats, its fiber is significantly shorter than that of Ad5. While the impact of the flexible interface between fiber shaft and knob domains has not been explored, our earlier studies addressed the question of whether shaft length and/or the flexibility imposed by the third repeat impact receptor binding. Interestingly, a soluble form of CAR has been shown to bind the Ad37 fiber knob (Roelvink et al., 1998; Seiradake et al., 2006) despite its inability to mediate binding of the virus to the cell surface (Arnberg et al., 2000a; Wu et al., 2001). By fusing the Ad37 fiber knob to the long and flexible shaft of Ad5, we were able to strongly increase virus binding and infectivity compared to a virus equipped with the wild-type Ad37 fiber (Wu et al., 2003). To differentiate whether length and/or flexibility of the fiber shaft are crucial for CAR binding, we generated mutants of the Ad5 fiber with either the flexible shaft repeat being replaced by the corresponding rigid repeat of

Ad37 or by shortening the shaft of Ad5 to match that of Ad37 in length. A significant impact of a rigid fiber shaft alone on virus binding and infection demonstrated that flexibility of the shaft is indeed critical for virus binding to CAR. Further, our experiments implied that the length of the fiber shaft plays an important role in receptor interaction as well, confirming earlier results of Shayakhmetov and Lieber (Shayakhmetov and Lieber, 2000). The impact of both, flexibility as well as length is likely due to the inability of the virus to allow simultaneous fiber knob-CAR and penton base-integrin binding without the steric flexibility provided by a long and flexible fiber shaft (Wu et al., 2003). Hence, we suggested that the fiber knob of species D Ads binds to a primary cellular receptor whose orientation permits simultaneous binding of the penton base to α_V integrins.

The beginning of the receptor-binding C-terminal knob domain of the fiber protein is defined by a well-conserved TLWT motif. The fiber knob contains a small number of segments with strongly conserved residues, although the sequences in-between those segments are highly variable. This can be attributed to antigenic variations between different serotypes and differences in receptor usage. However, there is an increased similarity between members of the same species (Chroboczek et al., 1995). Trimerization of the fiber protein is in part mediated by the presence of the knob domain, which has been shown to trimerize autonomously when expressed recombinantly with only small parts of the fiber shaft attached (Hong and Engler, 1996). The structure of each fiber knob monomer is composed of an eight-stranded anti-parallel β-sandwich structure, with three monomers forming the three-bladed propeller-like structure of the fiber knob trimer (van Raaij et al., 1999; Xia et al., 1994).

1.4.2 Adenovirus receptors

Similar to the human immunodeficiency virus (HIV), adenovirus entry into the cell requires association with two specific cellular receptors, one for attachment and a second one for internalization. While HIV binds to disparate receptors (CD4 and CCR5) via two separate domains within the same envelope glycoprotein (gp120 and gp41) (Kwong et al., 1998; Salzwedel and Berger, 2000), adenovirus employs two different capsid proteins for this task. The primary attachment receptor is bound by the knob domain of the fiber protein, while α_V integrin, representing the secondary receptor that mediated internalization, is bound by the penton base protein (Wickham et al., 1993). A conserved RGD motif in one of the penton base surface loops makes contact with α_V integrins at the cell surface. Penton binding to integrins may further allow the virus to stay attached to the cell surface upon release of the fiber proteins from the capsid (Nakano et al., 2000). Integrins represent a large family of heterodimeric membrane proteins that mediate cell adhesion, cell migration and differentiation, but have also been usurped by a number of viruses for cell entry (Stewart and Nemerow, 2007). In accordance with the five fold symmetry of the penton base complex, each penton can likely bind up to five integrin molecules (Chiu et al., 1999). Recruitment of these integrins by penton base then triggers a series of cell signaling events (E. Li et al., 1998a; E. Li et al., 1998b) that promote receptor-mediated endocytosis of the virus particle. The dependence of adenovirus entry on integrins was initially identified using the CAR-tropic species C Ad2 (Wickham et al., 1993). Recently, the penton base-integrin interaction was also shown to be critical for adenoviruses that use CD46 as primary attachment receptor (Murakami et al., 2007; Shayakhmetov et al., 2005a). However, species F adenoviruses Ad40 and Ad41 do not contain the integrin-binding RGD motif and exhibit a delay in their uptake, indicating that other entry pathways might exist (Albinsson and Kidd, 1999).

However, a prerequisite for the internalization-mediating interaction of

penton base with α_V integrins is the attachment of the virus particle to one of the primary attachment receptors described below.

Coxsackie and adenovirus receptor CAR

Early studies of the receptor usage of Ad2, a member of species C, found that the virus competes with Coxsackie virus type B3 for the same receptor (Lonberg-Holm et al., 1976). This receptor, a 46 kDa cell surface protein (calculated 38 kDa, migrating at 46 kDa in SDS-PAGE, likely due to glycosylation) was later identified as the coxsackievirus and adenovirus receptor (CAR) (Bergelson et al., 1997; Tomko et al., 1997). CAR is a type I membrane protein that belongs to the immunoglobulin superfamily. It is comprised of a cytoplasmic tail, a helical transmembrane domain and two immunoglobulin-like extracellular domains, D1 and D2 (Freimuth et al., 1999). In subsequent studies investigating adenovirus usage of this receptor, the fiber proteins of most members of adenovirus species A, C, D, E and F were found to bind CAR, with species B being a general exception (Roelvink et al., 1998). Competition studies using mutated recombinant Ad5 fiber knobs indicated a CAR binding site on the side of the fiber knob (Roelvink et al., 1999). These results were confirmed by a co-crystal structure of the Ad12 fiber knob with the domain I (D1), the membrane-distal IgV domain of CAR (Bewley et al., 1999). This structural analysis revealed a binding site at the interface of two adjacent knob monomers that encompasses the surface loops AB, CD and the β-strands E and F of one fiber knob monomer and the FG loop of the adjacent monomer. The fiber knob trimer is capable of binding three copies of the CAR D1 domain. The model for the Ad12-CAR binding site has been validated for other adenoviruses from species C and D (Howitt et al., 2003; Kirby et al., 2000; Seiradake et al., 2006). The equilibrium dissociation constant (K_D) for the Ad2 fiber knob to a single CAR D1 domain was measured between 20 and 25 nM (Lortat-Jacob et al., 2001). However, binding of the fiber knob to cell surface CAR is influenced by avidity effects, allowing tighter binding with an estimated K_D of around 1 nM.

While CAR is a well characterized receptor for coxsackievirus and adenovirus, its physiological role as well as tissue distribution and regulation of expression are not completely understood at this time. In polarized epithelial cells, CAR localizes at the apical pole of the lateral surface. It has been shown to co-localize with tight junction markers, and data showing that soluble CAR (C. J. Cohen et al., 2001) as well as anti-CAR antibodies (Walters et al., 2002) disrupt the formation of tight junctions suggests, that CAR is an integral part of tight junctions. Tight junctions are critical for cell polarity by forming a barrier that separates the apical and basolateral surfaces of polarized epithelial cells (B. R. Stevenson and Keon, 1998). This barrier restricts paracellular transit of macromolecules and ions, thus maintaining the regulated transcellular transport (Fanning et al., 1999). A correlation between CAR expression and cell adhesion as well as endothelial permeability has been observed, suggesting that CAR contributes to the barrier function of tight junctions (C. J. Cohen et al., 2001; Raschperger et al., 2006). In fact, an excess of expressed fiber protein released by Ad infected cells upon lysis is able to disrupt cell junctions in close proximity, thereby facilitating apical escape of virus released to the basolateral surface of endothelial cell layers (Walters et al., 2002). Also, disruption of the tight junctions might render CAR molecules, that are otherwise sequestered within tight junctions, accessible to Ad infection (C. J. Cohen et al., 2001). In solution, CAR has been shown to form dimers with a low-affinity association (van Raaij et al., 2000). It has been suggested that the high affinity binding of fiber knob to CAR disrupts the low-affinity CAR dimers involved in junction formation (Coyne and Bergelson, 2005).

Interestingly, besides adenovirus, two other unrelated viruses interact with primary receptors that are sequestered within tight junctions. coxsackievirus, just as adenovirus, uses CAR as receptor while reovirus binds to cells via the junctional adhesion molecule (JAM) that is homologous to CAR (Barton et al., 2001).

Sialic acid as a receptor for certain Ad types

The preferential tropism of Ad37 for the eye, and its poor transduction of CAR expressing lung epithelial cells suggested that this Ad type uses a distinct receptor. This was supported by the finding that a single amino acid mutation on the top surface of the Ad37 fiber knob (in the CD loop), located well outside the CAR binding region at the side of the knob, can ablate receptor binding of the virus (Huang et al., 1999). Arnberg and colleagues demonstrated that Ad37 binding to A549 human lung epithelial cells was sensitive to the removal of sialic acid from the cell surface by neuraminidase treatment. This led them to propose that Ad37 could attach to cells via sialic acid saccharides (Arnberg et al., 2000a). Subsequently, Ad19a, that shares the fiber protein of Ad37, and Ad8 have also been identified to bind to cells in a sialic acid dependent way (Arnberg et al., 2000b). Unlike other species D adenoviruses, these three serotypes are common causes of epidemic keratoconjunctivitis (EKC) (Ford et al., 1987). It has been suggested that the attachment of these viruses to host cells depends on a charge-dependent interaction between the positively charged fiber knobs of Ads 8, 19a and 37, that have a remarkably high isoelectric point (pI > 9), and the negatively charged sialic acid on cell surface glycoproteins (Arnberg et al., 2002).

A crystal structure of the Ad37 fiber knob in complex with sialyl-lactose (Burmeister et al., 2004) identified the location of the sialic acid binding site at the top of the fiber knob trimer. Due to its trimeric conformation, the fiber knob can bind up to three sialylated carbohydrates. The affinity of the sialyl-lactose binding site of Ad37 was estimated at a K_D of 5 mM. This is a fairly weak affinity for virus attachment to a cellular receptor, though it is in a similar range as that of influenza virus hemagglutinin binding to sialyl-lactose (K_D ~3mM) (Sauter et al., 1989). Despite the low affinity of its binding site on the Ad37 fiber knob, sialic acid could still play a significant role in the attachment of this virus due to potential avidity effects, similar to the attachment mechanism of influenza virus that depends on the simultaneous binding to

several cell surface sialic acid moieties via its hemagglutinin.

Comparison of the known fiber sequences of species D Ads indicated a well-conserved binding site for sialic acid in most strains. Nevertheless, serotypes other than Ad8, Ad19a and Ad37 exhibit a different tropism and are not known to be a common cause of EKC. Thus, binding to sialic acid cannot fully explain the ocular tropism of these Ads. The exact role that sialylated carbohydrates play in the attachment of species D adenoviruses remains unclear at this point, and a separate protein molecule is likely involved in the interaction and possibly affects binding and tropism of species D adenoviruses.

CD46 promotes binding of species B adenoviruses

A cell surface protein that might be involved in Ad37 attachment to the cell surface is the membrane cofactor protein (CD46). We were able to detect a direct interaction between this receptor and the fiber knob protein of Ad37. An analysis of this interaction is described in chapter I. In addition to these findings, a growing number of studies have indicated, that species B adenoviruses use CD46 as a cellular receptor. Some of the first studies reported that certain species B adenoviruses such as Ad3 does not compete the CAR binding species C viruses Ad2 and Ad5 (Defer et al., 1990; S. C. Stevenson et al., 1995). Subsequently it was found that none of the species B Ads bind to cells via CAR (Roelvink et al., 1998). Human CD46 was subsequently identified as a receptor for species B Ads 11 and 35 (Gaggar et al., 2003; Segerman et al., 2003b). Further, CD46 was shown to mediate infection of Ads 16, 21 and 50 as well, while species B Ads 3, 7 and 14 were suggested to not use this receptor or to use it with very low affinity (Tuve et al., 2006). However, it remains to be fully established whether these Ads are able to bind to CD46.

CD46 has also been found to function as receptor for a number of other viruses including measles virus (Dorig et al., 1993), human

herpesvirus 6 (Santoro et al., 1999) and bovine viral diarrhea virus (Maurer et al., 2004), as well as a receptor for a number of bacterial pathogens such as *Neisseria gonorrhoea*, *Neisseria meningitidis* (Källström et al., 1997) and group A *Streptococci* (Rezcallah et al., 2005).

CD46 is a ubiquitously expressed type I membrane glycoprotein that belongs to a family of proteins designated regulators of complement activation (RCA) (Hourcade et al., 1989; Liszewski et al., 1991). In humans, CD46 is expressed on all nucleated cell types. Like all members of the RCA protein family, it inhibits complement activation by interacting with fragments of the complement components C3 and C4. CD46 functions intrinsically by serving as a cofactor for the serine protease factor I in the cleavage and inactivation of C3b and C4b that are deposited on the same cell as the CD46 molecule, thereby preventing complement damage to the host cell. The RCA proteins are structurally related by sharing repeated amino acid motifs, termed short consensus repeats (SCRs) that are composed of ~60 partially highly conserved amino acids. CD46 contains four N-terminally located SCRs, followed by a region rich in serines, threonines and prolines (termed STP region), a small segment of unknown function, a hydrophobic transmembrane domain and a cytoplasmic tail. SCRs 1, 2 and 4 contain one N-linked glycan each, while the STP region is a site of extensive O-glycosylation. Alternative splicing allows the generation of multiple isoforms of CD46 with variations in the STP domain and the cytoplasmic tail.

The four SCR domains of CD46 mediate ligand association with the binding site for C3b being located in SCRs 3 and 4 while the recognition of C4b requires the additional presence of SCR 2 (Adams et al., 1991). Neither N-, nor O-linked oligosaccharides have a notable influence on binding of C3b or C4b. However, the N-glycans in SCRs 2 and 4 were found to be necessary for the cofactor activity of CD46 (Liszewski et al., 1998). The hemagglutinin of measles virus (MV) has a CD46 binding site distinct from that of the complement components (Manchester et al., 1995). The presence of SCRs 1

and 2 is necessary and sufficient to mediate MV attachment and subsequent entry into the cell (Manchester et al., 1997). Further, the N-linked oligosaccharide in SCR 2 was found to be critical for MV attachment to CD46 (Maisner et al., 1996).

To locate the Ad binding site on CD46, I generated cell lines stably expressing chimeras of CD46 and the closely related decay acceleration factor (DAF, CD55) (Manchester et al., 1995). Like CD46, CD55 contains four amino-terminal SCR domains however it does not mediate Ad binding (Lublin and Atkinson, 1989; Lukacik et al., 2004). My findings, detailed in chapter II, indicated that the binding site for the adenovirus fiber protein is comprised of SCRs 1 and 2 of CD46. In support of this, studies involving competition assays with CD46-specific antibodies and CD46 ligands as well as binding assays with CD46 mutants indicated a binding region that is stretched along the glycan free side of SCRs 1 and 2 (Fleischli et al., 2005; Gaggar et al., 2005; Sakurai et al., 2006). Further studies suggested that the N-linked glycans of CD46 are not critical for the Ad-CD46 interaction (Fleischli et al., 2005; Gaggar et al., 2005; Sakurai et al., 2006).

An important clue to the specific residues of species B Ad fiber knobs that are involved in CD46 binding came from a study that found a single point mutation (R279N) in the HI loop of Ad11 fiber knob that blocked CD46 dependent cell attachment (Gustafsson et al., 2006). The precise binding site of CD46 and the Ad11 fiber knob was later identified by Persson and colleagues who solved the crystal structure of the Ad11 fiber knob in complex with SCRs 1 and 2 of CD46 (Persson et al., 2007). Remarkably, the conformation of fiber knob-bound CD46 differs from that of unbound CD46. Instead of exhibiting a bend of ~60° between the two amino-terminal domains, the molecule assumes a straightened conformation upon fiber knob binding, resulting in a notable shape-complementarity between the fiber knob and CD46 and creating a large continuous binding surface.

Receptor X as a potentially new Ad receptor

While species B adenoviruses are subdivided in groups B1 and B2 based on genetic differences, this classification does not closely correspond with their receptor usage. Antibody competition studies as well as virus transduction assays led to the proposal of a new classification of species B adenoviruses according to the attachment receptors used. At the same time, a separate, yet to be identified receptor for the potentially non CD46-binding Ads 3, 7 and 14 as well as the CD46-tropic Ad11 was proposed (Tuve et al., 2006). This receptor, designated X, is thought to be a primate-specific, abundantly expressed glycoprotein that interacts with the adenovirus fiber knob at a lower affinity than CD46. Due to their limited expression pattern, CD80 and CD86, that have previously been suggested as receptors for Ad3, are unlikely to represent receptor X.

CD80 and CD86

Like all species B adenoviruses, Ad3 does not use CAR to infect cells and the role of CD46 as receptor for Ad3 is still controversial. Affinity purification of Ad3 fiber knob ligands from cell membrane fractions yielded the proteins CD80 and CD86 that belong to the immunoglobulin superfamily (Short et al., 2004). Subsequent studies suggested that not only Ad3 but all species B Ads can transduce cells in a CD80- and CD86-dependent fashion (Short et al., 2006). However, antibody competition assays indicated that Ad3 transduction of HeLa cells did not depend on either CD80 or CD86. The authors suggested that CD80 and CD86 mediate Ad transduction of certain hematopoietic cells, though only in the absence of other attachment receptors. Hence, it remains uncertain what role, if any, these molecules play in species B Ad infection *in vivo*.

Heparan sulfates

A KKTK motif in the proximal fiber shaft domain of Ads 2 and 5 has been suggested to mediate virus binding to heparan sulfate glycosaminoglycans (HS-GAG) (Dechecchi et al., 2001; Dechecchi et al., 2000). Studies demonstrating that mutations of this motif significantly reduced CAR-independent adenovirus transduction of the liver suggested an important role of HS-GAGs for the liver tropism of Ad5 based vectors (T. A. Smith et al., 2003b; T. A. Smith et al., 2003c). However, direct binding of the KKTK motif to HS-GAGs has not yet been demonstrated. Furthermore, mutations of the putative HS-GAG binding motif could alter the flexibility of the fiber shaft which could influence Ad internalization independent of HS-GAG binding. This is supported by observations that vectors carrying the mutated fiber protein were still able to bind to cells despite their inability to mediate transduction (Bayo-Puxan et al., 2006; Kritz et al., 2007). Hence, the role of an interaction between HS-GAGs and the adenovirus fiber shaft is still somewhat unclear. However, heparan sulfate proteoglycans are thought to play a role in adenovirus attachment mediated by coagulation factors (Kalyuzhniy et al., 2008).

Coagulation factors can indirectly modulate Ad association with cells

For most adenoviruses, binding of the fiber protein to the cellular receptor CAR and subsequent attachment of penton base to α_v integrins have been established as the first key steps in infection. However, this pathway cannot explain the predominant infection of liver cells by Ad5 or Ad5 based vectors *in vivo* despite low expression levels of CAR on these cells (Connelly, 1999). For example, vectors equipped with a fiber protein that has been mutated to abolish CAR binding exhibit an unchanged infection pattern of certain cell types *in vivo* (Alemany and Curiel, 2001). Aside from adenovirus fiber binding to cellular receptors, recent studies revealed a new mechanism for transduction of hepatocytes *in vivo* that implicates a novel, alternative

pathway for cell entry of adenovirus.

In particular, a role of several vitamin K dependent coagulation factors in the transduction of hepatocytes by Ad5 (Parker et al., 2006; Shayakhmetov et al., 2005b) has been suggested. Subsequent studies singled out coagulation factor X (FX) to be the critical factor for mediating CAR independent infection of liver cells in a mouse model (Kalyuzhniy et al., 2008; Waddington et al., 2008). FX was found to bind to, or near the hyper variable regions (HVRs) of the Ad5 hexon trimer via its Gla domain. The serin protease domain of the virus-bound FX then makes contact to the host cell (Waddington et al., 2008), likely mediated through cell surface heparan sulfate proteoglycans (HSPGs) (Parker et al., 2006).

Binding of FX to the viral hexon protein of different serotypes correlates with virus transduction and transgene expression *in vitro* and *in vivo*. Assessment of which adenovirus serotypes might use FX mediated cell binding to infect hepatocytes revealed that species D virus lacked the ability to interact with FX. These new findings could provide important information for the choice of Ad vectors for gene therapy applications that seek to avoid transduction of liver cells.

1.5 Adenovirus vectors

About a quarter of all gene therapy trials in the U.S involve the use of adenovirus as a vector, often for the treatment of cancer or cardiovascular diseases (Campos and Barry, 2007). The ability of adenovirus to efficiently transduce post-mitotic cells is an important factor for *in vivo* applications. A majority of the adenoviral vectors used, including the first ones developed, are based on the CAR-binding species C Ad5. To ensure a lack of autonomous replication, certain endogenous viral gene cassettes are typically deleted from Ad vectors. The adenovirus *E1* gene products are required for the activation and expression of the early and late genes, thus the ability of adenovirus to replicate depends critically on the *E1* gene cassette. A deletion of the *E1* region results in a replication deficient virus that is dependent on a cell line providing the *E1* genes products in trans for propagation. The cell line 293 is an *E1* expressing cell line, derived from human embryonic kidney cells, that complements *E1* deleted vectors and allows their propagation (Graham et al., 1977). Vectors with a deletion of the *E1* and sometimes in the *E3* genes are categorized as first-generation vectors. The deletion of gene cassettes from the adenovirus genome allows the insertion of larger therapeutic genes. The packaging of up to a total of 38 kb of DNA can be achieved without negatively affecting virus titer and growth rate (Bett et al., 1993). The deletion of the *E1* region permits the insertion of up to 5.1 kb of DNA, while the additional deletion of the *E3* region allows insertions up to 8.2 kb. The *E3* genes are not essential for adenoviral replication in tissue culture, though there is a possibility that they could provide certain benefits *in vivo* due to the interaction of their gene products with the host immune system.

A benefit of the additional *E3* deletion is the decreased likelihood of recombination events between the vector and the packaging cell line that lead to replication-competent viral progeny. This is a common problem of *E1* deleted vectors where recombination between the viral genome and the complementing cell line could result in the vector regaining the deleted gene

cassette (Lochmuller et al., 1994). Thus, vectors have to be carefully assessed for replication competence prior to their application.

A further problem of these first generation vectors is their potential to stimulate a potent innate and adaptive immune response leading to the destruction of transduced cells. This is likely due to low levels of replication taking place even in the absence of the *E1* genes, which limits use of these vectors mostly to short-term applications such as vaccination or cancer therapy (Yang et al., 1994a; Yang et al., 1994b). Moreover, pre-existing antibody/T cells to Ad5 in most adults can lead to decreased efficacy or even unanticipated problems in vaccine trials (Moore et al., 2008).

To address the problem of low-level gene expression and replication in *E1* deleted viruses, vectors with multiple gene deletions, usually *E2* and *E4*, were generated (Amalfitano et al., 1998; Gorziglia et al., 1996; Lusky et al., 1998). These vectors, termed second-generation, have the additional advantage of allowing for the insertion of larger therapeutic gene cassettes. Cell lines providing the missing gene products *in trans* have been created to allow propagation of these vectors. Since the deletion of *E2* includes removal of the gene encoding the adenovirus polymerase, no replication can take place even in the presence of a functional *E1A* gene (Amalfitano et al., 1998), resulting in a reduced immune response and sustained transgene expression by transduced cells (Hu et al., 1999).

The most radical approach to gene deleted adenovirus vectors are so called helper-dependent vectors (HDAds) (Alba et al., 2005; D. J. Palmer and Ng, 2005). Deletion of all viral genes from their genome minimizes immune response and allows transgene insertions of up to 37 kb (Clemens et al., 1996). These vectors allow long-term gene expression without the chronic toxicity inherent to first- and second-generation vectors. Due to the complete lack of viral genes these vectors depend on the expression of all critical gene products *in trans*. However, the generation of functional trans-complementing cell lines has not been possible, thus making virus propagation dependent on

helper viruses that provide the missing gene functions. An initial caveat of this approach was the difficult separation of the replication-deficient, transgene carrying vector from the helper virus (Sandig et al., 2000). Specific generation of HDAds was improved by the use of the Cre-*loxP* system (Parks et al., 1996). The packaging signal of the helper virus genome is flanked by *loxP* sites, resulting in its excision upon infection of a Cre recombinase-expressing packaging cell line. Further improvement of this system by the generation of packaging cell lines expressing high levels of Cre or other recombinases (Ng et al., 2001) allowed the production of high virus titers, with levels of helper virus contamination as low as 0.1-0.4%. Additional purification by CsCl gradient centrifugation could reduce contamination levels to 0.01-0.02% (D. Palmer and Ng, 2003). These levels of contamination with a helper virus that is equivalent to a first-generation Ad vector caused no reduced transgene expression nor increased toxicity in mouse models (Maione et al., 2001; Reddy et al., 2002). However, whether this is true in humans has not been determined. Despite the progress made, the clinical application of HDAds will require further reduction of helper virus contamination. To address this issue the use of non-Ad helper viruses such as herpes simplex virus-1 (Kubo et al., 2003) or baculovirus (Cheshenko et al., 2001) have been evaluated. However, HDAd yields obtained were low, rendering large-scale production impossible.

A further problem of HDAd generation is the possibility of a homologous recombination between the *E1* deleted helper virus and the *E1* containing packaging cell lines, which could result in replication-competent adenovirus. This issue has been addressed by the incorporation of stuffer DNA within the *E3* region of the helper virus (reviewed in D. J. Palmer and Ng, 2005). In order to be efficiently incorporated into the virus capsid, the Ad genome has to be between ~27.7 kb and ~38 kb in size (Bett et al., 1993; Parks and Graham, 1997). While not preventing the homologous recombination itself, the insertion of stuffer DNA would leave the vector

genome unpackageable in the event of a recombination, due to its size exceeding the packaging limit.

A problem all therapeutic approaches using the described, mostly Ad5-based vectors have in common, is the strong innate immune response upon systemic administration. This innate immune response is triggered by the Ad capsid proteins and does not depend on viral gene expression or replication. Intravascular delivery leads to a majority of the viral particles being sequestered by the liver, likely due to a tropism based on blood factor-mediated attachment of the capsid to hepatocytes (Kalyuzhniy et al., 2008; Waddington et al., 2008). This leads to significant production of inflammatory cytokines and chemokines and the subsequent recruitment of leucocytes to the transduced liver (Muruve et al., 2004). Other problems of these Ad5-based vectors include the high prevalence of neutralizing antibodies to Ad5 capsid proteins in the general population as well as a high immunogenicity of this virus, making re-administration of the vector (e.g. during vaccination) problematic (Abbink et al., 2007). Lastly, poor expression of the receptor CAR on certain cell types limits the application of Ad5-based vectors. This receptor is frequently down-regulated on the more malignant tumor isolates (Anders et al., 2003; Fuxe et al., 2003; Hemminki et al., 2003) and is not expressed on most hematopoietic cells types (Iacobelli-Martinez et al., 2005; Segerman et al., 2000).

These problems are being addressed by the development of novel vectors that are based on or incorporate capsid proteins of different Ad serotypes. Since hexon, the most abundant capsid protein of adenovirus, is a major target for neutralizing antibodies (Sumida et al., 2005), Ad vectors with hexon substitutions are being evaluated in preclinical trials. These vectors can be fully based on other serotypes or have a substitution of the hexon protein only. Even Ad5 vectors with modified hypervariable regions in the original hexon protein have been successfully tested (Roberts et al., 2006). In addition to the adaptive immune response, Ad5 based vectors are inhibited by

an innate immune response as well due to their preferential targeting of hepatocytes. As described earlier, it has been demonstrated that the strong liver tropism is mediated by a blood factor-hexon complex. This is limited to certain serotypes (Waddington et al., 2008) and could be addressed by the use of alternative hexon proteins as well. Vectors containing a substitution of the penton protein have been investigated (Sumida et al., 2005), but did not successfully evade antibody neutralization. A recent publication demonstrated that a change of the fiber knob domain allowed escape from preexisting capsid-specific neutralizing antibodies (NAbs) (Sarkioja et al., 2008). Even small changes in the knob portion of the fiber gene had a significant effect, which supports a suggestion that Ad neutralization depends on NAbs against several major capsid proteins, not just hexon (Gahery-Segard et al., 1998; Rahman et al., 2001).

More importantly, the use of alternative fiber proteins allows a modification of the tissue tropism of the vector. With CAR being poorly expressed or absent on most hematopoietic cell types (Iacobelli-Martinez et al., 2005; Segerman et al., 2000) and down-regulated on certain malignant tumor cells (Anders et al., 2003; Fuxe et al., 2003; Hemminki et al., 2003), fiber proteins from viruses using alternative receptors have gained increased attention. In particular, the incorporation of fiber knobs from the CD46-binding members of species B has become increasingly popular. Havenga and colleagues conducted an extensive study of Ad5-based vectors carrying fiber proteins from a wide range of other Ad serotypes (Havenga et al., 2002). Human cancer and primary cells are important targets for gene therapy; however a large number of these cell lines has low or absent expression of CAR and therefore are refractory to CAR-tropic adenovirus vectors. In a majority of tested cancer cell lines a significant, sometimes dramatic improvement in transgene expression was achieved by vectors carrying a non-Ad5 fiber protein (Havenga et al., 2002). In 80% of these cases, the fiber proteins causing the most pronounced improvement were derived from

species B Ads, in particular Ad16, Ad35 and Ad50. The results seen in primary cells were even more striking. With the exception of hepatocytes, all tested cell lines showed improved transduction efficiencies by fiber-chimeric vectors, and each time the most effective fiber was derived from species B Ads. Dose response experiments with human isolates indicated that comparable transgene expression could be achieved at 100-fold lower particle counts, if the vector used carried an Ad16 fiber. This reduction in vector dose is likely to significantly reduce vector toxicity and immune response.

Besides the use of fiber proteins from other Ad serotypes, the incorporation of foreign peptide sequences into surface loops of the fiber knob to re-direct vector tropism are being investigated (Nicklin et al., 2005) Introduction of an α_V integrin-binding RGD peptide allowed CAR-independent vector targeting and significantly improved gene delivery to primary tumor cells (Dmitriev et al., 1998; Hidaka et al., 1999). Moreover, addition of a poly-lysine sequence (K7) to the fiber knob enabled adenovirus vectors to bind cell surface heparan sulfates, thus allowing successful gene transfer to numerous cell lines in the absence of CAR (Bouri et al., 1999; Wickham et al., 1997).

Thus, an underlying theme of research in the area of adenovirus biology is that increased understanding of the virus structure and association with cellular factors and receptors is providing further insights toward improved methods of gene transfer. This could benefit the treatment of important human diseases such as genetic diseases or cancer as well as the development of vaccine delivery applications using adenoviral vectors.

1.6 Thesis objective

In this thesis project, I sought to characterize the interaction of adenovirus with the integral cell membrane protein CD46. Due to the increasing focus on adenoviruses as vectors for clinical gene transfer applications, further insights into the molecular basis of virus attachment and CD46 association in particular, could provide valuable information for the selection of novel adenovirus vectors. Thus, I compared CD46-dependent cell transduction of the species D Ad37 virus with that of a CD46-binding member of species B to evaluate the role of this receptor in the attachment of different Ad species. Further, I used antibody competition data as well as functional analysis of different CD46-expressing cell lines to locate the Ad binding site on CD46 and compared this to the known binding sites of other CD46-using pathogens. I also identified and defined the features of the Ad fiber protein that are critical for CD46 association using structural, biochemical and functional assays. Lastly, I obtained detailed kinetic data for the Ad-CD46 interaction by analyzing the binding of recombinant CD46 to the Ad fiber knob by surface plasmon resonance. The data obtained from my studies allows a more complete understanding of adenovirus receptor interactions. This could help in the selection of improved gene delivery vectors, but also have implications for the characterization of newly emerging, clinically relevant adenovirus strains.

2. Chapter I:
Analysis of species D Ad37 receptor usage

2.1 Introduction

Species D adenovirus type 37 (Ad37), together with Ad8 and Ad19, is a major cause of epidemic keratoconjunctivitis (EKC), a severe and highly contagious ocular infection (Ford et al., 1987). While most adenoviruses, with the general exception of species B, use the coxsackievirus adenovirus receptor (CAR) as attachment receptor, the specific tropism of EKC-causing viruses for the eye, and in some cases the genital tract, cannot be explained by the expression pattern of this receptor that is expressed on a variety of cells (Bergelson et al., 1997). Moreover, despite the expression of CAR on A549 lung epithelial cells, Ad37 was found to bind poorly to these cells (Huang et al., 1999). The fiber protein mediates the receptor attachment of CAR-binding adenoviruses, while species B Ads lack the CAR binding site in the knob domain of their fiber. Ad37 fiber knob, by contrast, is able to bind CAR immobilized on a solid support, albeit at a low affinity. However, we previously showed that the short and rigid shaft domain of Ad37 fiber further impairs binding of CAR on the cell surface and prevents the effective usage of this receptor for virus attachment (Wu et al., 2003).

The search for the attachment receptors of these non CAR-binding serotypes led to the identification of CD46 as cellular receptor for species B adenoviruses (Gaggar et al., 2003; Segerman et al., 2003b). The initial observation that attachment of a species B adenovirus to a permissive cell line could be efficiently blocked by the recombinant fiber knob domain confirmed, that receptor-binding of the virus is mediated by this domain. The fiber knob was then used to precipitate proteins from cell membrane lysates. Analysis of the precipitated proteins resulted in the identification of CD46 as the interacting receptor for certain species B adenoviruses.

Independent of the identification of CD46 as species B Ad receptor, our group found species D Ad 37 to interact with CD46. Ad37 had been previously reported to attach to sialic acid glycoconjugates on the cell surface (Arnberg et al., 2000a) as well as to unidentified, glycosylated 50- and 60-kDa proteins on conjunctival epithelial cells in a calcium dependent manner (Wu et al., 2001). Lentil lectin chromatography allowed the separation of glycoproteins from detergent-solubilized membranes of these cells. Separation of the isolated proteins by sodium dodecyl sulfate polyacrylamide gel electrophoresis (SDS-PAGE) and subsequent mass spectrometry analysis of bands corresponding in size identified four plasma membrane proteins. Out of these four candidates, CD46 was identified to be a receptor for Ad37 by immunodepletion analysis.

Part of the effort to identify CD46 as potential Ad37 receptor was to demonstrate that the fiber knob domain of this virus can bind directly to CD46. I expressed soluble recombinant CD46 and the recombinant fiber knob domain of Ad37 to analyze direct interaction between fiber knob and receptor. Further, I compared the CD46-dependence as well as the influence of sialic acid on attachment of vectors displaying either species D Ad37 or a species B fiber protein. Unexpectedly, I also discovered an enhancing effect of the recombinant Ad37 fiber knob on virus transduction. Further experiments to evaluate the potential of Ad37 fiber knob to enhance adenovirus transduction of murine hematopoietic stem cells and the human histiocytic lymphoma cell line U-937 (shown in Figures 2.6B and 2.7) resulted from a collaboration with Dr. Ronald Nepomuceno.

2.2 Material and methods

Cells and viruses

The Chinese hamster ovary cell line CHO-K1, the human embryonic kidney cell line 293 and the U-937 human histiocytic lymphoma cell line were purchased from the ATCC (Manassas, VA). 293-EBNA human embryonic kidney cells, constitutively expressing the EBNA-1 protein of Epstein-Barr virus, were obtained from Invitrogen (Carlsbad, CA). Murine $CD44^{hi}$ lineage-negative hematopoietic stem cells (mHSCs) (Ritter et al., 2006) were obtained from the laboratory of Dr. Martin Friedlander (The Scripps Research Institute). The generation of CHO cell lines stably expressing human isoforms of CD46 (CHO-CD46) is described in chapter II. Cells were maintained in F-12 medium (CHO cells), DMEM (293 and 293-EBNA cells) or RPMI (U-937 cells and mHSCs), supplemented with 10% fetal calf serum (FCS) (Omega Scientific, Tarzana, CA), 10 mM HEPES pH 7.55, 4 mM L-glutamine, 1 mM sodium pyruvate, 0.1 mM nonessential amino acids, 100 units/ml penicillin and 100 μg/ml streptomycin. Transfected CHO cells were maintained in F-12 medium supplemented as described above, with the addition of 0.5 mg/ml G418 sulfate. All tissue culture reagents were obtained from Invitrogen (Carlsbad, CA), unless otherwise noted.

Virus propagation and purification

The replication-deficient Ad5-based vectors used in this study are E1/E3-deleted and contain a cytomegalovirus promoter-driven GFP reporter gene cassette. They express either the endogenous Ad5 fiber (Ad5.F5), or fibers from Ad16 (Ad5.F16) (C. Hsu et al., 2005), Ad35 (Ad5.35F) (T. A. Smith et al., 2003c) or Ad37 (Ad5.F37) (Wu and Nemerow, 2004) due to an insertion of the respective fiber gene in the virus backbone. For the propagation of adenovirus and adenoviral vectors, 293 cells were grown to

about 80% confluency and infected with the respective adenoviral vector at a multiplicity of infection (MOI) of 200 particles per cell. Cells were harvested 72 hours post infection and lysed by three freeze-thaw cycles. Cellular debris was pelleted and the virion-containing supernatant was loaded onto a 16-40% cesium chloride gradient and spun for 3 hours at 30,000 rpm and 4°C in an SW40Ti rotor (Beckman Coulter, Fullerton, CA). The band containing mature virions was carefully extracted from the gradient. Following a second purification on a 16-40% cesium chloride gradient for additional purity, the virus was dialyzed into a buffer consisting of 10 mM Tris pH 8.0, 150 mM sodium chloride, 2 mM magnesium chloride and 10% glycerol. The viral protein concentration was determined with the Bio-Rad Protein Assay (Bio-Rad, Hercules, CA) and used to calculate the viral particle concentration with 1 μg protein = $4x10^9$ virions. The virus was aliquoted, flash-frozen and stored at -80°C.

Expression and purification of a soluble form of CD46 (sCD46)

The entire extracellular domain of the C isoform of CD46 was amplified by PCR from a mammalian expression plasmid coding for the C2 isoform of CD46 (Post et al., 1991), using Expand DNA polymerase (Roche) and the primers 5'-GCTAGCTTGTGAGGAGCCACCAACATTTGA-3' (NheI site underlined) and 5'-GCGGCCGCATCCAAACTGTCAAGTATTCCT-3' (NotI site underlined). The PCR product was gel purified and cloned into pCR2.1-TOPO (Invitrogen) according to the manufacturer's instructions. Plasmid DNA was amplified from the culture of a colony of transformed cells. Purified plasmid DNA and the mammalian expression vector pCEP-Pu-C-His (Kohfeldt et al., 1997), that adds a C-terminal 6x His tag to the expressed protein, were digested with the restriction enzymes NheI and NotI (New England Biolabs, Beverly, MA). Digested vector and insert were gel purified and ligated with T4 DNA Ligase (Invitrogen). The sequence of the resulting plasmid was verified by DNA sequencing. 293-EBNA cells (Invitrogen) were

transfected with the plasmid using FuGENE 6 transfection reagent (Roche) according to the manufacturer's instructions. Following several rounds of selection in DMEM containing 5 μg/ml puromycin, transfected and selected cells were grown in 40 15cm culture dishes to a confluency of ~80%, washed twice with PBS and incubated in serum-free DMEM containing 5 μg/ml puromycin for 5-6 days. To purify the secreted soluble CD46 (sCD46), the culture medium was centrifuged to remove cells and cellular debris and subsequently incubated with 1 ml Ni-NTA Agarose resin (Qiagen, Valencia, CA) for 1 hour. The resin was washed with 10 mM sodium phosphate pH 7.0, 300 mM NaCl and 10 mM imidazole by gravity flow. Bound sCD46 was eluted from the resin with a buffer composed of 10 mM sodium phosphate pH 7.0, 300 mM NaCl and 300 mM imidazole. Purified sCD46 was dialyzed against PBS and analyzed by SDS-PAGE and Western blotting.

Recombinant fiber knob constructs

A DNA fragment corresponding to the residues 172 to 365 of the Ad37 fiber protein was obtained by digesting a plasmid encoding the Ad37 fiber knob and part of the shaft domain (Wu et al., 2001) with the restriction enzymes BamHI and NotI. Following gel purification, this fragment was ligated into the BamHI/NotI cloning site of the kanamycin-resistant bacterial expression vector pET-28a(+) (Novagen Madison, WI), using T4 DNA Ligase (Invitrogen). The vector adds a 6x His tag, a 6 amino acid thrombin cleavage site and an 11 amino acid T7 tag to the N-terminus to the expressed fiber knob protein.

Ad16 fiber knob DNA was amplified by PCR from a plasmid containing the Ad16 fiber gene (pDV156; Denby et al., 2004) using Expand High Fidelity polymerase (Roche, Indianapolis, IN) and the primers 5'-CGCGGATCCGACTCTTCCAATGCTATCAC-3' (BamHI site underlined) and 5'-TGGTGCGGCCGCTCAGTCATCTTCTCTG-3' (NotI site underlined). The amplified DNA fragment, encoding residues 151 to 353 of the Ad16 fiber

protein, was cloned into pCR2.1-TOPO using the TA-Cloning Kit according to the manufacturer's instructions (Invitrogen, Carlsbad, CA). The resulting plasmid was digested with BamHI and NotI and the isolated DNA fragment encoding the fiber knob was subcloned into the bacterial expression vector pET-28a(+).

An ampicillin-resistant bacterial expression vector encoding residues 387 to 581 of the CAR-binding Ad5 fiber protein with an added N-terminal 6x His tag was previously generated by Eugene Wu (Wu et al., 2004). Correctness of the sequence of all fiber knob plasmids was verified by DNA sequencing.

Fiber knob expression and purification

The fiber knob encoding plasmids were used to transform BL21(DE3) *Escherichia coli* (*E. coli)* cells (Invitrogen) according to the manufacturer's instructions. Following selection on Luria-Bertani broth-agar plates (LB-plates) containing the appropriate antibiotic, a colony was picked and used to inoculate a culture of Luria-Bertani broth (LB) containing either 100 μg/ml ampicillin or 50 μg/ml kanamycin. A 1 liter culture was grown at 37°C to an optical density of 0.8 at a wavelength of 600 nm. Protein expression was induced with 1 mM isopropyl β-D-thiogalactopyranoside (IPTG) for 4 hours at 30°C. Cells were pelleted and lysed by incubation with 40 ml BugBuster Protein Extraction Reagent (Novagen, Madison, WI) supplemented with 20 U/ml of Benzonase (Sigma), 1 mg/ml of Lysozyme (Sigma, St. Louis, MO), 150 mM NaCl, 10 mM imidazole and Complete EDTA-free Protease Inhibitor Cocktail (Roche) for 20 min at 4°C. Cell debris was pelleted by centrifugation for 20 min at 12,000 x g and 4°C. The supernatant was incubated with 1 ml of Ni-NTA Agarose (Qiagen, Valencia, CA) or TALON Metal Affinity Resin (Clontech, Mountain View, CA) for 1 hour, rocking at 4°C. The resin was washed with 10 ml wash buffer 1 (20 mM sodium phosphate pH 7.0, 300 mM NaCl, 20 mM imidazole and 1% Triton X-100 for Ni-NTA Agarose or 20 mM

Tris pH 8.0, 300 mM NaCl, 10 mM imidazole and 1% Triton X-100 for TALON) and 10 ml wash buffer 2 (same as wash buffer 1 but without Trition X-100) by gravity flow. Bound protein was eluted with 20 mM sodium phosphate pH 7.0, 500 mM NaCl, 300 mM imidazole (Ni-NTA Agarose) or 20 mM Tris pH 8.0, 500 mM NaCl, 300 mM imidazole (TALON) and subsequently dialyzed into 20 mM Tris, pH 7.4, 100 mM NaCl.

Binding of soluble CD46 to immobilized fiber knob

Wells of a 96-well enzyme-linked immunosorbent assay (ELISA) plate (Immulon 4 HBX; Dynex Technologies, Chantilly, VA) were coated overnight with 1 μg of bovine serum albumin (BSA), purified Ad37 fiber knob, or purified Ad5 fiber knob diluted in 100 μl phosphate buffered saline (PBS). Wells were briefly blocked with Superblock in PBS (Pierce) and incubated with different amounts of sCD46 diluted in BLOTTO in PBS (Pierce), containing 1 mM calcium chloride for 1.5 h at room temperature. Wells were washed with PBS-$CaCl_2$, incubated with the anti-CD46 rabbit polyclonal antibody H-294 (Santa Cruz Biotechnology), washed, incubated with a horseradish peroxidase-conjugated goat anti-rabbit antibody, and washed again. The ELISA was developed with ABTS [2,2'-azino-bis(3-ethylbenzthiazoline-6-sulphonic acid)] substrate (Pierce) for 1 hour and analyzed by measuring absorbance at a wavelength of 405 nm.

Radioactive labeling of viruses

Ad5.16F or Ad5.37F particles were labeled by incubating 1 mCi of $Na^{125}I$ (Amersham, Piscataway, NJ) with 50 μg virus diluted in 100 μl of PBS (pH 7.4) and one Iodo-Beads Iodinating Reagent bead (Pierce Biotechnology, Rockford, IL) for 8 min at room temperature. Labeled virus was separated from free iodine using a PD-10 desalting column (Amersham), according to the manufacturer's instructions. The specific activity of ^{125}I-labeled virus was determined to be 3.33×10^6 and 3.26×10^6 cpm/μg of virus protein for Ad5.16F and Ad5.37F, respectively.

Virus binding assays

CHO-CD46 (BC1 isoform) and CHO-null cells were detached from tissue culture flasks with 10 mM EDTA in PBS, washed with serum-free medium and diluted to 10^6 cells in 120 μl serum-free medium. 500 radioactively labeled Ad5.16F or Ad5.37F virions per cell were added in 50 μl serum-free medium. Cells were incubated in the presence of virus for 1 hour at 4°C before being loaded onto a 200 μl oil cushion (86% silicone oil, 14% mineral oil) and centrifuged for 2 x 4 min at 13,000 x g. To determine the effect of cell-bound sialic acid on virus binding, cells were incubated in the presence 1 or 10 mU/ml neuraminidase in 20 μl serum-free medium for 1 hour at 37°C, prior to the addition of virus. The sample tubes were flash-frozen in liquid nitrogen and the bottom portion of the tubes that contained the cells separated from the unbound virus was cut and subject to analysis in a gamma counter. The percentage of virus bound to cells was calculated by dividing counted cell-bound activity by total activity of virus added to the cells.

Virus transduction assays

To analyze virus transduction, $5x10^4$ CHO-CD46 cells/well (C2 isoform) were cultured in a 24-well tissue culture plate. Cells were incubated with 1, 8 or 10 mU/ml of neuraminidase from *Vibrio cholerae* (Roche Applied Science, Indianapolis, IN), or buffer as control, in serum-free F-12 medium for 30 min at 37°C. Cells were washed and $5x10^6$ particles of Ad5.16F or Ad5.37F, diluted in serum-free medium, were added and incubated for 1 hour on ice. Cells were washed three times with medium and incubated for 16-20 hours at 37°C in F-12 medium containing FCS. The cells were detached with trypsin, resuspended in FACS buffer consisting of 20 mM Tris-buffered saline, 0.2% sodium azide, and 0.2% bovine serum albumin and analyzed for GFP transgene expression by acquiring 10,000 cells on a FACScan flow cytometer and analyzing fluorescence using CellQuest software (BD Biosciences, Billerica, MA).

Fiber knob competition assays

$5x10^4$ CHO-CD46 cells or $2x10^5$ U-937 cells were plated in 24-well tissue culture plates in F-12 and RPMI medium, respectively. Cells were incubated with 600 (CHO-CD46) or 1000 (U-937) particles/cell of Ad5.16F or Ad5.37F in the presence of varying concentrations of purified Ad fiber knob as indicated in the figure legends for 1 hour on ice. Cells were washed three times with medium and incubated for 16-20 hours at 37°C. GFP transgene expression was analyzed by FACS as described above.

Ad37 fiber knob binding to virus capsid

To measure Ad37 fiber knob interaction with Ad5 virions, 40 μg of Ad37 fiber knob were mixed with 40 μg of Ad5.F5 virus, in the presence of increasing amounts of NaCl in complete RPMI medium, in a final volume of 200 μl. After incubation for 1 h on ice, the mixture was layered over a step gradient of 290 μl of 40% Histodenz and 190 μl of 80% Histodenz, both in N-2-hydroxylpiperazine-N'-2-ethanesulfonic acid-buffered saline (HEPES) pH 8.0. Gradients were centrifuged at 47,000 rpm in an SW55Ti rotor (Beckman Coulter, Fullerton, CA) for 2 h at 4°C. Samples banded between the Histodenz layers were extracted with a needle and syringe, mixed with reducing SDS sample buffer, separated by SDS–PAGE, and transferred to nitrocellulose membranes for immunoblotting. Ad37 fiber knob was detected using an anti-T7 tag antibody horseradish peroxidase (HRP) conjugate. Following detection using the SuperSignal Substrate System (Pierce, Rockford, IL), the blots were stripped and re-probed for endogenous Ad5.F5 fiber protein using the anti-fiber monoclonal antibody 4D2 (NeoMarkers, Fremont, CA) and a peroxidase-conjugated anti-mouse secondary antibody.

Structural analysis

A map of the electrostatic surface potential of the Ad37 fiber knob was generated using the programs PDB2PQR (Dolinsky et al., 2004) and APBS (Baker et al., 2001). Visualization and analysis of this map as well as the crystal structure of Ad37 fiber knob in complex with sialyl lactose were done using the program PyMOL (DeLano, 2002).

2.3 Results

2.3.1 Expression of soluble CD46

Attachment of most adenoviruses to their known cellular receptors is mediated by the knob portion of the fiber protein (Shenk, 1996). After the identification of CD46 as potential receptor for Ad37 (Wu et al., 2004), I investigated whether the fiber knob of this virus is capable of direct binding to a recombinant soluble form of CD46 (sCD46). To express sCD46, the DNA sequence corresponding to the entire extracellular domain of the C isoform of CD46 was amplified by PCR and inserted into the mammalian episomal expression vector pCEP-Pu–*C-His* (Kohfeldt et al., 1997) that adds a C-terminal 6x His tag as well as an N-terminal BM-40 signal peptide that directs the gene product to the culture medium (Figure 2.1A). The vector contains the latent origin of Epstein-Barr virus (*oriP*) and a gene encoding Epstein-Barr nuclear antigen 1 (EBNA-1), allowing its extrachromosomal maintenance. Binding of EBNA-1 to *oriP* also dramatically increases gene expression of plasmids carrying *oriP*. This effect is further enhanced by the use of an EBNA-1 expressing cell line (for a review: Leight and Sugden, 2000). This sCD46-expression vector was used to transfect 293EBNA cells. Since the plasmid contains only the extracellular domain of CD46, the expressed protein accumulated in the culture medium from where it was purified by immobilized metal ion affinity chromatography (IMAC) (Figure 2.1B and C). Yields of 40 to 80 μg sCD46 protein were obtained from 40 15cm culture dishes.

2.3.2 Expression of recombinant fiber knob

For receptor-binding analysis, I expressed recombinant forms of the Ad37 and the Ad5 fiber knob. Since parts of the shaft domain of the fiber protein are needed to retain trimeric organization of the fiber knob (Hong and Engler, 1996), the constructs I generated encompassed the entire knob

domain and a small part of the fiber shaft. DNA sequences corresponding to the knob domains and the final shaft repeat of the fiber proteins were amplified from the Ad5, Ad16 and Ad37 genomes and cloned into expression vectors adding either a 6x His tag (Ad5 fiber knob) or both, a T7- and 6x His tag (Ad16, Ad37 fiber knob) to the N-terminus of the protein (Figure 2.1D). The recombinant proteins were expressed in *E. coli* and purified by IMAC. Initial trials with Ni-NTA agarose resin showed considerable contamination with bacterial proteins. This problem was overcome by the use of cobalt-based TALON metal affinity resin (Figure 2.1E). While nickel-based resins (Ni-NTA Agarose) are known to bind certain bacterial proteins containing exposed His residues (Kasher et al., 1993), the reduced affinity of TALON for individual His residues causes a higher specificity for proteins containing a 6x His tag, thus reducing contamination with host proteins.

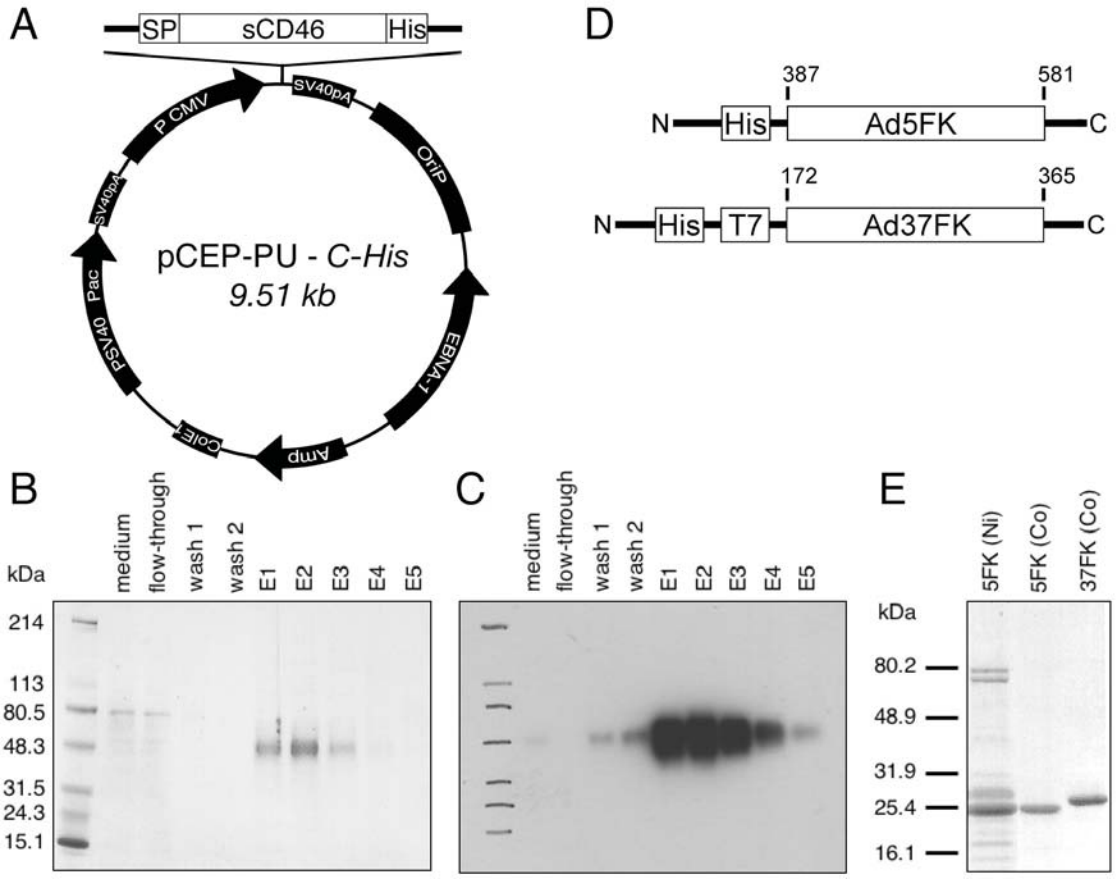

Figure 2.1. **Purification of recombinant proteins.** (A) The entire extracellular domain of the C isoform of CD46 was inserted into the pCEP-Pu-*C-His* vector that adds the signal peptide of BM-40 (SP) to the N-terminus to direct the gene product to the culture medium and a 6x His tag (His) to the C-terminus of the protein sequence. The recombinant soluble CD46 was purified from the culture medium of transfected 293EBNA cells by IMAC. Culture medium, column flow-through, wash fractions and elutions 1 to 5 were analyzed by SDS-Page (B) and anti-CD46 Western blotting (C). (D) Recombinant fiber knob constructs corresponding to residues 385-581 of the Ad5 fiber (Ad5FK) and 172-365 of the Ad37 fiber (Ad37FK) that contained an added 6x His tag or a 6x His tag and a T7 tag at their N-terminus were generated, respectively. (E) The recombinant proteins were purified from transformed *E. coli* by immobilized metal affinity chromatography (IMAC) using either Ni-NTA agarose (Ni) or TALON Metal Affinity Resin (Co). Elution fractions were analyzed by SDS-Page. Purification of the Ad16 fiber knob is shown in chapter IV.

2.3.3 Binding of sCD46 to immobilized fiber knob

Purification of the recombinant Ad5 and Ad37 fiber knobs and sCD46 enabled me to investigate binding between these proteins in an ELISA format (Figure 2.2). Ad37 fiber knob (FK37), CAR-binding Ad5 fiber knob (FK5) or BSA as negative control were immobilized in an Immulon 4 HBX assay plate. Binding of sCD46 was detected by ELISA in the presence of calcium. sCD46 showed low, albeit significant ($p<0.05$) binding to FK37, but failed to recognize FK5, as determined by comparison to nonspecific binding to BSA ($p = 0.2$). This experiment indicated that FK37 is capable of a low but specific interaction with the extracellular domain of CD46.

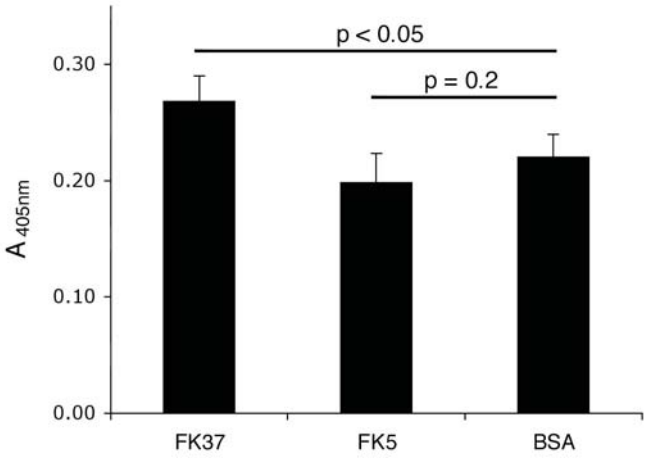

Figure 2.2. **Soluble CD46 binds to immobilized Ad37 fiber knob.** Binding of sCD46 to either Ad37 fiber knob (FK37), Ad5 fiber knob (FK5) or bovine serum albumin (BSA) immobilized on an ELISA plate was detected using a non-function blocking anti-CD46 antibody. Data represents the means and standard deviations of quadruplicates. P-values were calculated using Student's T-test.

2.3.4 Generation of a CHO cell line stably expressing CD46

In order to verify the role of CD46 in Ad37 attachment to cells, a cell line stably expressing CD46 was generated. For this purpose, I acquired a vector expressing the BCI isoform of human CD46 from K. Liszewski (Gunning et al., 1987; Liszewski et al., 1994). Further details of this vector and the different CD46 isoforms are described in chapter II. CD46-negative

CHO cells were transfected with this plasmid and subjected to several rounds of selection. Antibody staining of expressed cell surface CD46, followed by cell sorting, was used to select for clones with high expression levels. Expression of CD46 on the surface of transfected cells, but not on mock-transfected cells, was verified by antibody staining (Figure 2.3A).

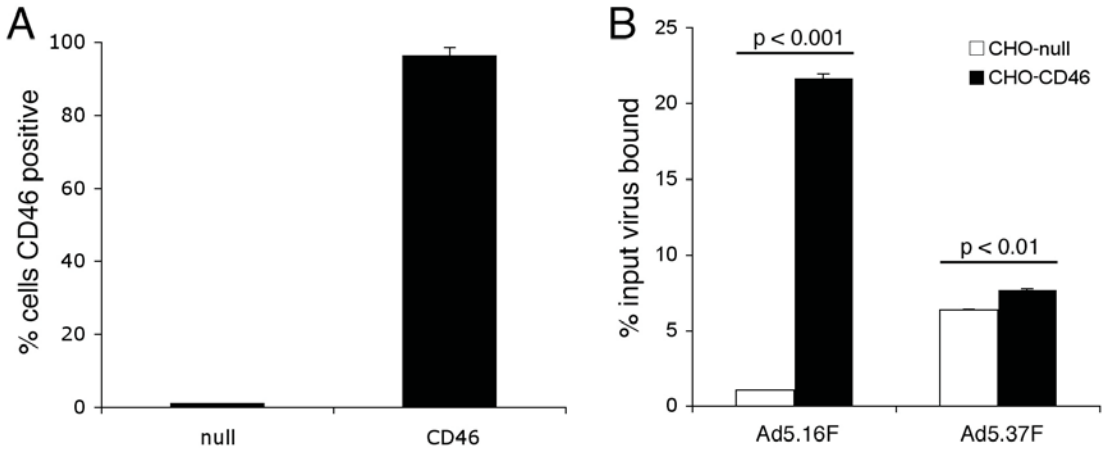

Figure 2.3. **CD46 expression enhances binding of Ad5.16F and Ad5.37F to the cell surface.** (A) CHO cells were stably transfected with the BCI isoform of CD46. CD46- (CD46) and mock-transfected cells (null) were incubated with a fluorescently conjugated anti-CD46 antibody and analyzed for receptor expression by flow cytometry. (B) CHO cells transfected with CD46 (CHO-CD46) or the empty vector (CHO-null) were incubated with radiolabeled Ad5.16F or Ad5.37F virus. After 1 h at 4ºC, cells were centrifuged through a cushion of mineral and silicone oil to separate unbound virus from the cells. Cell-bound virus was counted in a gamma counter. Data represents means and standard deviations of triplicates. Significance of results was assessed by Student's T-test.

2.3.5 Binding of Ad5.16F and Ad5.37F to CD46 expressing CHO cells

Next, I sought to compare cell attachment of an adenovirus vector carrying the Ad37 fiber protein (Ad5.37F) to that of a vector with the Ad16 fiber protein (Ad5.16F) (Figure 2.3B). The use of these Ad5-based adenoviral vectors ensures that observed differences in attachment or transduction are specific for the fiber proteins. Both viruses were radiolabeled with ^{125}I and subsequently used to analyze binding to CHO cells that stably express CD46 or to CD46-negative CHO-null cells as control. Ad5.16F showed strong

binding to CD46-expressing cells, while no efficient attachment to mock-transfected cells was observed. Expression of CD46 improved Ad5.37F binding only slightly, albeit significantly ($p<0.01$). However, Ad5.37F also showed considerable attachment to CD46-negative CHO cells, suggesting that other molecules on the cell surface besides CD46 (i.e. sialic acid) could mediate attachment.

2.3.6 Sialic acid dependence of adenovirus binding

Previous publications proposed a role of sialic acid in the attachment of Ad37 to the cell surface (Arnberg et al., 2000a; Burmeister et al., 2004). To verify that sialic acid (SA) binding is involved in Ad37 infection of host cells, I treated CD46 expressing CHO cells with different amounts of neuraminidase to remove SA moieties from cell surface glycoproteins, and infected them with either Ad5.16F or Ad5.37F (Figure 2.4A). The adenovirus vectors used in this assay carry a gene encoding green fluorescent protein (GFP), which enabled me to assess virus transduction by measuring GFP transgene expression. Surprisingly, neuraminidase treatment of CHO-CD46 cells increased Ad5.16F transduction. This effect has been observed previously for other Ad serotypes (Arnberg et al., 2000a; Bergelson et al., 1997) and is likely due to SA residues on various glycoconjugates interfering with adenovirus binding in a charge dependent way (Arcasoy et al., 1997). Removal of those charges from the cell surface by neuraminidase treatment may facilitate virus attachment. In consensus with the proposed role of SA as an attachment receptor, removal of SA from the cell surface reduced Ad5.37F infection. Next, I compared how neuraminidase treatment impacts binding of Ad5.37F to the cell surface in the presence or absence of CD46 (Figure 2.4B). Removal of SA in the absence of CD46 reduced virus binding by about 50%. This effect was clearly less pronounced in the presence of CD46, indicating that both, CD46 and SA are involved in Ad37 attachment to cells.

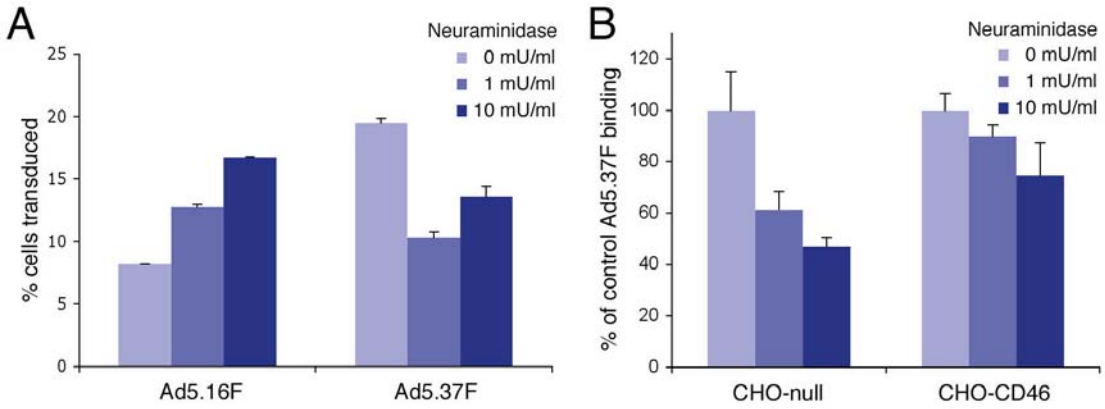

Figure 2.4. **Ad5.37F binding to CD46-positive and -negative cells is sensitive to neuraminidase treatment.** (A) CHO-CD46 cells were treated with different concentrations of neuraminidase for 30 min at 37ºC before being incubated with Ad5.16F or Ad5.37F for 1 h on ice. Cells were washed, incubated overnight at 37ºC and assayed for transgene expression by flow cytometry. (B) CHO-null or CHO-CD46 cells were incubated with the indicated concentrations of neuraminidase for 30 min at 37ºC and subsequently incubated with radiolabeled Ad5.37F for 1 h at 37ºC. Virus binding was assayed as described in Figure 2.3. Data represents means and standard deviations of triplicates.

2.3.7 Ad37 fiber knob enhances adenovirus transduction

In an effort to demonstrate that Ad37 attachment to CD46 is fiber knob dependent, infection with Ad5.16F or Ad5.37F was competed by the addition of purified fiber knobs (Figure 2.5A). CHO-CD46 cells were preincubated with the purified fiber knobs of Ad16 (FK16), Ad37 (FK37) and CAR-specific Ad5 (FK5) as control, before the addition of Ad5.16F or Ad5.37F virus. As expected, FK16 efficiently blocked infection of Ad5.16F while FK5 had no effect. Both, FK16 as well as FK5 exhibited a modest inhibitory effect on Ad5.37F. While in the case of FK16 this could be interpreted as interference with CD46 binding, the equally inhibitory effect of CAR-specific FK5 rather suggests a non-specific interaction or that Ad5.37F can, to a limited degree, recognize CAR. Remarkably, FK37 significantly increased Ad5.16F infection by about 40%. It also enhanced rather than inhibited Ad5.37F infection, albeit at a level somewhat less pronounced. The infection-enhancing effect of FK37 is an interesting observation that suggests its possible use to improve the

gene-delivery to non-permissive cells. For example transduction of $CD44^{hi}$ mouse hematopoietic stem cells (mHSC) is very inefficient by conventional Ad5-based vectors, due to the absence of CAR and human CD46 on those cells. However, the presence of recombinant FK37 increased the number of transduced cells dramatically in a dose dependent way and thus enabled efficient gene delivery (Figure 2.5B).

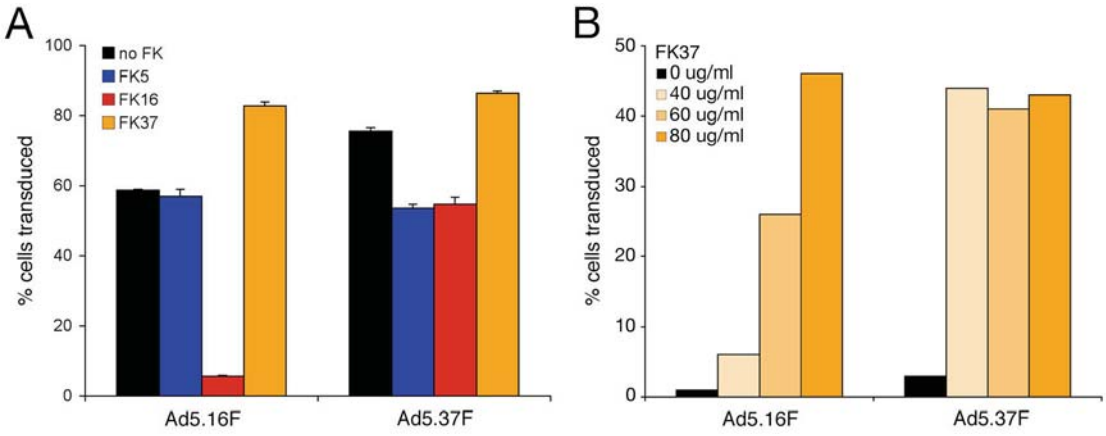

Figure 2.5. **Recombinant Ad37 fiber knob enhances Ad transduction**. (A) CHO-CD46 cells were incubated with Ad5.16F or Ad5.37F virus alone or in the presence of 30 ug/ml FK5, FK16 or FK37 for 1 h on ice. Cells were washed and incubated overnight at 37ºC. Cells were assayed for transgene expression by flow cytometry. Data represents means and standard deviations of triplicates. (B) mHSCs were incubated with Ad5.16F or Ad5.37F in the presence of varying concentrations of FK37 for 1 h on ice. Cells were washed and incubated overnight at 37ºC before being assayed for transgene expression by flow cytometry.

We were able to demonstrate that FK37 attaches to the capsid of virions in a charge-dependent manner. For this purpose, Ad5.5F virions were incubated with FK37 in the presence of increasing NaCl concentrations and subsequently separated from unbound fiber knobs by centrifugation through a density cushion (Figure 2.6A). Salt concentrations in excess of 200 mM blocked the attachment of FK37 to virions. The treatment of cells with neuraminidase dramatically reduced the transduction-enhancing effect of FK37 on Ad5.5F virus, indicating a role of cell-surface sialic acid. The CD46-specific transduction by Ad5.16F in the absence of FK37 was not negatively

affected (Figure 2.6B) by neuraminidase treatment. These results suggest that the FK37 acts as a bridge between the virus capsid and cell-associated sialic acid glycoconjugates, mediating indirect attachment of virions to the cell surface.

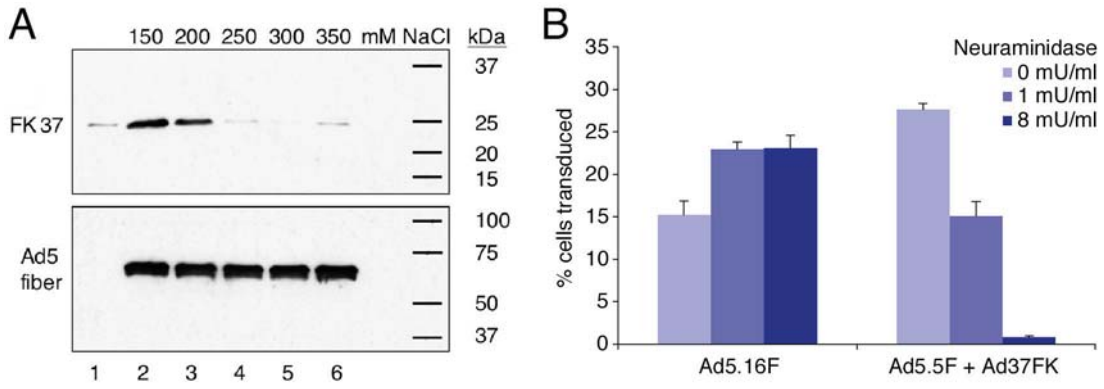

Figure 2.6. **Ad37 fiber knob binds to the virus capsid in a charge dependent manner and mediates transduction in a sialic acid-dependent way.** (A) FK37 was mixed with Ad5.5F in the presence of increasing amounts of NaCl (lanes 2 to 6), incubated for 1 h on ice and subsequently ultra centrifuged through 40% Histodenz onto an 80% Histodenz cushion. Samples from the interface were analyzed by Western blot with an anti-T7 tag antibody that detects the recombinant FK37 (upper panel). The blot was then stripped and reprobed with the monoclonal 4D2 anti-Ad5 fiber antibody to verify equal loading (lower panel). Lane 1 was loaded with 37FK alone as a control. (B) U-937 cells were treated with different concentrations of neuraminidase at 37ºC. After 30 min, cells were incubated for 1 h on ice in the presence of either Ad5.16F as control or Ad5.5F and FK37. Cells were washed, incubated overnight and assayed for transgene expression by flow cytometry. Data represents means and standard deviations of triplicates.

2.4 Discussion

Recombinant forms of soluble CD46 (sCD46) and the fiber knob domains of different adenoviruses were successfully expressed and purified. Measuring direct binding of sCD46 to immobilized Ad37 fiber knob (FK37) showed a significant, albeit low interaction in solution. The generation of a cell line stably expressing CD46 enabled me to compare the CD46-specificity of cell attachment of Ad5.37F, an adenoviral vector carrying the species D Ad37 fiber protein, to that of a vector displaying the fiber protein of Ad16 (Ad5.16F), a member of species B. These experiments indicated that the attachment of Ad16 depends to a much higher level on the expression of cell surface CD46 than Ad37 attachment. Further experiments addressed the suggested role of sialic acid as receptor for Ad37. Inhibition of cell transduction occurred when sialic acid residues were removed from the cell surface by neuraminidase treatment. A vector with species B Ad16 fiber, by contrast, was not negatively affected. While incubation of CD46-negative CHO cells with neuraminidase lowered Ad5.37F binding considerably, the inhibiting effect of neuraminidase treatment appeared to be reduced in the presence of cell surface CD46. Together my results suggest that besides sialic acid, CD46 does play a role in mediating Ad37 attachment to the cell surface.

While an interaction of Ad37 with CD46 could be demonstrated, the comparably low dependence of virus attachment on CD46 expression suggests that this protein might not necessarily be a critical primary attachment receptor for Ad37. However, the Ad37-CD46 interaction might have additional consequences besides infection. There is considerable evidence that engagement of CD46 by pathogens may downregulate parts of the innate immune response. Measles virus as well as human herpes virus 6, both of them CD46-tropic, have been shown to suppress production of the cytokine interleukin-12 in human monocytes upon infection (Karp et al., 1996; A. Smith et al., 2003a). Iacobelli-Martinez and colleagues (Iacobelli-Martinez et al., 2005) demonstrated that Ad37 as well as CD46-utilizing species B

members Ad16 and -35 reduced production of IL-12 and other proinflammatory cytokines in human peripheral blood mononuclear cells. This is likely due to an interference with interferon gamma (IFN-γ) signaling events and subsequent blocking of the expression of the C/EBPβ transcription factor that is responsible for the gene transcription of numerous proinflammatory cytokines. This down regulation of IFN-γ-related cytokine production was only triggered by vectors carrying CD46-binding fibers, not by CAR-utilizing Ads. In a second study it was shown that Ad37 and species B viruses, unlike CAR-tropic Ads, induce activation of Toll-like receptor nine (TLR9). Activation of TLR9 by CD46-binding adenoviruses results in type I interferon (IFN-1) production and subsequent expression of IFN-1-dependent cytokines (Iacobelli-Martinez and Nemerow, 2007). Importantly, this effect on regulation of the innate immune response was preferentially caused by viruses that interact with CD46, Ad37 and species B viruses.

In addition to CD46, sialic acid has been proposed as a receptor for Ad37 (Arnberg et al., 2000a). A crystal structure of the Ad37 fiber knob in complex with sialyl lactose provides further insight into this interaction and the potential role of sialic acid (SA) in Ad attachment (Burmeister et al., 2004). The binding site for SA is located on the top surface of the positively charged fiber knob, which is able to bind three SA molecules due to its trimeric organization (Figure 2.7). With few exceptions (potentially Ad15), this binding site appears to be conserved among species D viruses. Contrary to earlier reports (Arnberg et al., 2000a) this site can bind α(2,3)- as well as α(2,6)-linked sialyl-lactose (Burmeister et al., 2004). The equilibrium dissociation constant (K_D) of sialyl-lactose binding to the Ad37 fiber knob was estimated to be 5 mM, which is a range not unusual for binding of SA to other proteins (Dormitzer et al., 2002; Sauter et al., 1989). However, it remains unclear how this site can mediate the high-affinity binding observed for Ad37 virions (Arnberg et al., 2002; Huang et al., 1999). Potentially, multiple contacts between virus and cell surface sialic acid glycoconjugates could result in

strong avidity effects. Influenza virus attachment for example depends exclusively on viral hemagglutinin binding to SA despite a K_D of ~3 mM for the individual binding site (Sauter et al., 1989). Alternatively, recognition of a separate protein molecule simultaneous with or independent of SA binding might be required for efficient attachment. This is supported by studies involving protease treatment of cells that implicate a protein component in Ad37 attachment (Cashman et al., 2004).

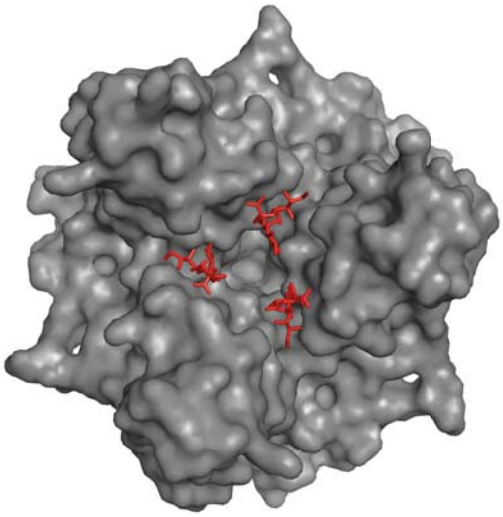

Figure 2.7. **The Ad37 fiber knob trimer has three binding sites for sialic acid.** Top view of the Ad37 fiber knob trimer (gray) with three sialyl lactose molecules (red) bound close to the threefold axis. While the sialic acid residues make contact with the fiber knob, the galactose residues of the sialyl lactose are pointed away from the binding site, thus allowing sialic acid binding independently of attached residues. Figure is based on the structure of the Ad37 fiber knob in complex with sialyl lactose (PDB-ID 1UXA).

The remarkably high positive charge of Ad37 fiber knob with a calculated isoelectric point of ~9.4 (Nepomuceno et al., 2007) makes it likely that charge-dependent interactions play a role in the binding of the negatively charged SA (Arnberg et al., 2002; Burmeister et al., 2004). This highly positive charge also plays a role in the enhanced transduction observed in our studies involving FK37, likely causing binding of the positively charged

recombinant soluble Ad37 fiber knob to the negatively charged hexon proteins (Q. G. Li et al., 1997) of the virus capsid (Figure 2.8). We could demonstrate that FK37 likely acts as a bridge by binding to the virus in a charge dependent manner and subsequently mediating virus attachment to the cell by interaction with sialic acid glycoconjugates on the cell surface. The observed improvement in gene-delivery by FK37-Ad complexes was especially remarkable in human myeloid cells and mouse haematopoietic stem cells. These cell types are refractory to infection by the commonly used Ad5-based vectors.

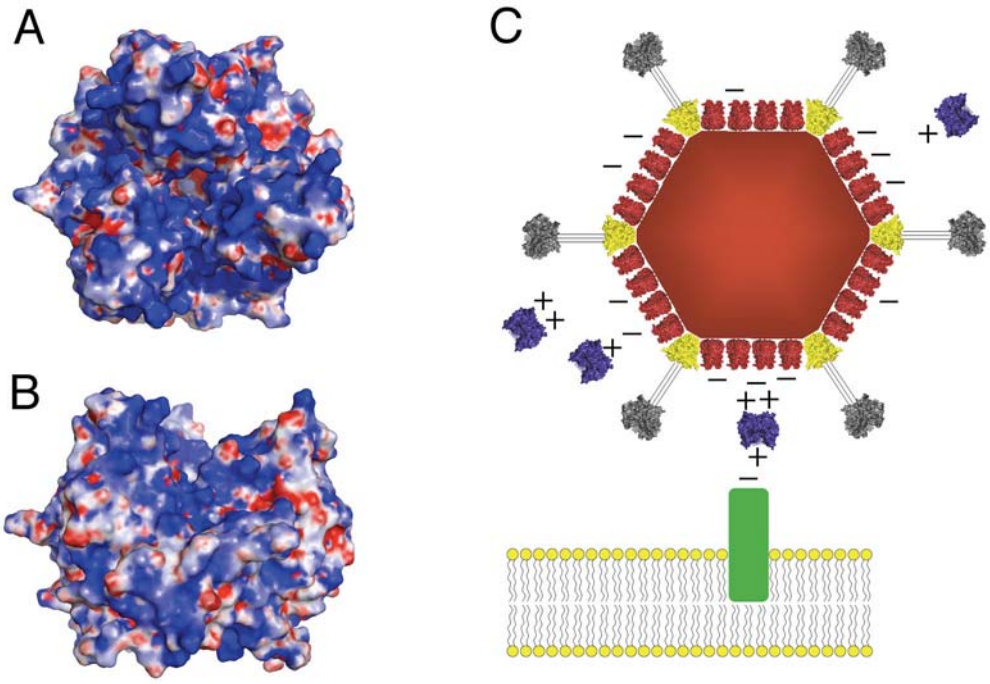

Figure 2.8. **The positively charged Ad37 likely acts as a bridge between the virus capsid and sialic acid molecules on the cell surface.**
(A, B) A map of the electrostatic surface potential of the Ad 37 fiber knob was calculated from the published Ad37 fiber knob structure (PDB-ID 1UXE). Figure shows the top (A) and side (B) of the fiber knob domain. Coloring indicates electrostatic surface potential from +10 kT (blue) to -10 kT (red). (C) Model of the Ad37 fiber knob acting as a bridge between the virus capsid and cell surface molecules. The positively charged FK37 (blue) likely attaches to the negatively charged hexon molecules (red) of the virus capsid and mediates attachment to sialic acid glycoconjugates (green) on the cell surface.

The mechanism of FK37 facilitating virus-cell binding may also play a role in normal infection of Ad37. Excess fiber protein expressed in the cell during viral replication could interact with the capsids of newly synthesized virions (Ad37 hexon has the same negative charge as Ad5 hexon) and cause additional avidity effects strengthening attachment to cell surface sialic acid glycoconjugates.

In conclusion, the relatively weak dependence of Ad37 attachment on CD46 expression and the unresolved role of sialic acid glycoconjugates in virus transduction indicated that Ad37 exhibits a complicated set of interactions with multiple cell molecules and thus might not be an optimal candidate to further study the detailed interactions of adenovirus attachment to CD46. Encouraged by the strong and highly CD46-dependent attachment of Ad5.16F, I chose to investigate the molecular basis of species B Ads binding to CD46.

3. Chapter II:
Identification of the binding site for species B adenoviruses on CD46

3.1 Introduction

CD46, an integral membrane protein, can be expressed in multiple isoforms that are derived from a single gene by alternative splicing. However, only four of these isoforms are commonly expressed in human cells. All isoforms of CD46 share an identical amino-terminus consisting of four short consensus repeats (SCRs), also referred to as complement control protein modules (Figure 3.1). SCRs 1, 2 and 4 each have a single N-linked carbohydrate moiety. The SCR domains are followed by a region rich in serines, threonines and prolines (STP region) that are heavily O-glycosylated. The STP region that is derived from three exons, designated A, B and C, is subject to alternative splicing. The major isoforms contain either C alone or B and C together. The STP region is followed by a 12 amino acid sequence of unknown function and the hydrophobic transmembrane domain. The carboxy-terminus consists of an alternatively spliced cytoplasmic tail (CYT) with a length of either 16 (CYT-1) or 23 amino acids (CYT-2). Based on the splicing of the STP region and the cytoplasmic tail the major isoforms of CD46 are termed BC1, BC2, C1 and C2. The relative expression levels of CD46 isoforms are genetically controlled and inherited, with three phenotypes identified in the population (Riley-Vargas et al., 2004). While most cells express CD46 isoforms in a phenotype-specific pattern, a predominance of specific isoforms has been noted for certain tissues. For example, the BC isoforms are preferentially expressed in the kidneys while brain cells express only the C isoforms (Johnstone et al., 1993).

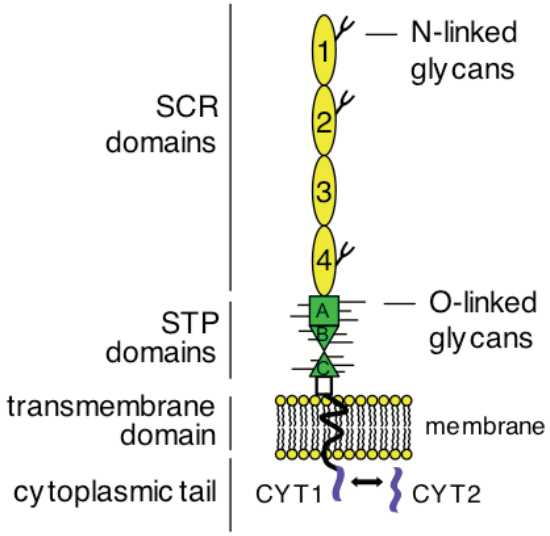

Figure 3.1. **Diagram of the CD46 structure.** The N-terminus of CD46 consists of four short consensus repeats (SCR) (yellow). SCRs 1, 2 and 4 carry one N-linked glycan each. The SCR domains are followed by an alternatively spliced serine, threonine and proline rich region (STP) that is heavily O-glycosylated (green). Next is a short sequence of unknown function (white) that connects to the hydrophobic transmembrane domain (black) and an alternatively spliced cytoplasmic domain (blue), the 16 amino acid CYT-1 or the 23 amino acid CYT-2.

The cytoplasmic tail domains both contain putative signaling motifs that trigger cell signalling events upon crosslinking of CD46 molecules. The different sequence characteristics of CYT-1 and CYT-2 suggest distinct interactions with signaling complexes (S. Russell, 2004). This is supported by a report that provided evidence for different signaling outcomes depending on the tail domain (Marie et al., 2002). Further, the two non-homologous cytoplasmic tails seem to be responsible for differential processing of CD46 preprotein to the mature forms (Liszewski et al., 1994). These tail-specific signaling effects could indicate a regulatory mechanism that is controlled by variations in the ratio of CD46 isoforms. However, nearly all cells express both, CYT-1 as well as CYT-2, making it unlikely that this regulation takes place at a cellular level (Post et al., 1991; S. M. Russell et al., 1992). More likely is a regulation by selective recruitment of isoforms to different signaling complexes (S. Russell, 2004). Despite these findings, the roles of the cytoplasmic tails in signaling are still poorly understood. Little is known about the impact of alternative splicing of the STP regions as well, though sporadic

reports indicate that the BC isoforms cleaves cell-bound complement component C4b with higher efficiency than the C isoforms, thus offering enhanced protection against activation of the classic complement pathway (Liszewski and Atkinson, 1996).

The binding site for complement component C3b has been located in SCRs 3 and 4 of CD46 while the site for C4b consists of SCRs 2, 3 and 4, suggesting that SCR1 is dispensable for complement regulation (Adams et al., 1991). Interestingly, certain cell types of New World monkeys express a form of CD46 that is lacking this domain and yet have a functionally intact complement activation system (E. C. Hsu et al., 1997). The deletion of SCR1 could have an evolutionary implication with regards to avoiding infectious pathogens that might depend on this domain for efficient attachment. For example the measles virus (Edmonston strain) binding site was located stretched along SCRs 1 and 2 in various studies employing antibody competition, mutagenesis and chimeric receptor constructs, as well as peptide mapping (reviewed in Manchester et al., 2000). Absence of SCR1 would prevent efficient attachment of the virus and inhibit infection. The binding sites of CD46-binding pathogens are diverse, though most contact regions are located within the SCR domains. Human herpesvirus 6, for example, binds to a site located in SCRs 2 and 3 (Greenstone et al., 2002), while *Neisseria gonorrhoeae, Neisseria meningitidis* and *Streptococcus pyogenes* attach to SCRs 3 and 4 (Giannakis et al., 2002; Källström et al., 2001).

I used a panel of cell lines expressing different CD46 isoforms to examine whether each of the CD46 isoforms were capable of mediating adenovirus infection. My findings suggested an interaction of the adenovirus fiber knob with the conserved SCR domains of CD46 rather than the alternatively spliced STP region. Identification of a function blocking antibody and transduction studies with chimeric CD46 constructs allowed me to more precisely locate the species B adenovirus binding site within SCRs 1 and 2 of CD46. Selection and maintenance of transfected cell lines and flow cytometry cell sorting were performed with the help of Tina-Marie Mullen.

3.2 Material and methods

Cells and viruses

CHO-K1 cells were maintained in F-12 medium supplemented with 10% fetal calf serum (FCS) (Omega Scientific, Tarzana, CA), 10 mM HEPES pH 7.55, 4 mM L-glutamine, 1 mM sodium pyruvate, 0.1 mM nonessential amino acids, 100 units/ml penicillin and 100 μg/ml streptomycin. Transfected CHO cells were maintained in F-12 supplemented as above, with the addition of 0.5 mg/ml G418 sulfate (pHβ-Apr1.neo and pSFFV.neo based plasmids) or 0.4 mg/ml Zeocin (pcDNA3.1-Zeo+ based plasmids). All tissue culture reagents were obtained from Invitrogen (Carlsbad, CA) unless noted otherwise. An Ad5 vector expressing the fiber protein of Ad16 (Ad5.16F) (C. Hsu et al., 2005) was described in chapter I.

Receptor constructs

Plasmids based on the pHβ-APR1.neo vector (Gunning et al., 1987) that express the CD46 isoforms C1, C2 or BC1 under the control of the β-actin promoter were obtained from Kathryn Liszewski (Liszewski et al., 1994). To generate a construct encoding to the BC2 isoform of CD46, a DNA sequence corresponding to SCRs 1 to 4 and the STP domains B and C was amplified from the previously described CD46-BC1 plasmid by PCR, using the primers BC2-1 5'-GAGTGCAAGCTTGCCACCATGGAGCCTCCCGGC CGCCG-3' (HindIII site underlined) and BC2-2 5'-TCCTCCTTTGAAGATA TCTGTACGGGACAACACAA-3'. Further, a DNA sequence corresponding to the domain of unknown significance, the transmembrane domain and the cytoplasmic domain 2 of CD46 was amplified from the CD46-C2 plasmid using the primers BC2-3 5'-CCTACTTACAAGCCTCCAGTCTCAAATT ATCCAGG-3' and BC2-4 5'-CCCGGGAAGCTTACTCACTCAGCCTCTCT GCTCTGCTG-3' (HindIII site underlined). A subsequent PCR, using the gel-purified products of both previous PCRs as template and the primers BC2-1

and BC2-4, generated a cDNA fragment encoding the CD46-BC2 isoform, framed by HindIII restriction sites. All PCRs were performed using Taq polymerase (Invitrogen). The fragment was digested with the restriction enzyme HindIII and ligated into the HindIII site of pHβ-APR1.neo vector (Gunning et al., 1987) that places expression under the control of the β-actin promoter. Additionally, the insert was also ligated into the pcDNA3.1-Zeo+ vector (Invitrogen), placing expression under the control of the CMV promoter. The correct orientation of the insert and correctness of the sequence was verified by DNA sequencing. Expression plasmids encoding the receptor decay acceleration factor (DAF, CD55) or the chimeric receptors DM1 and DM12 were obtained from Marianne Manchester (Manchester et al., 1995) and are based on the pSFFV.neo vector that contains the SFFV-LTR promoter.

Generation of CD46-expressing cell lines

CHO-K1 cells were transfected with the expression plasmids described above using the FuGENE 6 transfection reagent (Roche, Indianapolis, IN) according to the manufacturer's instructions. Individual clones were selected over 4 weeks for stable expression with either 500 μg/ml G418 (Invitrogen, Carlsbad, CA) for the vectors pHβ-Apr1.neo and pSFFV.neo or 500 μg/ml Zeocin (Invitrogen) for the vector pcDNA3.1-Zeo+. To obtain higher and more uniform expression of the different CD46 isoforms, cells were subject to several rounds of staining with the anti-CD46 antibody H-294 (Santa Cruz Biotechnology) and a PE-conjugated goat anti-rabbit secondary antibody and subsequent sorting for equally high CD46 expression by FACS. To verify equal expression levels of the receptor DAF and the chimeric receptors DM1 and DM12, cells were stained with either the the anti-DAF antibody I-19 or the anti-CD46 antibody N-19 that recognizes SCR1 of CD46 present in DM1 and DM12 (Santa Cruz Biotechnology, Santa Cruz, CA) and a PE-conjugated rabbit anti-goat secondary antibody prior to being analyzed by FACS.

Virus transduction assays

$5x10^4$ cells/well of CHO cells stably expressing an isoform of CD46, CD55 or a chimeric receptor were cultured in 24-well tissue culture plates in complete F-12 medium. The cells were washed once with serum-free F-12 medium prior to the addition of $5x10^7$ Ad5.16F virions in 250 μl serum-free medium. Following a 1 hour incubation at 4°C, the cells were washed three times with fresh medium and incubated for 16-20 hours at 37°C in F-12 medium containing FCS. To analyze GFP expression of transduced cells, 10,000 cells were acquired by flow cytometry on a FACScan flow cytometer and fluorescence was analyzed using CellQuest software (BD Biosciences, Billerica, MA).

Antibody competition experiments

50,000 CHO-CD46 (BC1) cells/well were cultured in a 24-well tissue culture plate. Cells were washed with serum-free F-12 medium and incubated in the presence of serum-free medium alone or 40 μg/ml of an antibody directed against the N-terminal 19 amino acids of either CD46 (N-19, Santa Cruz) or CD55 (I-19, Santa Cruz Biotechnologies) diluted in serum-free medium in a total volume of 270 μl. After 1 hour at room temperature, 30 μl of serum-free medium, containing $8.3x10^6$ Ad5.16F virions was added to the cells and incubated for an hour at 37°C. The cells were washed three times and incubated for 16-20 hours in F-12 medium containing FCS, before being analyzed for GFP transgene expression by FACS as described above.

3.3 Results

3.3.1 Expression of different CD46 isoforms

Four CD46 isoforms are commonly observed on the surface of human cells. To perform comparative studies of Ad binding to different CD46 isoforms, expression vectors containing the BC1, C1 and C2 isoforms were obtained from Kathryn Liszewski (Liszewski et al., 1994) and a vector containing the BC2 isoform was generated in our laboratory (Figure 3.2A). All CD46 constructs were cloned into the pHβApr1.neo expression vector (Gunning et al., 1987) that allows protein expression under the control of the β-actin promoter. Since expression levels of the BC2 isoform were observed to be very low, a new construct based on the expression vector pcDNA3.1-Zeo+ was generated that placed expression of the BC2 isoform under the control of the CMV promoter. After initial transfection and selection, expression levels of the different CD46 isoforms were observed to be vastly different. Therefore, several rounds of receptor selection by flow cytometry cell sorting were performed to achieve high and more uniform CD46 expression as assessed by staining with an anti-CD46 antibody and subsequent analysis by flow cytometry. Ubiquitous expression of CD46 in the cell lines was verified by immunostaining (Figure 3.2B). The cells were found to be almost uniformly CD46 positive. However, despite repeated efforts to maintain equal levels of expression, the BC2 isoform was found on the cell surface at slightly diminished levels.

3.3.2 Adenovirus uses all four isoforms of CD46 with similar efficiency

To determine which of the four isoforms were capable of mediating adenovirus infection, I analyzed transduction of an Ad5 vector carrying the fiber protein of Ad16 (Ad5.16F) (Figure 3.2C). The cells were incubated with virus for 1 hour, then washed and analyzed the next day for expression of the GFP transgene encoded by the Ad vector. A mock-transfected cell line served

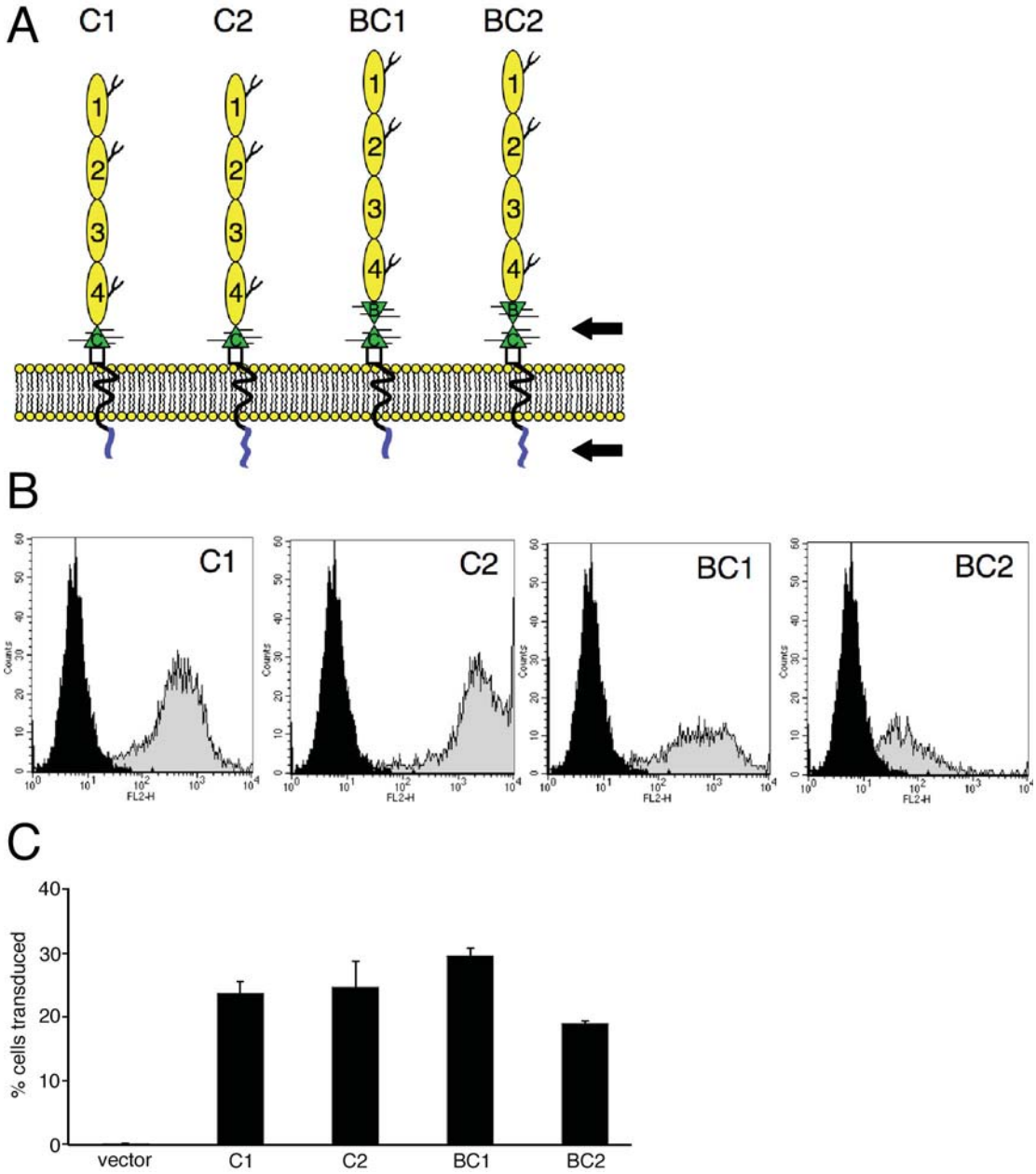

Figure 3.2. **All four CD46 isoforms commonly expressed by human cells can mediate adenovirus infection.** (A) The four isoforms commonly expressed on human cells. Alternative splicing (indicated by arrow) results in either the STP domain C expressed alone or together with domain B (green). Both versions are expressed with either splicing variant of the cytoplasmic tail domain (blue). (B) Stably transfected cells expressing individual isoforms of CD46 were stained with an anti-CD46 antibody and analyzed for CD46 expression by flow cytometry (grey). Mock-transfected cells lacking CD46 are shown as control (black). (C) CD46 expressing cell lines were incubated with Ad5.16F virus for 1 hour at 4°C before being washed with fresh medium and analyzed for transgene expression 16-20 hours post infection by flow cytometry. Data represents means and standard deviations of triplicates.

as negative control in these experiments to verify the CD46-specificity of the infection. While no significant infection was observed in the absence of CD46, all four isoforms supported transduction at similar levels. A slightly decreased level of transduction was observed in cells expressing the BC2 isoform. I attributed this to a decreased receptor expression level of this isoform that was observed in multiple experiments.

3.3.3 Antibody directed against the N-terminus of CD46 blocks species B adenovirus transduction

To verify the role of CD46 in species B adenovirus transduction, I performed competition experiments using an anti-CD46 antibody. These studies showed that Ad5.16F transduction of CD46-expressing CHO cells could be efficiently blocked by an anti-CD46 antibody while an anti-DAF antibody, used as a control, did not inhibit transduction significantly (Figure 3.3). The epitope of the function-blocking anti-CD46 antibody is located in the N-terminal 19 amino acids of the protein, a site within the SCR1 domain of CD46. This suggested that the adenovirus-binding site on CD46 comprises the most membrane-distal domain of this protein. This location is similar to that of measles virus rather than that of most other pathogens or the natural ligands of CD46, the complement components C3b and C4b.

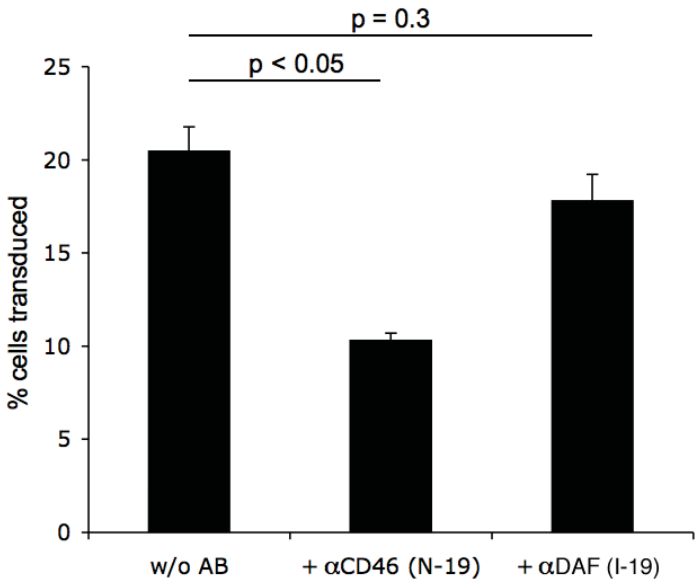

Figure 3.3. **An antibody specific for the N-terminus of CD46 significantly inhibited Ad5.16F transduction.** CD46 expressing CHO-BC1 cells were preincubated with 40 μg/ml of an antibody directed against the N-terminal 19 amino acids of either CD46 or DAF, or with buffer as control, for 30 minutes at 37 °C. Ad5.16F virions were addend to the cells and incubated for 1 hour on ice. The cells were washed and analyzed for expression of the GFP transgene by flow cytometry. Data represents means and standard deviations of triplicates. P-values were determined by Student's T-test.

3.3.4 Generation of cell lines expressing chimeric CD46 receptors

Like CD46, decay acceleration factor (DAF, CD55) belongs to the family of regulators of complement activation (RCA) (Lublin and Atkinson, 1989). It is structurally very similar to CD46, with four amino-terminal SCR domains and an STP domain (Lukacik et al., 2004). However, DAF has a glycosyl-phosphatidylinositol membrane anchor instead of the transmembrane domain of CD46. Despite its structural similarity, DAF does not function as receptor for ligands of CD46 such as measles virus, adenovirus or human herpesvirus 6. However, it can bind different pathogens including echovirus and coxsackie virus (Spiller et al., 2000). To gain further insight into the precise location of the adenovirus-binding site, I acquired chimeric constructs composed of CD46 and DAF domains from Marianne Manchester (Figure 3.4A). These constructs are based on DAF but have either SCR1 alone (DM1) or SCRs 1 and 2 (DM12) swapped for the

corresponding SCRs of CD46 (Manchester et al., 1995). CHO cells were transfected with individual constructs and selected for stable expression. The previously used CD46-C1 cell line served as a positive control and a cell line stably expressing DAF was generated as a negative control. DAF, DM1 and DM12 are expressed by the pSFFV.neo vector that contains the SFFV-LTR promoter (Fuhlbrigge et al., 1988). Cells were analyzed for receptor expression by immunostaining with an antibody specific for the N-terminal 19 amino acids of either CD46 or DAF (Figure 3.4B). However, the detected expression levels of DM12 were lower, to a certain degree, than those of the other constructs.

3.3.5 The binding site for species B adenoviruses is composed of SCRs 1 and 2

The generated cell lines expressing the chimeric receptors were assayed for Ad5.16F transduction by measuring GFP transgene expression (Figure 3.4C). DAF expressing cells showed a low level of infection when compared to mock-transfected CHO cells. However, this effect was less pronounced in repeated experiments. Transduction of cells expressing the DM1 construct did not exceed the levels of CD46-negative mock-transfected cells. Cells expressing the DM12 construct, by contrast, showed substantial transduction, close to that of cells expressing CD46. The remaining difference might be due to lower expression levels of the DM12 construct compared to those of CD46. These results indicate that SCR domains 1 and 2 of CD46 are necessary and sufficient for species B Ad binding. Since the chimeric constructs based on DAF are missing the transmembrane domain of CD46 as well as the cytoplasmic domain, this data further suggests that CD46 serves solely as receptor for adenovirus infection and likely does not require CD46-mediated signaling events. If signaling events transmitted by the cytoplasmic domain of CD46 were critical for infection, I would have expected a lack of efficient virus transduction of cells expressing the GPI-anchor linked DM12 receptor.

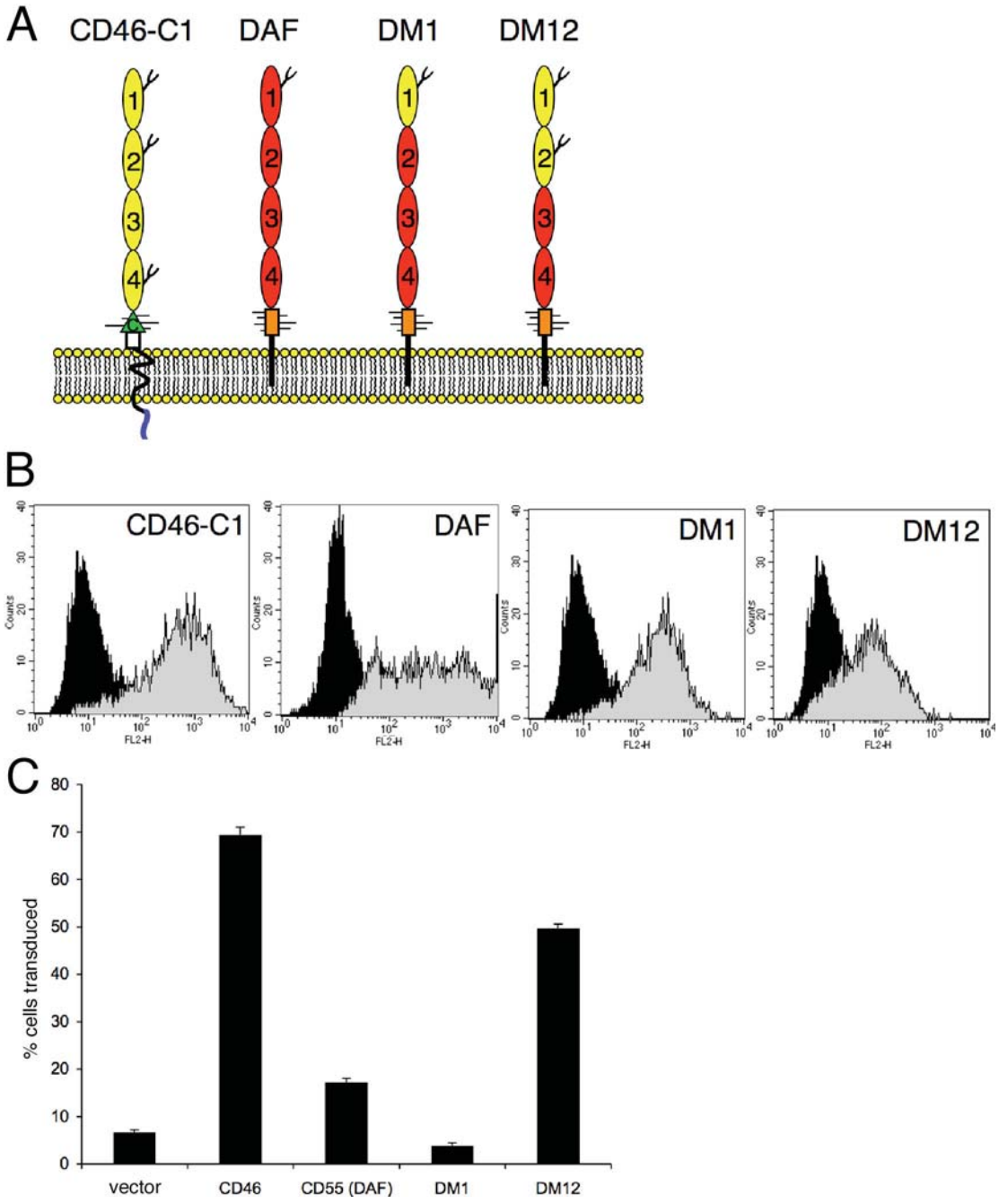

Figure 3.4. **CD46 SCRs 1 and 2 are necessary and sufficient for species B Ad transduction.** (A) CD46-C1, DAF and two chimeric receptors based on DAF with either SCR1 alone or SCR1 and 2 of DAF (red) replaced by the corresponding domains of CD46 (yellow). (B) Stably transfected cells were stained with an antibody against the N-terminal 19 amino acids of either CD46 (CD46-C1, DM1, DM12) or DAF (DAF) and analyzed for receptor expression by flow cytometry (grey). Mock-transfected cells lacking the receptor are shown as control (black). (C) Cells were incubated with Ad5.16F virus for 1 hour at 4°C before being washed with fresh medium and analyzed for transgene expression 16-20 hours post infection by flow cytometry. Data represents means and standard deviations of triplicates.

3.4 Discussion

To analyze the usage of specific CD46 isoforms by adenovirus, I generated CHO-based cell lines expressing the four common isoforms of this receptor. However, a loss of CD46-BC2 expression in transfected cells over time was observed despite evaluation of two different expression vectors and selection of stably expressing cells. Resequencing of the vector confirmed that the BC2 expression construct corresponded to that of the other vectors used. This situation of unstable BC2 expression has been described by other groups (Segerman et al., 2003b) and could be related to downregulation due to isoform-specific signaling effects of the receptor. I attempted to overcome this problem by specifically selecting cells with high expression levels by flow cytometry cell sorting. This allowed adequate expression of BC2 cells for up to two weeks.

The selected cells enabled me to investigate the impact of these isoforms on adenovirus infection with a vector carrying the species B fiber protein of Ad16 (Ad5.16F). I chose to perform these studies by analyzing transgene expression rather than virus binding to ensure that potential isoform-specific effects on later stages of infection would not be missed. My studies indicated that all isoforms promote virus transduction at comparable levels. The mild decrease of transduction observed in cells expressing CD46-BC2 is likely caused by the lower expression levels of this isoform. My results are supported by a separate study that addressed differences in isoform-specific CD46-usage by species B adenovirus (Gaggar et al., 2003). Although this study found isoform-specific differences in transduction levels, these differences correlated with the expression levels of the respective CD46 isoforms.

In stark contrast, piliated *Neisseria gonorrhoeae* has been shown to preferentially adhere to CHO cells expressing the BC- but not the C-isoforms

(Källström et al., 1997). This is due to the location of the binding site for the *N. gonorrhoeae* pilus that has been shown to comprise SCRs 3 and 4 and likely the STP region of CD46 (Källström et al., 2001). The isoform-independent CD46-usage of adenovirus could be an indication that the Ad binding region of CD46 is located in a more membrane-distal domain. However, the first published study to attempt locating the species B adenovirus binding site of CD46 relied on antibody competition assays to assign the contact region for Ad11 to the membrane-proximal SCR domains (SCRs 3 and 4) of CD46 (Segerman et al., 2003b). Subsequent studies used a panel of anti-CD46 antibodies to compete Ad3 infection with inconclusive results (Sirena et al., 2004), though it is still a matter of discussion whether Ad3 actually binds to CD46, an issue that will be discussed in a chapter IV. I made the observation that an antibody specific for the amino-terminal 19 amino acids of CD46 could efficiently inhibit CD46-mediated infection, suggesting that the binding site for the Ad16 fiber knob comprises this membrane distal domain. A more precise localization of the binding site was made possible by the expression of chimeric CD46/DAF receptor constructs. In virus transduction experiments, I was able to demonstrate that the membrane-distal SCRs 1 and 2 of CD46 are required to promote species B Ad infection. This suggests a binding region similar to that of measles virus (Figure 3.5) and also matches the scheme of pathogen binding sites on RCA family proteins generally consisting of at least two consecutive SCR domains (Riley-Vargas et al., 2004).

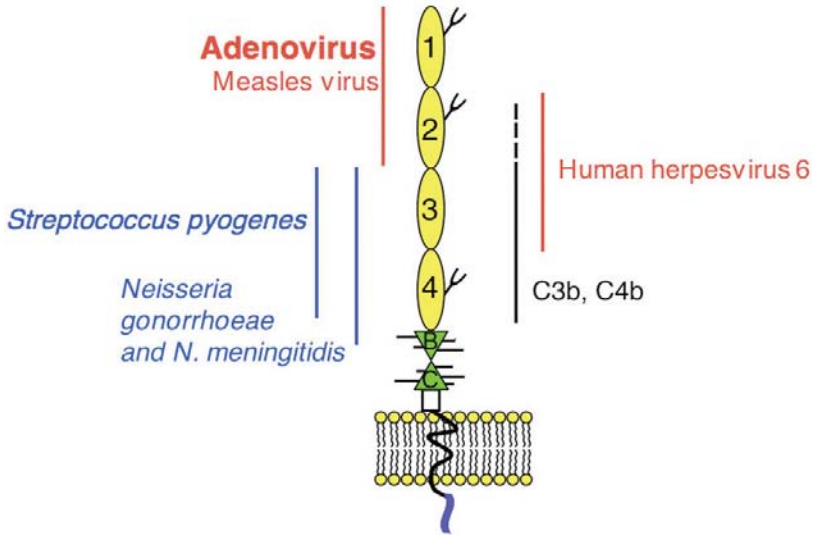

Figure 3.5. **Binding sites of different pathogens on CD46.**
The approximate locations of the binding sites for viral (red) and bacterial (blue) pathogens on CD46 are shown in the diagram. The binding site for species B adenovirus maps to SCRs 1 and 2, similar to that of measles virus. The binding sites for the natural CD46 ligands C3b and C4b are located in SCRs 3 to 4 and 2 to 4, respectively (black).

Later studies employed competition experiments as well as infection assays with hybrid receptors and mutated CD46-constructs to map the adenovirus binding site more precisely (Fleischli et al., 2005; Gaggar et al., 2005; Sakurai et al., 2006). While these studies consistently indicated a critical importance of SCRs 1 and 2 for Ad binding, the precise locations of the assigned binding sites in CD46 differed considerably. Two of these studies further demonstrated that the N-linked glycans on the membrane-distal domains of CD46 did not critically contribute to attachment of species B Ads (Fleischli et al., 2005; Gaggar et al., 2005). This is in agreement with my earlier results, showing an increase rather than decrease in Ad5.16F infection upon removal of sialic acid moieties by neuraminidase treatment. The N-linked glycans appear to be of more critical importance for the infection of measles virus (E. C. Hsu et al., 1997; Maisner et al., 1996) or *N. gonorrhoeae* (Källström et al., 2001).

An interesting observation made in Ad transduction studies of hybrid CD46 constructs was that efficient engagement of the receptor depends on an appropriate distance of the binding domain from the cell surface, likely because of steric constraints (Fleischli et al., 2005). We described a similar role for length in the attachment of CAR-tropic Ads to the cell surface. Our studies indicated that a certain length of the Ad fiber shaft in CAR-binding adenoviruses – in addition to its flexibility – was required to mediate efficient virus transduction and avoid steric hindrance upon binding to the cell-surface receptor (Wu et al., 2003). The finding that all CD46 isoforms support virus transduction, including chimeric receptors that are linked to a GPI-anchor, suggests that CD46-related signaling events are likely not required for efficient Ad infection. Given the fact that integrin-binding is still needed for efficient cell entry of CD46-tropic adenoviruses (Murakami et al., 2007; Shayakhmetov et al., 2005a), the role of CD46 is likely that of a primary attachment receptor, similar to CAR.

In conclusion, I was able to demonstrate that all four common isoforms of CD46 are able to mediate infection of a species B adenovirus, likely at comparable levels. Contrary to the findings of a previous study (Segerman et al., 2003b), an antibody competition experiment indicated involvement of the membrane-distal CD46 domain in virus interaction. Further studies using chimeric CD46/DAF constructs allowed me to locate the binding site more precisely by demonstrating that SCRs 1 and 2 are necessary and sufficient for efficient virus transduction.

4. Chapter III:
Conservation of CD46 binding among species B2 adenoviruses

4.1 Introduction

The recently reported crystal structure of species B2 Ad11 fiber knob complexed with SCR1-2 of CD46 (Persson et al., 2007) has provided valuable insights into the molecular basis of species B adenovirus binding to CD46. The molecular model of this complex confirmed my earlier findings that SCRs 1 and 2 comprise the binding site for species B fiber knobs. Interestingly, the new structural data indicates that binding of the fiber knob leads to conformational changes in CD46. The previously published structure of an unliganded CD46 construct, comprised of SCRs 1 and 2, showed a pronounced bend of approximately 60° between the domains, with the two N-linked glycans covering a portion of the concave surface of the molecule (Casasnovas et al., 1999). However, superimposition of crystallographically independent molecules indicated a certain degree of flexibility between the two SCRs at the domain interface. Upon binding of the Ad11 fiber knob, the angle between the two SCRs becomes close to zero, thereby forming a rod-like segment (Figure 4.1A) (Persson et al., 2007). This realignment of the fiber knob-binding CD46 domains results in a notable shape-complementarity of the receptor-virus interface, forming a continuous contact area stretched across the side of two fiber knob subunits (Figure 4.1B,C). Along this site, three major contact regions, assigned to the fiber knob surface loops DG, HI and IJ, and the critical residues within these regions have been partially defined. One of the Ad11 fiber knob subunits binds to SCR1 and the interface of SCR1 and SCR2, thus contributing the majority of contacting residues. The second fiber knob subunit makes contact with the base of SCR2.

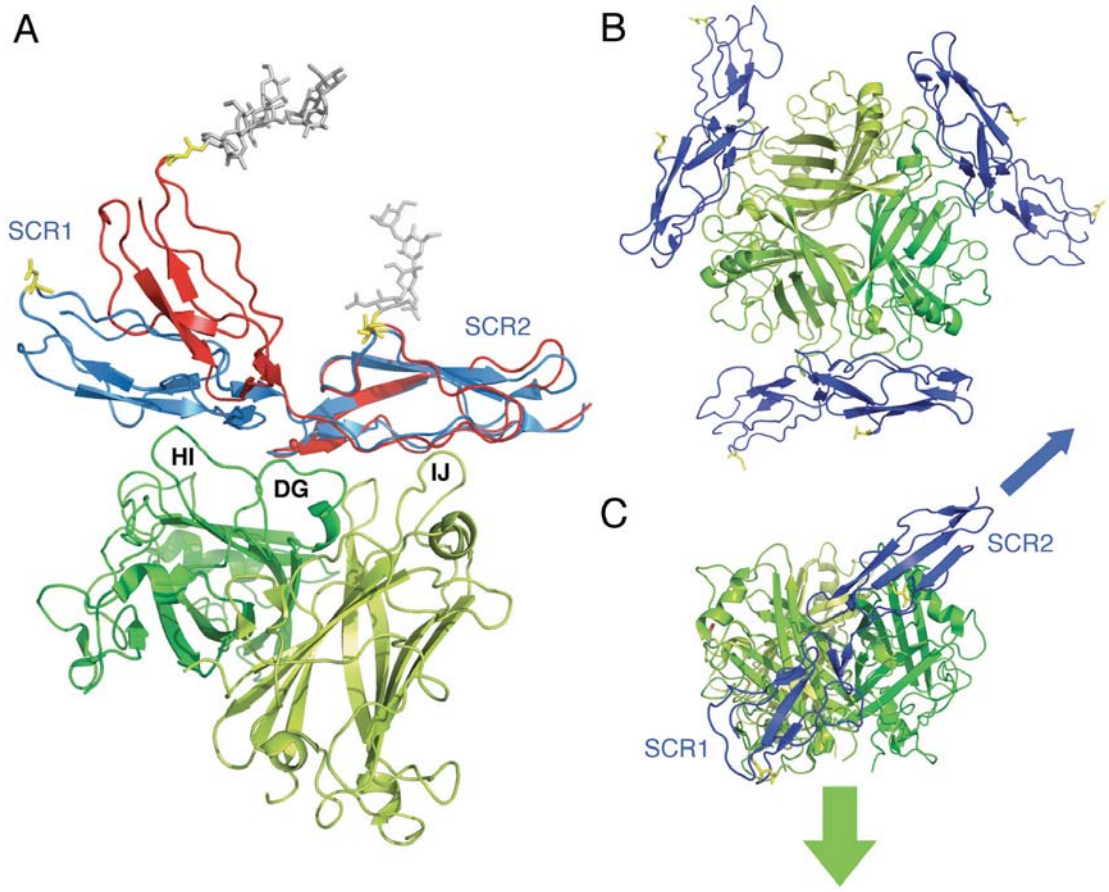

Figure 4.1. **Stucture of the Ad11 fiber knob in complex with the SCR1 and SCR2 domains of CD46.** (A) Unbound CD46 (red) exhibits a pronounced bend at the interface of the two SCR domains. Upon binding to the fiber knob, the CD46 molecule assumes a straightened conformation (blue) that results in a continuous binding surface stretched along the glycan free surface of both SCR domains. The glycosylated residues N49 and N80 of CD46 are highlighted in yellow and the glycans attached to the unliganded form of CD46 are shown in gray. The binding site encompasses the DG and HI loops of one Ad11 fiber knob subunit (dark green) and the IJ loop of a second subunit (light green). (B) Due to its trimeric conformation, the Ad fiber knob (green, viewed from the top) is capable of binding up to three CD46 molecules (blue). (C) The interface of CD46 (blue) bound to the virus is stretched diagonally across the side of the trimeric fiber knob (green, shown in side view). The green arrow indicates the axis of the fiber shaft, pointing towards the virus capsid. The blue arrow indicates the orientation of the C-terminal CD46 domains and the cell membrane. Figures were prepared using the program PyMOL and are based on the published structures of CD46 (PDB-ID 1CKL) and the Ad11-CD46 complex (PDB-ID 2O39).

The extensive contact area suggests tight binding that was confirmed by affinity measurements reporting an equilibrium binding constant (K_D) of

~2 nM. The main chain of the HI loop contributes a large van der Waals contact by interaction with the side chain of Y36 of CD46. Two key residues for the interaction are R279 and R280 of Ad11 fiber knob. R280 builds a salt bridge with E63 of CD46 that is critical for binding. R279, a residue that is required for efficient binding as noted in mutagenesis experiments (Gustafsson et al., 2006) does not interact directly with CD46. However, this residue is likely involved in orienting the HI and DG loops by interacting with its neighboring residues R280 and N247. The IJ loop of the fiber knob contributes to the interaction with two hydrogen bonds involving the side chain of Q305 and the main chain of T306. Owing to its trimeric conformation, the fiber knob can bind up to three CD46 molecules (Figure 4.1B).

Despite this new structural information, the relationship of the virus structure to the actual binding efficiency of different species B viruses to CD46 at the cell surface remains to be clarified. In my studies reported here, I compared the structural features of Ad35 fiber knob and properties of its association with cell surface CD46 with that of Ad11 in order to gain further insights into the molecular basis of CD46 interactions with different species B adenoviruses. My findings suggest that although there are certain structural differences in the CD46 binding regions of Ad35 and Ad11, these do not appear to greatly impact CD46 interactions on cell surfaces. These findings reveal the extent to which natural fiber modifications preserve CD46 binding efficiency, a situation that should influence the selection and development of novel adenoviral vectors.

4.2 Material and methods

Cells and viruses

All cells were maintained in DMEM supplemented with 10% fetal calf serum (FCS) (Omega Scientific, Tarzana, CA), 10 mM HEPES pH 7.55, 4 mM L-glutamine, 1 mM sodium pyruvate, 0.1 mM nonessential amino acids, 100 units/ml penicillin and 100 μg/ml streptomycin. CHO-K1 cells were stably transfected with an expression plasmid containing the C2 isoform of CD46 (Post et al., 1991) or the empty vector as a control as described in chapter II. Transfected CHO cells were maintained in DMEM supplemented as described above, with the addition of 0.5 mg/ml G418 sulfate (Invitrogen, Carlsbad, CA). Ad11p (Slobitsky strain) was obtained from the ATCC (Manassas, VA) and propagated in A549 human lung epithelial cells. An Ad5 vector expressing the fiber protein of Ad35 (Ad5.35F) (T. A. Smith et al., 2003c) was propagated in 293 cells. Viruses were propagated and purified as described in chapter I.

Labeling of adenovirus

Ad11 and Ad5.35F were fluorescently conjugated utilizing an Alexa Fluor 488 Labeling Kit (Invitrogen, Carlsbad, CA). Purified virus was dialyzed against PBS for 2 hours at 4°C. 0.6 mg of virus was diluted to a total volume of 500 μl with PBS. 50 μl of 1 M sodium bicarbonate (pH 8.3) was added and the entire mix was transferred to one vial of Alexa Fluor 488 reactive dye. After 1 hour incubation at room temperature in the dark, the labeled virus was dialyzed against three changes of 40 mM Tris pH 8.1, 150 mM NaCl, 2 mM $MgCl_2$ and 10% glycerol at 4°C in the dark to remove unbound dye molecules. Final virus concentration and dye incorporation were determined by UV spectroscopy using the following calculations:

$$c(virus) = [A_{260} - (0.08 * A_{280})] * 10^{12} * dilution \qquad [particles/ml]$$

$$c(dye) = \frac{A_{494} * dilution}{1.5 * 10^5} \quad [M]$$

$$c(capsomers) = \frac{c(virus) * 252 * 10^3}{6 * 10^{23}} \quad [M]$$

Dye/capsomer ratios were typically between 1.5 and 2.5. Infectivity of labeled virus was compared to that of mock-labeled virus (incubated without dye) to verify that labeling conditions maintained at least 90% of the original cell infectivity of the virus.

Expression and purification of recombinant fiber knob proteins

The expression of Ad5 fiber knob was described in chapter I. To obtain viral DNA, 15 µg of Ad11 or Ad5.35F in 200 µl Tris-buffered saline (TBS) pH 7.4 were incubated in the presence of 1 mg/ml proteinase K, 0.5% SDS, 1 mM EDTA and 50 mM HEPES for 1 hour at 55°C. Viral DNA was isolated by phenol-chloroform extraction and served as template for the amplification of cDNA corresponding to residues 121-323 of the Ad35 fiber and residues 118-325 of the Ad11 fiber by PCR. I used the sense primers 5'-CGCGGATCCAACAACGGTGACATTTGTATA-3' (Ad5.35F) and 5'-CGCGGATCCCTTACATTCAATTCAAACAACATTTG-3' (Ad11) (Bam HI sites underlined) and the antisense primers 5'-TGGTGCGGCCGCTTAGTTGT CGTCTTCTG-3' (Ad5.35F) and 5'-TGGTGCGGCCGCTCAGTCGTCTTC TCTGATGTAG-3' (Ad11) (Not I sites underlined). The fragments were subsequently cloned into the Bam HI/Not I site of the pET28a(+) vector (Novagen, Madison, WI). Recombinant protein was expressed in BL21(DE3) cells (Invitrogen, Carlsbad, CA) and purified using TALON Metal Affinity Resin (Clontech) as previously described in chapter I. The 6x His tag of Ad11 and Ad35 fiber knob was subsequently cleaved by dialyzing the protein into buffer containing 20 mM Tris pH 8.0, 150 mM NaCl and 2.5 mM $CaCl_2$ and incubating it with 0.2 U/mg of protein thrombin protease (Novagen, Madison, WI) for 2 hours at room temperature. Cleaved 6x His fragments as well as

uncleaved protein molecules were removed by incubation with TALON Metal Affinity Resin. The flow-through was diluted with an equal volume of 20 mM Tris pH 8.0 and further purified by anion exchange chromatography on an ÄKTA FPLC system using a Resource Q 1 ml anion exchange column (GE Healthcare, Piscataway, NJ) in 20 mM Tris pH 8.0 with a NaCl gradient from 20 mM to 500 mM. Fiber knobs diluted in loading buffer (80mM Tris pH 6.8, 2% SDS, 10% glycerol, 0.2% bromophenol blue, 5% β-mercaptoethanol) were analyzed by SDS-PAGE with or without prior boiling. Protein bands were stained with SimplyBlue protein stain (Invitrogen, Carlsbad, CA). To verify their trimeric conformation, the fiber knob proteins were analyzed by size exclusion chromatography using an ÄKTA FPLC system and a HiPrep 16/60 Sephacryl S-200 HR gel filtration column (GE Healthcare, Piscataway, NJ). Fiber knob protein, or a mixture of bovine serum albumin (~66 kDa) and albumin from chicken egg white (~45 kDa) (Sigma, St. Louis, MO) as size standards, were run in a buffer consisting of 10 mM Tris pH 8.0 and 150 mM NaCl at a constant flow rate of 0.3 ml/min at 4°C.

Crystallization, data collection and processing

Ad35 fiber knob was concentrated to 13 mg/ml in 20 mM Tris pH 8.0, 100 mM NaCl using Ultrafree-0.5 PBTK centrifugal filter units (Millipore, Billerica, MA). Initial crystal screens were performed by sitting drop vapor diffusion using the Crystal Screen and Crystal Screen 2 kits (Hampton Research, Aliso Viejo, CA). Diffraction quality crystals were obtained after 2 weeks at 22.5°C by hanging drop vapor diffusion using 0.1 M MES pH 6.5, 10% (v/v) 1,4-Dioxane, 1.6 M $(NH_4)_2SO_4$ as precipitant. Diffraction data from the crystals was collected by flash freezing the crystal soaked in the mother liquor containing 25% glycerol for five minutes at the GM/CA CAT beamline at Advanced Photon Source (APS; Chicago, IL). A set of 200 images was collected from a single crystal with an oscillation angle of 1º and a crystal to detector distance of 350 mm. X-ray diffraction data was processed using

HKL2000 suite of programs (Otwinowski and Minor, 1997).

The crystals diffracted to better than 2.7 Å resolution. All images were processed, integrated and scaled in the I4 space group with unit cell dimensions of **a**=173.9 Å and **c**=154.1 Å. A total of 923,306 observations with 57,497 unique reflections were recorded, which amounted to an overall completeness of nearly 91% with an R_{merge} of 15%. The final data reduction statistics are shown in Table 4.1. The Wilson B of the Data is 67 $Å^2$ (Wilson, 1942). The crystal packing analysis showed a solvent content of ~71% for a total of two trimeric fiber knobs in the asymmetric unit (B. W. Matthews, 1968). The higher solvent content is reflected in higher B-factors for the residue in the refined structure.

Data analysis and structure solution

The Ad35 fiber knob structure was solved by molecular replacement using the program Phaser (Read, 2001; Storoni et al., 2004) with a trimer of Ad11 fiber knob (Persson et al., 2007), (PDB ID: 2O39) as the search model. The initial phases obtained from the Phaser solution were improved by two fold and/or six fold NCS averaging using CCP4 (CCP4, 1994) and the RAVE suite of programs (Kleywegt and Jones, 1994). The electron density was averaged into a mask corresponding to a trimer of Ad35 fiber knob. After 15 cycles of NCS averaging, the Rfactor and CC improved from 50% to 15% and 60% to 95%, respectively. The program O (Jones et al., 1991) was used for model building and CNS (Brunger et al., 1998) was used for structure refinement. The initial model of Ad35 was built into averaged electron density and every step of model building was followed by a round of refinement. The final refinement statistics are shown in Table 4.1. TOP3d from the CCP4 suite of programs (CCP4, 1994) and ALIGN (G.E. Cohen, 1997) were used for structure alignment. PyMOL (DeLano, 2002) was used for structure visualization, analysis and figure generation. Intra-/intersubunit contacts and individual accessible surface area were calculated using the programs

Contact and Areamol, respectively, from the CCP4 suite of programs. The Ad35 fiber knob coordinates and structure factors have been deposited in the Protein Data Bank with accession code 3BQ4.

Fiber Binding and virus competition assays

CHO cells were detached from culture flasks with Versene (Invitrogen, Carlsbad, CA) and washed with serum-free medium (DMEM). 10^5 cells per well were deposited into a 96-well plate, resuspended in 50 μl serum-free medium containing different amounts of fiber knob and incubated on ice. After 30 minutes, $3x10^9$ Alexa 488-labeled Ad particles in 50 μl medium were added to the cells in each well for 45 minutes on ice. The cells were pelleted, fixed in PBS containing 4% paraformaldehyde and diluted in PBS containing 0.2% bovine serum albumin and 0.2% sodium azide. 10,000 cells were acquired by flow cytometry on a FACScan flow cytometer and fluorescence was analyzed using CellQuest software (BD Biosciences, Billerica, MA). Background fluorescence of cells in the absence of virus was subtracted and the mean fluorescence intensity was normalized to 100 for cells incubated with virus in the absence of fiber knob.

4.3 Results

4.3.1 Expression and purification of adenovirus fiber knobs

Receptor binding of adenovirus requires proper trimerization of the fiber protein. A previous study reported that trimer formation of the fiber knob requires the entire knob domain as well as at least the knob-proximal 15 residues of the fiber shaft in the case of Ad2 (Hong and Engler, 1996). However, subsequent studies demonstrated trimerization of an Ad2 fiber knob construct containing only the last 12 amino acids of the C-terminal shaft domain (van Raaij et al., 1999) as well as trimer formation of the species B Ad3 fiber knob in the presence of 5 remaining shaft residues (Durmort et al., 2001). I designed an expression construct comprising the complete fiber knob sequence of Ad35 as well as 12 adjacent residues of the fiber shaft, corresponding to approximately one and a half shaft repeats. Further, I designed a construct encoding the Ad11 fiber knob and the C-terminal 15 residues of the shaft domain, corresponding to the construct used in the published Ad11-CD46 co-crystal structure (Persson et al., 2007). To obtain viral DNA, Ad11 virus and an Ad5-based vector carrying the Ad35 fiber gene (Ad5.35F) were propagated in 293 cells and purified by CsCl-gradient ultracentrifugation. Mature virions were digested with proteinase K and the DNA was subsequently purified using phenol-chloroform extraction. After PCR amplification, the corresponding fiber knob sequence was inserted into the pET28a(+) expression vector that adds a cleavable 6x His tag and a T7 tag to the N-terminus (Figure 4.2A).

The proteins were expressed in *E. coli* and purified by immobilized metal ion affinity chromatography (IMAC). Since crystallization of a protein can be impeded by the presence of a 6x His tag (Qi et al., 2007; Stevens, 2000), I removed this tag by thrombin cleavage. This allowed further purification by a second step of IMAC. Uncleaved protein molecules as well as all proteins non-specifically binding to the affinity resin were bound, while

the cleaved fiber knob would be released into the flow-through. To remove the thrombin protease as well as possibly remaining contaminants, the protein solution was further purified by FPLC using an anion-exchange column (Figure 4.2B-D). The process yielded up to 15 mg of purified Ad35 fiber knob protein (FK35) and up to 5 mg of purified Ad11 fiber knob protein (FK11) from 1 liter of bacterial culture.

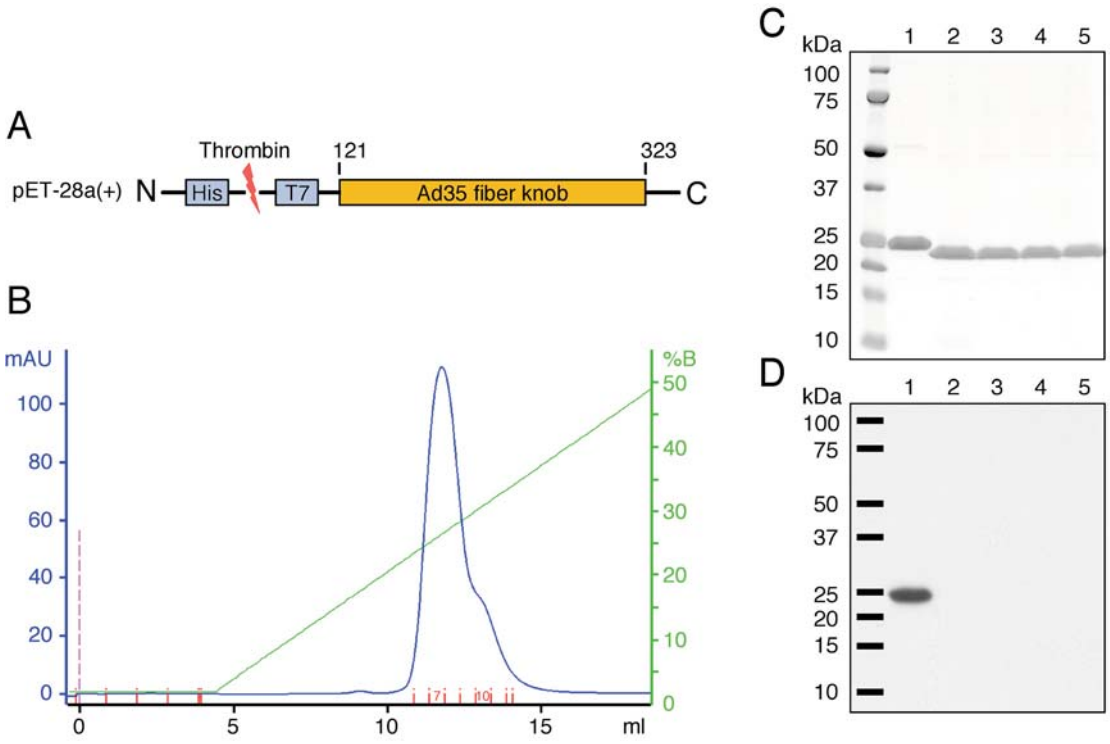

Figure 4.2. **Expression and purification of the Ad35 fiber knob**
(A) cDNA encoding residues 121 to 323 of the Ad35 fiber knob domain was inserted into the expression vector pET-28a(+) that adds a thrombin-cleavable 6xHis tag and a T7 tag to the N-terminus of the protein. (B) Following cleavage of the 6xHis tag the fiber knob protein was purified by FPLC on a Resource Q anion exchange column in Tris buffer pH 8.0 using a NaCl gradient from 20 to 500 mM NaCl. FK35 protein samples from different stages of the purification were analyzed by SDS-PAGE (C). Removal of the 6xHis tag was verified by Western blot analysis using an anti-6xHis tag primary antibody (D). Fiber knob protein purified from cell lysate using IMAC still contained the N-terminal 6xHis tag (lane 1) while thrombin cleavage removed this tag efficiently (lane 2). Potentially uncleaved molecules as well as proteins nonspecifically binding the resin were removed in a second step of IMAC (lane 3). Elution fractions 7 (lane 4) and 10 (lane 5) from the anion exchange chromatography are shown as well. Peak fraction 7 was used for subsequent experiments. The Ad11 fiber knob was purified in an analogous manner.

I verified that the purified fiber knobs retained a trimeric organization by gel electrophoresis under semi-native conditions and by size exclusion chromatography. Semi-native gel electrophoresis showed bands for both fiber knobs that migrated at a size of ~50 kDa, compared to ~23 kDa for the monomers, clearly indicating their multimeric state (Figure 4.3A). It has been shown previously that trimeric fiber knobs can run at the size of dimers in SDS-PAGE analysis (Durmort et al., 2001). To ensure that the fiber knobs had a trimeric organization, they were analyzed on a size exclusion column where they eluted at approximately the same retention volume as a marker protein of 66 kDa, indicating their trimeric conformation (Figure 4.3B).

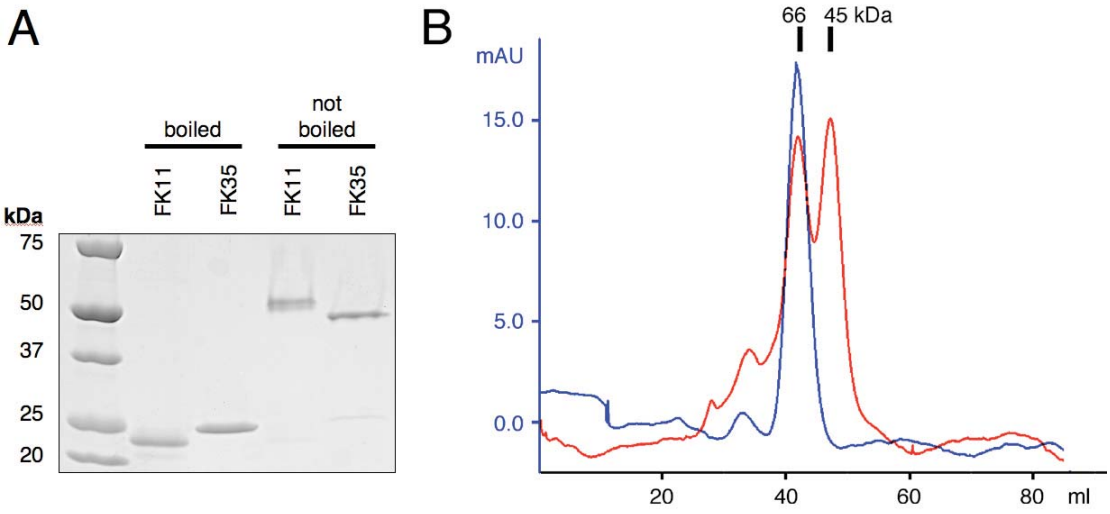

Figure 4.3. **Recombinant Ad11 and Ad35 fiber knobs retain trimeric organization.** (A) Purified FK11 and FK35 samples were run boiled or non-boiled on a polyacrylamide gel. Non-boiled samples show fiber knob multimers. (B) FK35 was analyzed by FPLC on a size exclusion column (blue curve). The elution profile of bovine serum albumin (66 kDa) and albumin from chicken egg white (45 kDa) (red curve) run under identical conditions indicated a trimeric conformation of FK35. Trimeric organization of FK11 was verified accordingly.

4.3.2 Crystallization of Ad35 fiber knob

The purified FK35 was concentrated to 10 mg/ml and crystallization trials were performed using sitting drop vapor diffusion. Spherulites and microcrystals were obtained after two weeks from a crystallization buffer consisting of 4 M sodium formate. However, subsequent trials with modified buffer compositions did not improve crystal growth. A crystallization buffer consisting of 1.6 M ammonium sulfate, 0.1 M MES monohydrate pH 6.5 and 10% v/v 1,4-Dioxane yielded crystal plates after two weeks (Figure 4.4A). Varying salt and Dioxane concentrations as well as pH of the mother liquor did not improve crystal quality. Instead, I obtained single crystals with a size of approximately 100 μm by hanging drop vapor diffusion after two weeks using a protein stock solution that was further concentrated to 13 mg/ml and the crystallization buffer described above (Figure 4.4B). The crystals were flash frozen after soaking in the mother liquor containing 25% glycerol for five minutes and data was collected by Drs. Glen Nemerow and Vijay Reddy at the GM/CA CAT beamline at APS, Chicago. Data processing and subsequent determination of the protein structure was performed by Drs. Sangita Venkataraman and Vijay Reddy (Table 4.1).

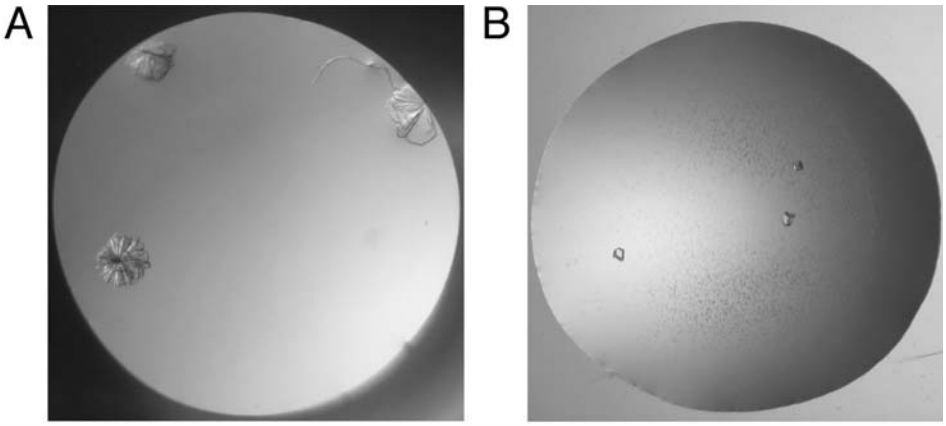

Figure 4.4. **Protein crystals of the Ad35 fiber knob**
Crystal plates were obtained by sitting drop vapor diffusion using a protein concentration of 10 mg/ml and a crystallization buffer consisting of 1.6 M ammonium sulfate, 0.1 M MES monohydrate pH 6.5 and 10% v/v 1,4-Dioxane. Single crystals (~100 μm) were obtained after two weeks by hanging drop vapor diffusion using the same crystallization buffer with FK35 concentrated to 13 mg/ml.

Table 4.1. Data statistics

Parameters	*Data*
Space group	I4
Resolution range (Å)	50 – 2.7 (2.8 – 2.7)[§]
Unit Cell:	
a, b (Å)	173.820
c (Å)	154.008
No. of unique reflections	57497
I/σ(I)	13.3 (2.0)
Completeness (%)	91.5 (68.4)
Rmerge* (%)	14.9 (62.4)
R factor/ free R (%)	33.2/35.2
No. of Protein atoms/asymmetric unit	8976
RMSD bond (Å)	0.010
RMSD angles (º)	1.7
Ramachandran statistics	
Most Favored region (%)	63.5
Additionally allowed region (%)	28.3
Generally allowed region (%)	6.5
Disallowed region (%)	1.7

Rmerge = ∑hkl |I -< I>| / ∑I
§Data in parentheses refer to the last resolution shell

4.3.3 Structure analysis of the Ad35 fiber knob and model of a complex with CD46

There are two copies of Ad35 fiber knob trimers in the crystallographic asymmetric unit. The tertiary structure of Ad35 fiber knob is similar to that of the previously solved structure of Ad11 (Persson et al., 2007) with which it shares 50% sequence identity (Figure 4.5A). The quality of the electron density that aided in unambiguous positioning of the side chains into the

density is shown in Figure 4.5B. The distinguishing features of the Ad11 and Ad35 fiber knob structures owe primarily to the surface loops that are implicated in CD46 binding in the Ad11 structure bound to CD46.

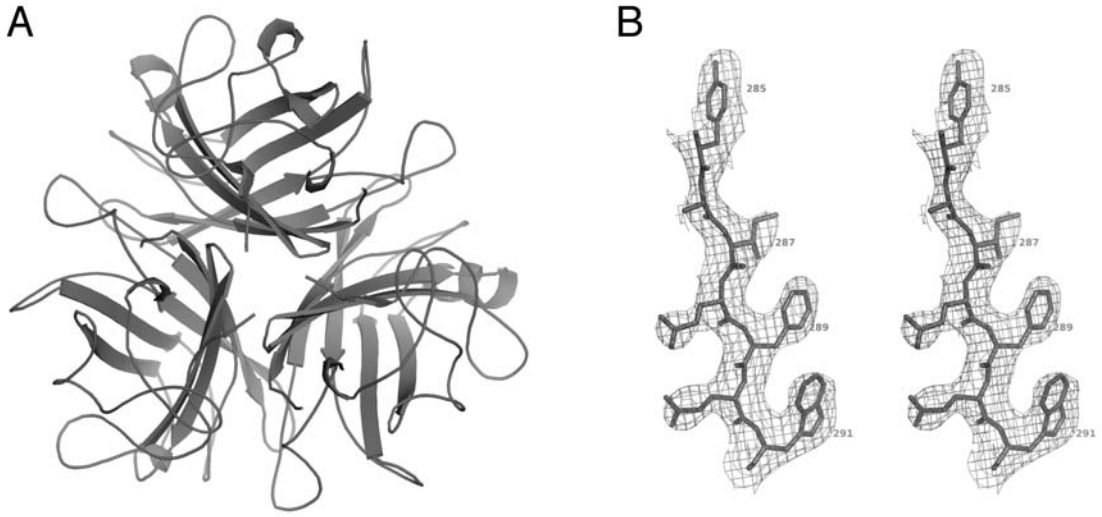

Figure 4.5. **Crystal structure of the Ad35 fiber knob trimer.** (A) A ribbon diagram of the Ad35 fiber knob trimer viewed down the threefold axis. (B) Stereo diagram showing the quality of fit of residues 285 to 291 of the Ad35 fiber knob into $2F_o - F_c$ electron density contoured at 1.0 σ.

In the crystal structure of Ad11 fiber knob bound to CD46, three regions, corresponding to the DG- (residues 245-247), the HI- (residues 279-285) and the IJ-loop of the fiber knob (residues 305-307) were identified that interact directly with the CD46 receptor domains (Figure 4.6). While the DG- and HI loops that bind to the first SCR domain originate from one subunit of the Ad11 trimer, the interactions in the IJ loop are contributed by the residues from the neighboring subunit. Thus the CD46 (SCR1 and SCR2) interacting regions span two of the three subunits of the Ad11 trimer. The Ad11 fiber knob is lacking two short β-strands (termed E, F) that are present in Ad35. Therefore, the loop termed DG in the Ad11 fiber knob corresponds to the FG loop in Ad35. A structural superimposition of the Ad11 and Ad35 fiber knobs reveals that the HI loop is structurally most conserved followed by the FG- and IJ loop (Figure 4.7).

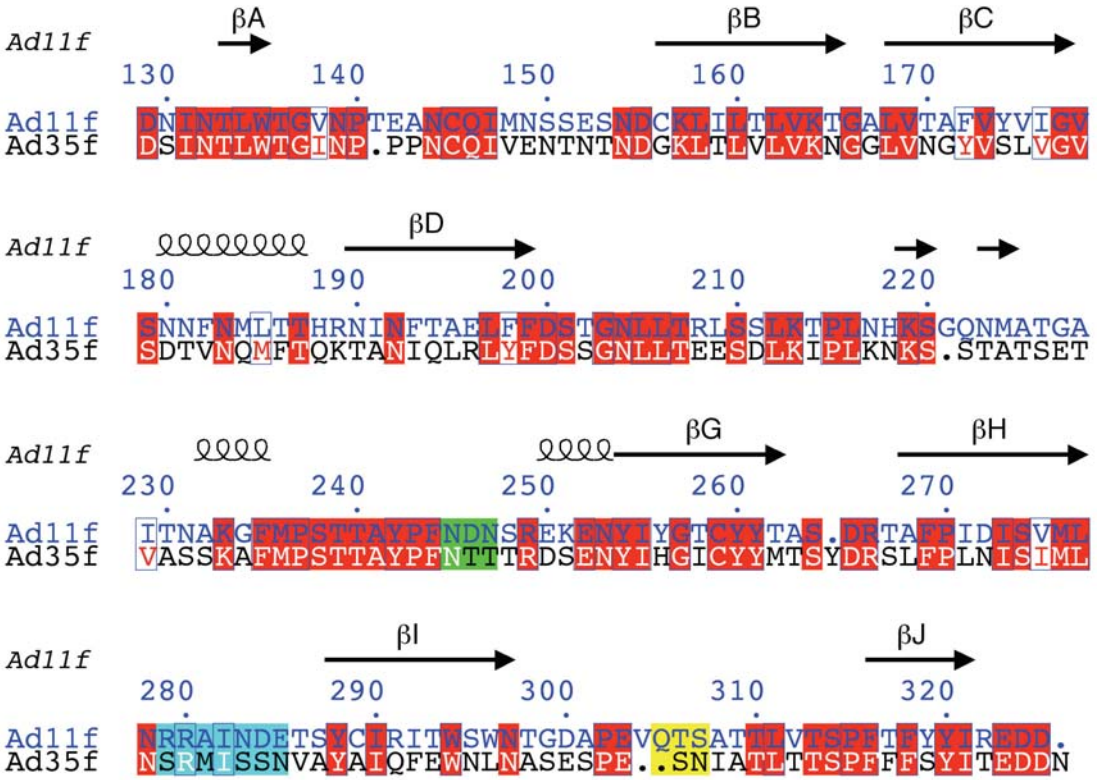

Figure 4.6. **Sequence alignment of Ad11 fiber knob monomer with Ad35 fiber knob monomer.** Residues in the FG, HI and IJ loops that interact with the CD46 receptor are highlighted in cyan, green and yellow, respectively. The conserved residues in the non-interacting regions are highlighted with a red background while similar residues are enclosed in blue boxes.

Of particular interest, the IJ loop in the Ad35 structure is shorter by two residues than the corresponding loop in the Ad11 structure. This results in the IJ loop of Ad11 fiber knob having closer proximity to the CD46 receptor and hence could result in a more favorable interaction at this region. In contrast, this interaction is predicted to be lacking in the Ad35 fiber knob-CD46 complex model.

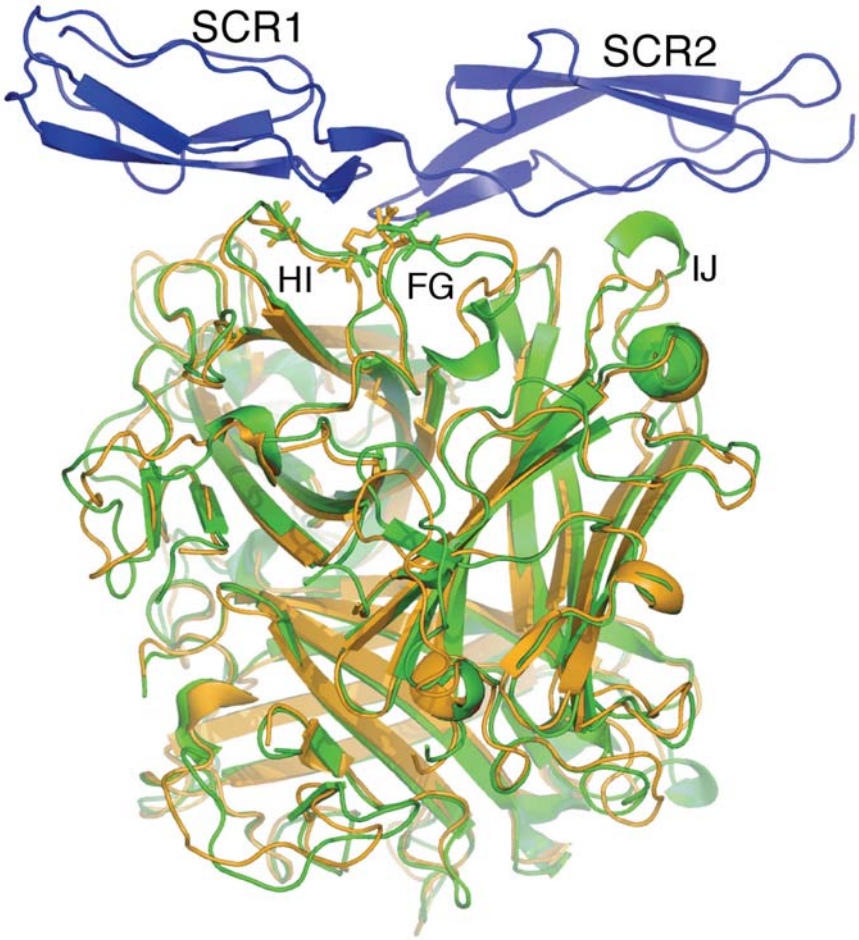

Figure 4.7. **Structural comparison of Ad35 fiber knob with Ad11 fiber knob bound to CD46.** Superimposition of the Ad35 fiber knob trimer (orange) onto the Ad11 fiber knob trimer (green) bound to CD46 (blue), showing the interacting surface loops. The conserved interacting residues in the FG (R280/R279, I282/I281 in Ad11/Ad35) and HI loops (N245/N243 in Ad11/Ad35) are shown in stick representation. Also indicated is the IJ loop that differs the most between the Ad11 and Ad35 fiber knob structures.

The buried surface area for the Ad11 fiber knob bound to CD46 is 1905 $Å^2$ while it was calculated to be 1715 $Å^2$ for the Ad35 fiber knob trimer. These values are in a similar range as the buried surface area of ~1880 $Å^2$ estimated in Ad-CAR association (Bewley et al., 1999). Based on the sequence alignment of Ad11 with Ad35 (Figure 4.6), the residues in all three interacting regions are most dissimilar between Ad11 and Ad35 sequences when compared to the corresponding non-interacting regions. However, a

comparison of residue-wise interactions at the three CD46-binding regions between the Ad11 and Ad35 structures reveals that the two fiber knobs are comparable in terms of the residue-wise buried surface area upon association with CD46 (Table 4.2). This is also true for the number and nature of contacts that are observed between the fiber knob and CD46 receptor. All the contact forming residues show a decreased accessible surface area when in association with the CD46 receptor (data not shown). Of particular significance, the salt bridge between E63 of CD46 and R280 and R279 of Ad11 and Ad35, respectively, is conserved.

Table 4.2. **Comparison of the normalized buried surface areas of selected amino acids in Ad11 and Ad35 upon association with CD46.**

Ad11		Ad35	
Residue Number	Normalized Buried Surface area (%)[$]	Residue Number	Normalized Buried Surface area (%)[$]
N245	20.3	N243	29.1
R280	26.6	R279	27.6
A281	18.8	M280	18.7
I282	25.4	I281	34.6
N283	25.7	S282	13.2
D284	39.8	S283	34.0
Q305	29.6	-[$$]	-[$$]
T306	46.6	-[$$]	-[$$]

[$] The % normalized buried surface area was calculated by dividing the buried surface area values of the amino acids in contact with CD46 by the accessible surface area for the same amino acid in isolation.
[$$] Corresponding residues are absent due to shorter length of the IJ loop in Ad35 fiber knob structure.

Further conserved residues in the CD46-contacting regions include N243 and N245 in the FG/DG loop and I281 and I282 in the HI loop of the

Ad35 and Ad11 fiber knob structures, respectively. Other contacts at the FG- and HI loops have corresponding interactions in Ad11 and Ad35 except for the IJ loop, where a few contacts are predicted to be absent in Ad35, owing to the shorter loop (Figure 4.7). Thus, the present Ad-CD46 structure models suggest that the Ad35 fiber knob might bind to the CD46 receptor in a similar fashion as to the Ad11 fiber, indicated by the similarities in the buried surface area and the contacts between the individual fibers with the CD46 receptor. However, a direct comparison of these two fiber knobs binding to cell surface CD46 has not been previously evaluated.

4.3.4 Analysis of Ad fiber knob binding to cells via CD46

In initial flow cytometry studies I examined the binding of fluorescently conjugated Ad11 as well as of a labeled Ad5 vector equipped with an Ad35 fiber (Ad5.35F) to CHO cells lacking CD46 (null) or to CHO cells expressing CD46 (Figure 4.8A). I observed that labeled virus/vector bound to CHO cells expressing human CD46 but did not show significant binding to CHO cells lacking this receptor, indicating the requirement for a specific receptor in virus-cell association.

I next used the CHO-CD46 cells to compare Ad35 and Ad11 fiber knob interactions in competition studies (Figure 4.8B, C). CHO-CD46 expressing cells were preincubated with varying amounts of FK35, FK11, or the Ad5 fiber knob (FK5) as a control, prior to the addition of labeled Ad11 or Ad5.35F virions. Flow cytometric analysis showed that FK35 and FK11 exhibited very similar capacity to inhibit Ad11 as well as Ad5.35F virus binding to cells while the CAR-specific FK5, as expected, did not impair binding. However, the FK5 construct potently blocked Ad5 attachment to CAR expressing HeLa cells (data not shown). These findings indicate, that despite having somewhat different CD46 binding regions, particularly in the IJ loop, the fiber knob domains of Ad35 and Ad11 promote very similar association with CD46 on host cells.

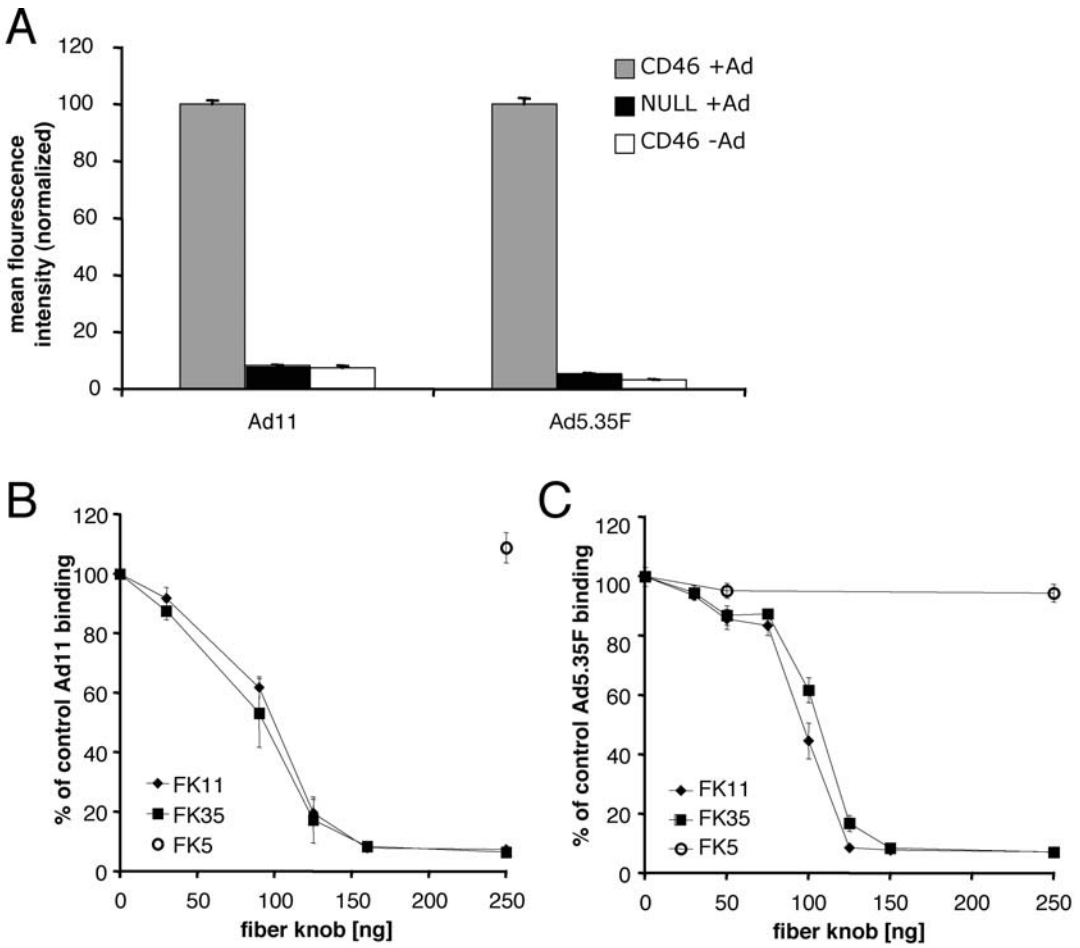

Figure 4.8. **Functional comparison of Ad11 and Ad35 fiber knobs binding to cellular CD46.** (A) CHO-K1 cells stably transfected with a plasmid expressing CD46 (CD46) or an empty expression vector (NULL) were incubated with Ad11 or Ad5.35F virus at 30,000 virus particles per cell. CD46 expressing cells in the absence of virus serve as background control. Mean fluorescence intensity was normalized to 100 for CD46 expressing cells incubated in the presence of virus. No efficient attachment of either virus was observed in the absence of cellular CD46. Data points represent means of triplicates. Error bars represent standard deviations. (B, C) CHO cells expressing CD46 were pre-incubated with different amounts of Ad11 fiber knob (FK11), Ad35 fiber knob (FK35) or Ad5 fiber knob (FK5) on ice for 30 minutes, before the addition of 30,000 virus particles per cell of Ad11 (B) or Ad5.35F (C) for 45 minutes on ice. Mean fluorescence intensity was measured by flow cytometry. Background fluorescence of cells in the absence of virus was subtracted and fluorescence of cells incubated with virus in the absence of fiber knob was defined as 100%. Data points represent means of triplicates. Error bars represent standard deviations. Graphs shown are representative for at least two independent experiments with separate protein preparations.

4.4 Discussion

While the recently published co-crystal structure of Ad11 fiber knob-CD46 provides structural details of the adenovirus receptor interaction (Persson et al., 2007), is not yet fully clear how these structural features relate to CD46 association. The degree to which other species B adenoviruses share the CD46-binding capabilities of Ad11 has also not been investigated. As both, Ad11 and Ad35 are candidates for new gene therapy vectors, a comparison of their receptor binding efficiencies may aid in the selection of optimal gene delivery vectors.

Recent mutagenesis studies identified critical residues in the Ad35 fiber knob that are likely to be involved in CD46 binding (Wang et al., 2007). The residues identified in Ad35 fiber knob that are likely to make direct contact to CD46 are located within the same CD46-binding regions identified in Ad11. This correlation of fiber knob regions involved in receptor binding, the DG/FG, HI and IJ loops, suggests that both virus types engage their primary receptor in a very similar fashion and likely with very similar strong binding (low nanomolar) affinity. However, previous studies measured Ad11 or Ad35 fiber knob association with CD46 at 2 nM and 15.35 nM, respectively (Persson et al., 2007; Wang et al., 2007). This almost eight-fold difference is somewhat surprising in light of the structural similarities between the Ad11 and Ad35 fiber knobs (Figure 4.7). However, the IJ loop in the Ad35 fiber knob trimer exhibits some structural differences with that of Ad11. In this region, the Ad11 fiber knob has two additional residues that are missing in Ad35. The extended IJ loop might allow a closer contact to CD46, which on a theoretical basis could enhance receptor interaction. Nonetheless, a measurement of the amount of buried surface area for Ad11 and Ad35 fiber knob in our studies revealed only a relatively minor difference overall.

Given the very similar structural features of CD46-binding domains of Ad11 and Ad35 fiber knob, I performed virus competition binding studies using recombinant fiber knobs in order to assess the efficiency of their

association with CD46 under physiological conditions. My binding assays are designed to allow multivalent association of fiber trimers with cell surface CD46 molecules, a situation that would more closely mimic vector–cell interactions. To ensure that fiber knob interactions were exclusively restricted to CD46, I used CHO cells expressing recombinant CD46. Importantly, CHO cells do not express an alternative species B receptor, designated X (Tuve et al., 2006), a situation that I confirmed by showing that Ad11 cannot efficiently bind to CHO cells in the absence of human CD46. Under these physiological conditions both, Ad11 and Ad35 fiber knob showed an almost identical ability to inhibit Ad binding to cells, thus indicating that each of these virus proteins possesses equivalent CD46 binding efficiency.

My findings thus differ from the previously published studies that showed different binding affinities to CD46 by distinct Ad types. One possible explanation for this discrepancy is that the previous studies measured the 1:1 interaction of a single CD46 SCR1-2 construct with a trimeric fiber knob molecule in solution or immobilized on a solid support, rather than on the cell surface. The binding of Ad11 to the truncated CD46 was analyzed in solution by isothermal titration calorimetry while the measurements on Ad35 fiber knob were performed on a solid support using surface plasmon resonance. Differences in steric hindrance or effects of the coupling chemistry on the ligand might influence the measured affinities, thus making a direct comparison of these results difficult. Since the fiber knob trimer has three potential CD46 binding sites, attachment of the fiber knob to the cell surface could well involve multivalent association with CD46 molecules, further stabilizing virus/fiber binding and the efficiency of cellular attachment. Moreover, the truncated version of CD46 (SCR1-2) employed in previous studies might interact somewhat differently than the full-length CD46 molecule used in my current studies.

Thus, my structural findings revealing relatively small differences in the CD46 binding surfaces of the Ad11 and Ad35 fiber knobs appear to be

consistent with the similar CD46 interactions on host cells. In this regard it is interesting to note that the difference in buried surface area upon CD46 binding by Ad11 and Ad35 fibers might even be smaller than calculated. My model is based on the assumption that CD46 upon binding to Ad35 fiber knob assumes a straightened conformation, comparable to the one seen in the CD46-Ad11 structure. However, the actual degree of bending between the two SCRs of CD46 is unknown and therefore, if it were slightly more pronounced, it could provide a more favorable interaction with the Ad35 fiber knob in the region of the IJ loop. Thus, the difference in buried surface areas in the two fiber knobs in this region might actually be less pronounced than suggested by the model. This possibility is supported by the very similar binding efficiencies observed in my competition studies.

In these studies, I demonstrated that, based on structural analyses and modeling as well as on cell based competition studies, the fiber knobs of Ad11 and Ad35 exhibit very similar binding to CD46 on cells. Importantly, my investigations also indicate the degree to which certain outer loops of the Ad fiber knob can tolerate alterations without impacting CD46 association on intact cells. This finding may help clarify CD46 association by Ad vectors based on species B2 viruses and indicate that both fiber types provide suitable alternatives for the development of gene therapy vectors.

5. Chapter IV:
Impact of structural variations in species B adenovirus fibers on CD46 binding

5.1 Introduction

Similar to my previously described investigations, most studies analyzing the mechanism of adenovirus binding to CD46 to date have focused on receptor binding by two species B2 adenoviruses, Ad11 and Ad35 (Pache et al., 2008; Persson et al., 2007; Wang et al., 2007). It was found that both viruses engage CD46 in a similar fashion and with similar efficiencies. Based on the co-crystal structure of Ad11 fiber knob in complex with CD46, a large continuous binding region in the virus fiber was shown to encompass the DG-, the HI- and the IJ-loops of the fiber knob domain. Moreover, a highly conserved arginine residue in the HI loop was found to form a critical salt bridge with CD46, and mutations targeting this amino acid profoundly reduced receptor association (Wang et al., 2007). However, the degree to which other members of species B use CD46 has not been extensively investigated.

Species B Ads are further divided into members of species B1 and B2. This division correlates more with tissue tropism rather than with receptor usage. The majority of species B adenoviruses use CD46 as their primary cellular receptor (Gaggar et al., 2003; Segerman et al., 2003b; Sirena et al., 2004) with the two N-terminal extracellular domains of CD46 mediating fiber association as demonstrated in a number of studies including the one presented here in chapter II (Fleischli et al., 2005; Gaggar et al., 2005). However, B1 and B2 Ads exhibit distinct tissue tropisms. While the members of species B2 are known to cause infections of the kidney and urinary tract, B1 adenoviruses are associated with infections of the upper respiratory tract. Whether these distinct tissue tropisms correlate with different CD46-

association among species B1 or B2 remains to be investigated.

In the research described in this chapter, I compared the association of the Ad16 fiber knob, a member of species B1, with CD46 to that of the Ad11 knob and provide a detailed kinetic analysis for the binding sites of both fiber types. In addition, I crystallized the Ad16 fiber knob and, in collaboration with Dr. Vijay Reddy, generated a comparative model of this protein in complex with CD46. The model of this complex as well as targeted mutagenesis studies of recombinant fiber knobs allowed me to identify a critical region in the FG loop of different species B Ad fibers that plays a key role in the interaction with CD46. These studies aid our understanding of Ad-CD46 association and may help guide the future development of improved viral vectors with enhanced receptor binding.

5.2 Material and methods

Cells and viruses

All cell lines based on CHO-K1 cells were maintained as previously described in chapter III. 293EBNA expressing the extracellular domain of the C isoform of (Wu et al., 2004) are described in chapter I and were maintained in DMEM supplemented with 10% fetal calf serum (Omega Scientific, Tarzana, CA), 10 mM HEPES pH 7.55, 4 mM L-glutamine, 1 mM sodium pyruvate, 0.1 mM nonessential amino acids, 100 U/ml penicillin and 100 μg/ml streptomycin with the addition of 5 μg/ml Puromycin.

Ad11p (Slobitsky strain) was obtained from the ATCC (Manassas, VA) and propagated in A549 cells. Ad5.16F (C. Hsu et al., 2005) was propagated in 293 cells. Propagation and purification of the viruses have been described in chapter I. Concentrations of purified viruses were determined by UV absorbance measurements. Viruses were fluorescently conjugated as previously described in chapter III using an Alexa Fluor 488 Labeling Kit (Invitrogen, Carlsbad, CA) under conditions that maintained at least 90% of the original infectivity.

Protein expression and purification

Generation of cDNA encoding recombinant fiber knob proteins corresponding to residues 118-325 of Ad11p fiber (Slobitzki strain) (FK11) and residues 151-353 of Ad16 fiber (FK16) has been described in previous chapters. Mutations in the fiber knob constructs were introduced using the QuikChange site directed mutagenesis kit (Stratagene, La Jolla, CA) according to the manufacturer's instructions. Briefly, mutant oligonucleotide primers are incorporated into the plasmid strands by PCR amplification using the polymerase PfuTurbo. The non-mutated, parental DNA template is then digested by the endonuclease DpnI that specifically cleaves methylated and hemimethylated DNA. The remaining synthesized, mutation-containing

plasmid DNA is used to transform competent *E. coli* cells that repair the nicks in the mutated plasmids. The following mutagenic primers (listed in 5'-3' orientation) were designed under consideration of guidelines proposed by Zheng et al. (Zheng et al., 2004).

FK16 R309Q	FWD	GTTACTGTCACACTAAACCAACGTATGCTAGCTTCTGGAATG GCCTATG
	REV	CATAGGCCATTCCAGAAGCTAGCATACGTTGGTTTAGTGTGA CAGTAAC
FK16 R310N	FWD	GTTACTGTCACACTAAACAGAAATATGCTAGCTTCTGGAATG GCCTATG
	REV	CATAGGCCATTCCAGAAGCTAGCATATTTCTGTTTAGTGTGA CAG
FK16 333VQ334	FWD	GCAGAGGAAGCCCCGGAAGTGCAAACTACCGAAGTCACT CTC
	REV	GAGAGTGACTTCGGTAGTTTGCACTTCCGGGGCTTCCTCT GC
FK16 T212M	FWD	GGAGCCTCAGAATATACTAACATGTTGTTTAAAAACAATCAA GTTAC
	REV	GTAACTTGATTGTTTTTAAACAACATGTTAGTATATTCTGAG GCTCC
FK16 ΔA276	FWD	CCATTTATAACATACACTGAGACCCTAAATGAAGATTAC
	REV	GGTCTCAGTGTATGTTATAAATGGATAGGCGGTGG
FK16 ΔY275	FWD	CCACCGCCTATCCATTTATAACAGCCACTGAGACC
	REV	GGTGGCGGATAGGTAAATATTGTCGGTGACTCTGG
FK16 ΔY275/ΔA276	FWD	AGCACCACCGCCTATCCATTTATAACAACTGAGACCCTAAA
	REV	TTTAGGGTCTCAGTTGTTATAAATGGATAGGCGGTGGTGCT

FK11 246A247	FWD	CCTTTCAATGATGCGAATTCTAGAGAAAAAGAAAACTAC
	REV	CTAGAATTCGCATCATTGAAAGGATAGGCAGTCGTG
FK11 246AA247	FWD	CCTTTCAATGATGCGGCGAATTCTAGAGAAAAAGAAAACTAC
	REV	CTAGAATTCGCCGCATCATTGAAAGGATAGGCAGTCGTG
FK11 246YA247	FWD	CCTTTCAATGATTATGCGAATTCTAGAGAAAAAGAAAACTAC
	REV	CTAGAATTCGCATAATCATTGAAAGGATAGGCAGTCGTG

All fiber knob constructs were expressed in BL21(DE3) *E. coli* cells (Invitrogen, Carlsbad, CA) and purified by immobilized metal affinity chromatography, removal of the 6x His tag and ion exchange chromatography as previously described in chapter III. To verify expression and trimerization, fiber knobs diluted in loading buffer (80mM Tris pH 6.8, 2% SDS, 10% glycerol, 0.2% bromophenol blue, 5% β-mercaptoethanol) were

analyzed by SDS-PAGE with or without prior boiling. Protein bands were stained with SimplyBlue protein stain (Invitrogen, Carlsbad, CA).

The soluble extracellular domain of the C isoform of CD46 (sCD46) was expressed in mammalian 293EBNA cells and purified as described in chapter I.

Competition of Ad transduction by soluble CD46

To verify the activity of the expressed sCD46 protein, 50,000 A549 cells/well were cultured in a 24-well tissue-culture plate. $6.5x10^6$ Ad5.5F or Ad5.16F particles (virus concentration was adjusted to infect ~5% of the cells) were preincubated with varying concentrations of sCD46 in serum-free medium. After 1 hour on ice, virus and sCD46 were added to the cells for 1 hour on ice. The cells were washed three times with medium and incubated overnight at 37°C. 10,000 cells were acquired by FACS and analyzed for GFP expression as previously described.

Surface plasmon resonance analysis of CD46-fiber binding

Surface plasmon resonance experiments were performed on a BIAcore 2000 system (GE Healthcare, Piscataway, NJ) at 25°C. CM5 sensor chips, *N*-hydroxysuccinimide (NHS), 1-ethyl 3-(3-dimethylaminopropyl)-carbodiimide hydrochloride (EDC), ethanolamine hydrochloride, Surfectant P20 and HSB-EP buffer were obtained from GE Healthcare (Piscataway, NJ). Carboxymethyl-dextran sodium salt (CM-dextran) was obtained from Sigma-Aldrich (St. Louis, MO). Between 50 and 80 resonance units (RU) of purified fiber knob protein diluted in 20 mM sodium acetate pH 4.0 were covalently immobilized on CM5 sensor chips using standard amine coupling chemistry in HSB-EP running buffer as recommended by the manufacturer. A reference flow cell was generated by activation and subsequent blocking without the immobilization of fiber knob. Binding studies were carried out by injecting sCD46 at concentrations of 49.6, 24.8, 12.4, 6.2, 3.1, 1.6 and 0.8 nM at flow

rates of 20 and 40 μl/min (FK11) or at concentrations of 827, 621, 414, 207, 103, 52 and 26 nM at flow rates of 40 and 50 μl/min (FK16, FK11 246AA247) in a running buffer consisting of 10 mM Tris pH 7.4, 150 mM NaCl, 3 mM EDTA, 0.005% Surfectant P20 and 100 μg/ml CM-dextran. All concentrations were analyzed in two replicate injections. Additional injections at flow rates varying from 25 to 75 μl/min were used to verify that binding was not influenced by mass transport effects (Morton and Myszka, 1998). Response from a reference flow cell was subtracted from the sensograms. Kinetic constants were obtained by global fitting of the data to a 1:1 interaction model. Kinetic analysis included double referencing (Myszka, 1999). Equilibrium data was extracted from sensograms to calculate equilibrium dissociation constants of FK16 and FK11 246AA247 independently of the kinetic analysis. Data analysis was performed using the software Scrubber 2.0 (BioLogic Software, Campbell, Australia).

Crystallization, data collection and processing

Purified FK16 was concentrated to 10 mg/ml in 20 mM Tris pH 8.0, 100 mM NaCl in Ultrafree-0.5 PBTK centrifugal filter units (Millipore, Billerica, MA). Equal volumes (1.5 ml) of the fiber knob sample and the reservoir solution containing 100 mM HEPES (pH 7.5), 0.7 M NaH_2PO_4 and 0.85 M KH_2PO_4 were used in the crystallization setups. Sitting drop vapor diffusion yielded crystals after 1 week at 22.5ºC. X-ray diffraction data for FK16 crystals was collected at the GM/CA CAT beamline at APS, Chicago. The crystals were pre-soaked in the mother liquor containing 25% glycerol for five minutes and flash frozen prior to data collection. The X-ray diffraction data consisted of a set of 176 images collected from a single crystal on a MAR300 CCD detector with an oscillation angle of 1º, a wavelength of 0.979 Å and a crystal to detector distance of 350 mm. The diffraction data was processed and scaled using HKL2000 suite of programs (Otwinowski and Minor, 1997) to a resolution of 2.4 Å resolution in the space group P6522. The overall

completeness of the data was 99% with an R_{merge} of 11.2%. The final data reduction statistics are shown in Table 5.1.

Data analysis and structure determination

The FK16 structure was solved using the molecular replacement program Phaser (Read, 2001; Storoni et al., 2004) with a trimer of the Ad11 fiber knob (Persson et al., 2007), (PDB id: 2O39) as the search model. Due to the presence of two trimers in the asymmetric unit, the phases were improved by two fold NCS averaging using CCP4 (CCP4, 1994) and the RAVE suite of programs (Kleywegt and Jones, 1994). The model was built using the program O (Jones et al., 1991) and later refined using CNS (Brunger et al., 1998). The data and the final refinement statistics are shown in Table 5.1. The program TOP3d from the CCP4 suite (CCP4, 1994) was used for structure alignments and to obtain the NCS matrix used in the density modification. Structure visualization, analysis and figure generation was done using PyMOL (DeLano, 2002). The Ad16 fiber knob coordinates and structure factors have been deposited in the Protein Data Bank with accession code 3CNC.

Sequence alignments

Amino acid sequences of fiber knobs were aligned using the program ClustalW2 (Chenna et al., 2003). Structure-based alignments were performed using the program TM-align (Y. Zhang and Skolnick, 2005). A phylogenetic tree diagram was created using the PHYLIP program package (Felsenstein, 2005).

Cell binding and competition assays

Fiber knob competition studies to evaluate CD46 interactions were performed as previously described (chapter III). Briefly, 10^5 CHO cells per sample were incubated with varying amounts of fiber knob for 30 min on ice prior to the addition of $3x10^9$ fluorescently labeled Ad particles for 45 min on ice. After pelleting, the cells were fixed, diluted and diluted in FACS buffer. 10,000 cells were acquired on a FACScan flow cytometer and analyzed using CellQuest software (BD Biosciences, Billerica, MA).

5.3 Results

5.3.1 Expression and purification of Ad16 fiber knob

I generated an expression plasmid by amplifying amino acids 151-353 of the Ad16 fiber and inserting the sequence in the pET28a(+) vector that adds an N-terminal T7 tag and a cleavable 6x His tag. This Ad16 fiber knob construct (FK16) encodes the final 11 C-terminal Ad16 fiber shaft residues in addition to the entire sequence of the fiber knob domain. Similar to the expression and purification of FK35 and FK11 (chapter III), FK16 was expressed in *E. coli* and subsequently purified by immobilized metal affinity chromatography (IMAC) and anion exchange chromatography (Figure 5.1). Following the removal of the 6x His tag by thrombin cleavage, the protein was further purified by a step of reverse IMAC to remove uncleaved FK16 molecules that were retained by the resin and anion exchange chromatography. The protein yields were comparable to those of FK11 and FK35 (i.e. 8 mg of purified protein per 1 liter culture). Trimerization of purified FK16 was verified by SDS-PAGE (data not shown)

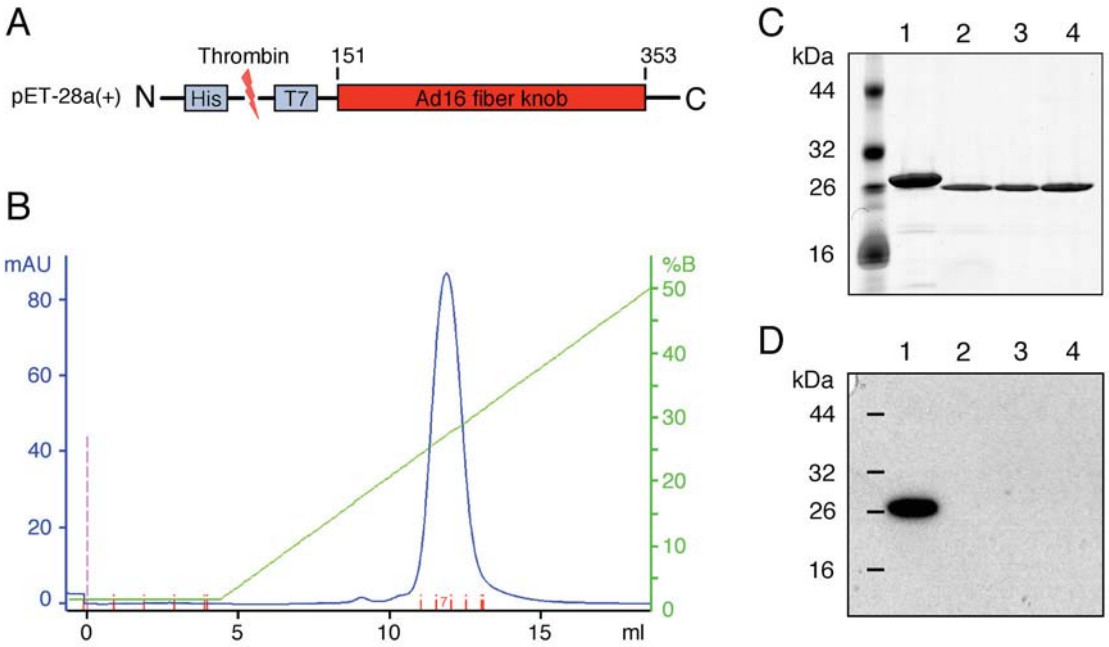

Figure 5.1. **Expression and purification of the Ad16 fiber knob**
(A) cDNA encoding residues 151 to 353 of the Ad16 fiber was inserted into the expression vector pET-28a(+) that adds a thrombin-cleavable 6xHis tag and a T7 tag to the N-terminus of the protein. (B) Following cleavage of the 6x His tag, the fiber knob protein was purified by FPLC on a Resource Q anion exchange column. (C) FK16 protein samples from different stages of the purification were analyzed by SDS-PAGE. (D) Removal of the 6x His tag was verified by Western blot analysis using an anti-6x His tag primary antibody. His-tagged fiber knob protein purified from cell lysate by IMAC (lane 1) and thrombin-cleaved protein without the His-tag (lane 2) contained a considerable amount of impurities. The contaminants as well as potentially uncleaved fiber knob were removed in a step of reverse IMAC (lane 3) and by anion exchange chromatography (elution fraction 7 is shown in lane 4).

5.3.2 Ad-binding activity of soluble CD46

Soluble CD46 (sCD46) was expressed and purified as described in chapter I (Figure 5.2A). To verify that this protein retained its ability to bind adenovirus, I used purified sCD46 to compete Ad infection of CD46-positive human lung epithelial A549 cells (Figure 5.2B). Infection with an Ad5-based vector carrying the Ad16 fiber (Ad5.16F) was efficiently inhibited (>50%) by preincubation of the virions with sCD46, while a control vector carrying the CAR-binding Ad5 fiber (Ad5.5F) was not affected.

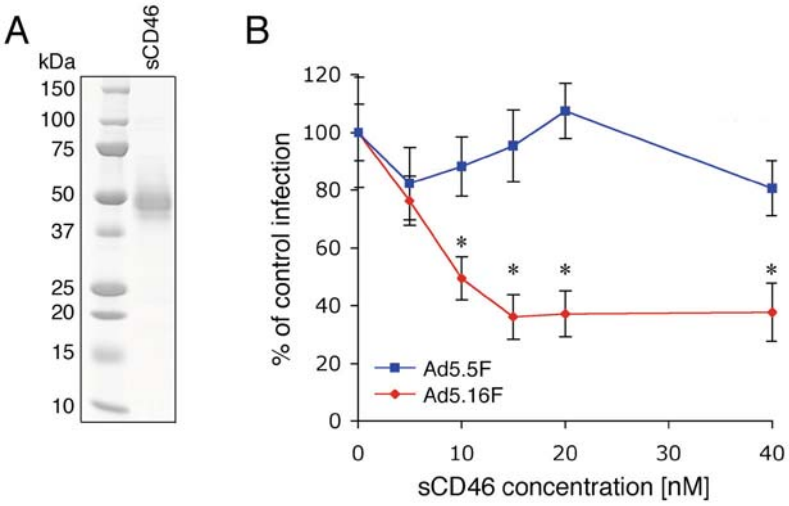

Figure 5.2. **Purified soluble CD46 (sCD46) inhibits CD46-dependent Ad infection.**
(A) Purified sCD46 analyzed by SDS-PAGE. (B) Ad5.5F or Ad5.16F virions were incubated with varying amounts of sCD46 for 1 hour on ice before being added to CAR- and CD46-expressing A549 cells. Following 1 hour incubation on ice, cells were washed three times and incubated over night at 37°C. Infection was determined by detection of GFP transgene expression using flow cytometry. In order to maximize the efficiency of sCD46 activity, the input Ad level was chosen to infect a small number of host cells (~ 5%). Data represents means and standard deviations of triplicates. Data points marked by (*) are significantly different ($p < 0.05$) from the control infection in the absence of sCD46, as determined by Student's T-test.

5.3.3 Kinetic analysis of fiber knob binding to CD46

Although most species B adenoviruses utilize CD46 as their primary receptor, little is known of their relative binding efficiencies. Surface Plasmon Resonance (BIAcore) was therefore used to measure the affinity and kinetics of the interaction between FK11 or FK16 and purified sCD46. Previous studies indicated that fiber knob binding to CD46 immobilized on a biosensor surface is complex due to avidity effects and cannot easily be modeled (Wang et al., 2007). Thus, I covalently coupled Ad fiber knobs to the biosensor surface and measured the association of soluble sCD46. These experiments measured the binding of an sCD46 molecule to a single binding site on the fiber knob without being influenced by potential avidity effects. The association rate (k_a) determined for sCD46 binding to FK11 (Figure 5.3A) was

1.865 x 10^6 M^{-1} s^{-1} and the dissociation constant (k_d) was found to be 0.0108 s^{-1}, resulting in an equilibrium dissociation constant (K_D) of 5.77 nM ($K_D = k_d/k_a$). The association rate constant for sCD46 binding to FK16 (Figure 5.3B) was similar to that of FK11 with a measured k_a of 1.315 x 10^6 M^{-1} s^{-1}. In striking contrast however, the dissociation rate constant obtained for FK16 was more than 50 fold higher than for FK11 with a k_d of 0.575 s^{-1}. These association/dissociation rate constants resulted in a calculated K_D of 437 nM for the binding of sCD46 to FK16, a more than 70 fold lower affinity than that of sCD46 with FK11. As the value determined for the dissociation rate constant for the FK16-sCD46 interaction is at the extreme edge of the recommended range for the biosensor used for these studies, I used equilibrium binding analysis (Morelock et al., 1995) to verify the K_D independent of the on- and off-rates (Figure 5.3C). Non-linear regression analysis revealed a K_D of 431 nM, confirming the overall affinity (K_D) calculated from the association and dissociation rate constants. Further, I verified that none of the sensograms used for the kinetic analysis were influenced by mass transport effects, which can cause inaccuracies in the calculated kinetic constants (Figure 5.3D, E) (Morton and Myszka, 1998).

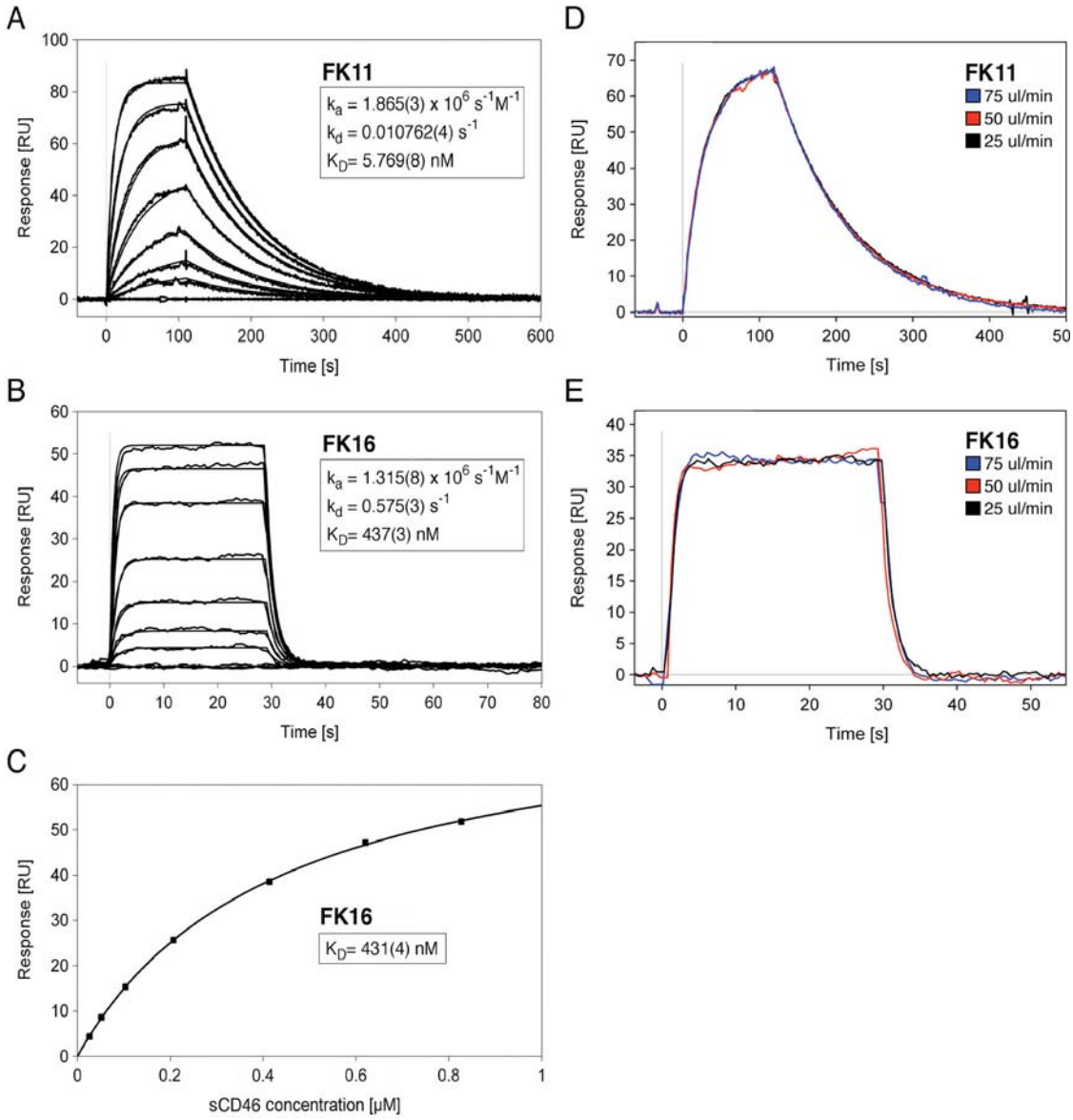

Figure 5.3. **BIAcore analysis of sCD46 binding to Ad fiber knob protein.** sCD46 was injected at varying concentrations over a sensor surface containing immobilized FK11 (A) or FK16 (B). Measured response curves were overlaid with a global fit to a 1:1 interaction model to obtain kinetic constants. Sensograms show one from a duplicate set of injections used for curve fitting. (C) The amount of sCD46 bound to FK16 at equilibrium was plotted against the concentration of injected sCD46. The equilibrium dissociation constant (K_D) was obtained by nonlinear curve fitting of the Langmuir binding model. Values in parentheses represent the error of the fitting procedure in the final digit. (D, E) Injections at different flow rates do not show flow rate-dependent variation of the sensograms, indicating that the binding measured for FK11 and for FK16 is not significantly influenced by mass transport effects.

5.3.4 Comparison of Ad11 and Ad16 binding to CD46-expressing cells

The BIAcore studies were designed to measure the binding of sCD46 to a single binding site on the fiber knob. Under physiological conditions, however, binding of the fiber knob to the cell surface is likely be influenced by avidity effects as revealed by the crystal structure of Ad11 fiber knob complexed with three CD46 molecules (Persson et al., 2007). To assess receptor binding under more physiological conditions, I analyzed fiber knob binding to CHO cells exogenously expressing CD46. In initial studies, I asked whether CD46 is required for efficient attachment of Ad11 or Ad5.16F. Both viruses efficiently bound to CHO-CD46 cells but not to CD46-negative CHO-NULL cells, demonstrating that CD46 is indeed required for cell attachment of these Ad serotypes (Figure 5.4A). Next, I compared the relative binding efficiency of fluorescently labeled Ad11 and Ad5.16F virions to CD46-expressing CHO cells in the presence of increasing amounts of purified Ad11 or Ad16 fiber knobs (Figure 5.4B, C). Flow cytometric analyses showed that FK11 was significantly better at inhibiting Ad11 as well as Ad5.16F attachment to CD46-CHO cells. The CAR-binding Ad5 fiber knob (FK5) did not block virus attachment, confirming the specific interaction of these species B Ads with CD46 (data not shown). These findings indicated that the Ad11 and Ad16 fibers possess distinct binding efficiencies to CD46 on the cell surface.

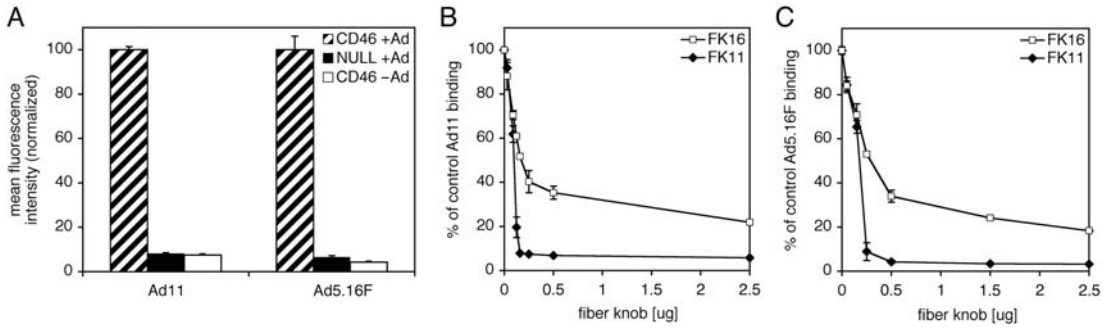

Figure 5.4. **Functional analysis of fiber knob binding to CD46 on cells.**
(A) Stably transfected CHO-K1 cells expressing either CD46 (CD46) or an empty vector (NULL) were incubated in the presence of 30,000 Ad11 or Ad5.16F virus particles per cell. Mean fluorescence intensity measured by flow cytometry was normalized to 100 for CD46 expressing cells incubated with virus. (B, C) CD46 expressing CHO cells were preincubated with different amounts of FK11 or FK16 prior to incubation with Ad11 (B) or Ad5.16F (C) virus. After subtracting the background fluorescence of cells in the absence of virus, the fluorescence of cells incubated with virus in the absence of fiber knob was defined as 100%. Data points represent means of triplicates. Error bars represent standard deviations.

5.3.5 Crystallization of the Ad16 fiber knob

In order to uncover the underlying molecular basis of the relatively low CD46 binding efficiency of Ad16 fiber knob, I decided to crystallize this protein to solve the 3D-structure. I concentrated purified FK16 to 10 mg/ml and obtained microcrystals by sitting drop vapor diffusion in initial crystal screens with two different crystallization buffers composed of either 0.1 M MES monohydrate pH 6.5 and 1.6 M $MgSO_4$ or 0.1 M HEPES pH 7.5, 0.8 M NaH_2PO_4 and 0.8 M KH_2PO_4. Crystal size was improved for both conditions by varying the composition of the crystallization buffers. Nevertheless, crystals grown in HEPES, NaH_2PO_4 and 0.8 M KH_2PO_4 appeared more promising. Given the fact that crystals grown from phosphate-based crystallization buffers frequently turn out to be composed of salt rather than protein, I tested the crystals with IZIT dye that selectively stains protein-crystals and verified that the crystals I obtained consisted of protein. Further refinement of the conditions for sitting as well as hanging drop vapor diffusion yielded the best crystals from a buffer consisting of 0.1 M HEPES (pH 7.5),

0.7 M NaH_2PO_4 and 0.85 M KH_2PO_4. However, crystals grown by hanging drop vapor diffusion turned out to be extremely fragile and were difficult to handle. Therefore, sitting drop vapor diffusion was used to grow the crystals used for data collection. Data from FK16 crystals was collected by Drs. Glen R. Nemerow and Vijay S. Reddy at the GM/CA beamline at APS, Chicago and the computational solution of the protein structure was performed by Sangita Venkataraman and Vijay S. Reddy.

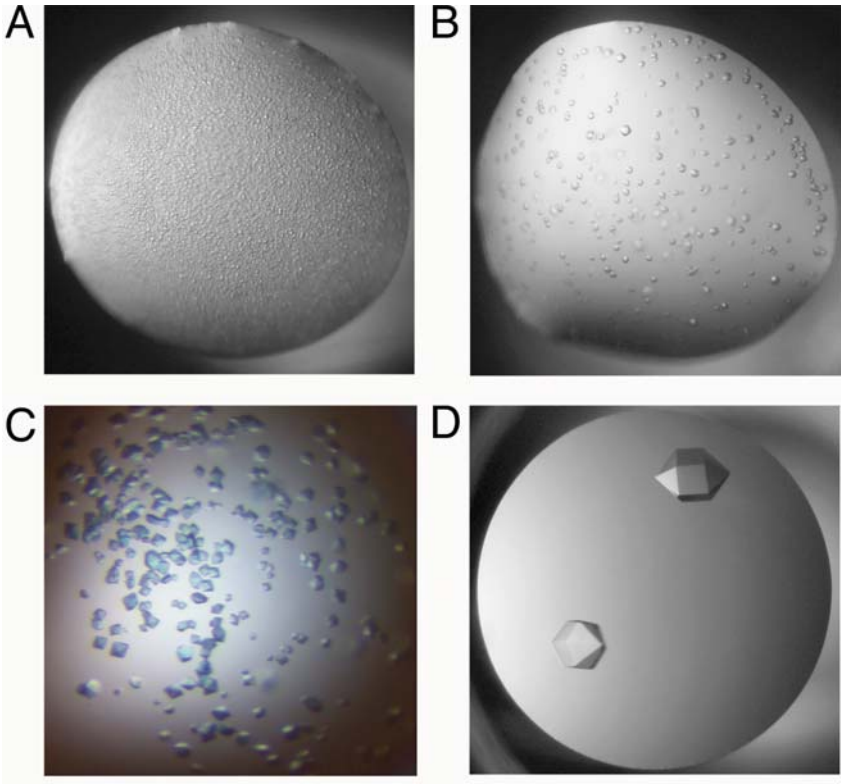

Figure 5.5. **Crystals of the Ad16 fiber knob protein.**
Initial crystallization trials by hanging drop vapor diffusion resulted in microcrystals (A). Crystal size could be improved by varying the concentrations of buffer components (B). Successful staining of the crystals with IZIT crystal dye (C) indicated that the observed crystals were composed of protein. Further changes in the crystallization conditions and the use of sitting drop vapor diffusion resulted in crystals up to 500 nm in size (D).

Table 5.1. **Data statistics**

Parameters	*Data*
Space group	P6522
Resolution range (Å)	50 – 2.4 (2.5 – 2.4)[§]
Unit Cell:	
a, b (Å)	167.830
c (Å)	262.161
No. of unique reflections	84274
I/σ(I)	45.4 (2)
Completeness (%)	99.3 (98.5)
Rmerge* (%)	11.2 (88.1)
R factor/ free R (%)	24.5 / 27.2
No. of Protein atoms/asymmetric unit	9168
No. of Solvent atoms/asymmetric unit	100
RMSD bond (Å)	0.007
RMSD angles (º)	1.5
Average B factor for all atoms ($Å^2$)	65.3
Ramachandran statistics	
Most Favored region (%)	83.2
Additionally allowed region (%)	14.3
Generally allowed region (%)	1.0
Disallowed region (%)	1.5

*$R_{merge} = \sum_{hkl} |I - < I >| / \sum I$
[§]Data in parentheses refer to the last resolution shell

5.3.6 Structure determination of the Ad16 fiber knob

The crystal structure of the Ad16 fiber knob was determined by molecular replacement using Ad11 fiber knob as search model (Table 5.1). Similar to the structure of Ad11 fiber knob, Ad16 fiber knob is a trimer (Figure 5.6) and there are two trimers in the crystallographic asymmetric unit. The structure of Ad16 showed significant deviation from Ad11 at the surface loops (Figure 5.7).

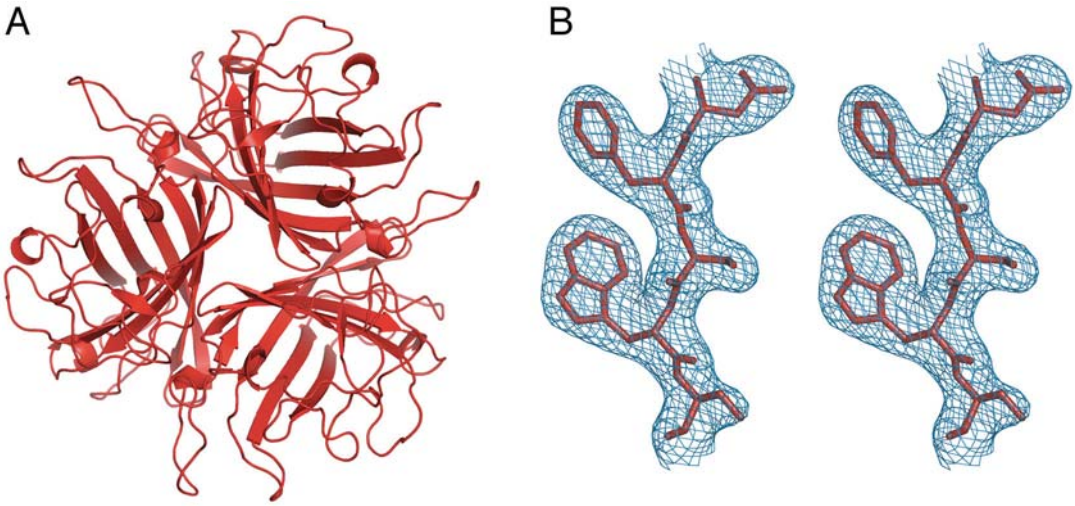

Figure 5.6. **Crystal structure of the Ad16 fiber knob.**
(A) Ribbon diagram showing the crystal structure of the Ad16 fiber knob trimer viewed down the threefold axis. (B) Stereo diagram showing the quality of $2F_o - F_c$ electron density for residues 289 to 293 of the Ad16 fiber contoured at 1.0s.

In order to gain better understanding of the mode of CD46 binding, the structure of the Ad16 fiber knob was superimposed onto the structure of the Ad11-CD46 complex (Persson et al., 2007). In the Ad11-CD46 complex, three loops of Ad11, designated HI, DG and IJ, were found to interact with the SCR domains of CD46. The DG loop in Ad11 fiber knob lacks the E and F β-sheets. Ad16 by contrast contains these β-sheets, forming the corresponding FG loop. The superimposition of Ad16 structure onto the structure of Ad11-CD46 complex revealed that the HI loop adopts similar conformations in both structures while the FG and IJ loop of Ad16 differ significantly from their

counterparts in Ad11. The FG loop is longer and the IJ loop is shorter in the Ad16 structure compared to the corresponding DG and IJ loops in the Ad11 structure. The differences in conformation and length of these loops were considered as potential causes for the reduced CD46 binding to the Ad16 fiber knob. CD46 attachment as shown in Figure 5.7 would likely require the extended FG loop of Ad16 fiber knob to bend out of the way due to steric constraints. Therefore, an analysis of buried surface areas based on this model, as shown for the Ad35 fiber knob in chapter III, would not give a true estimate of the surface area involved in CD46 association Ad16 fiber knob.

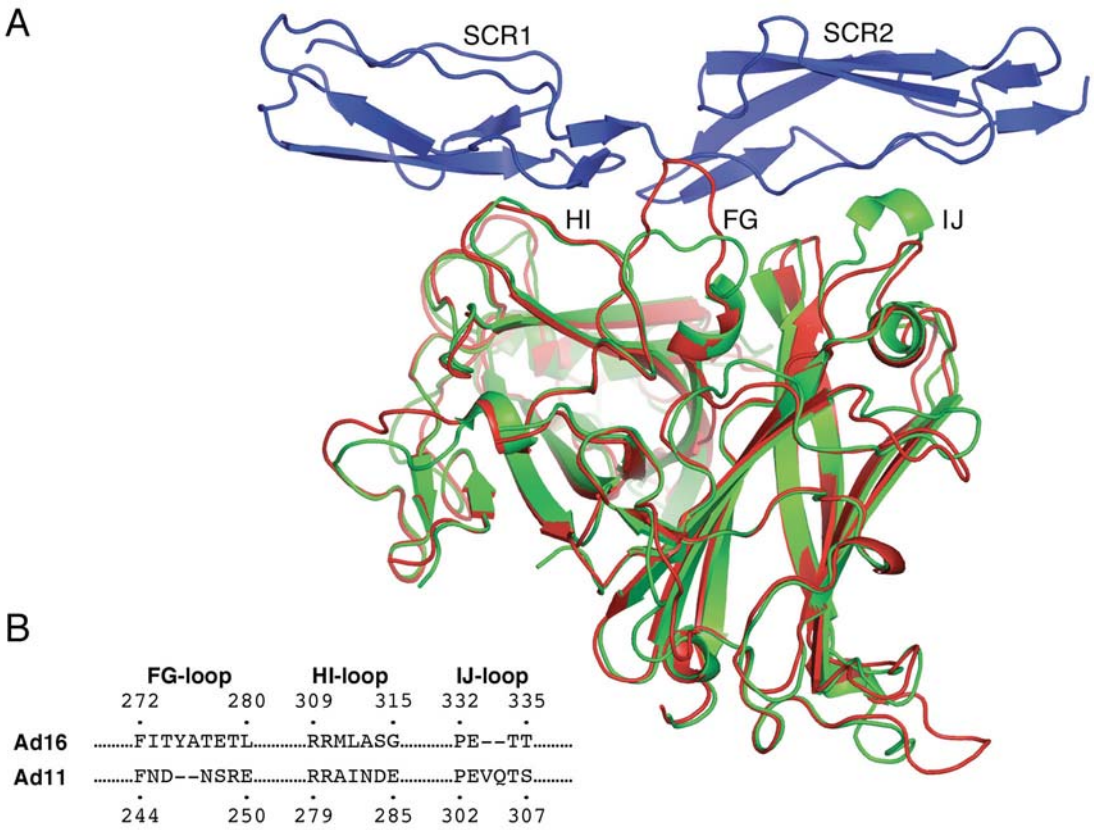

Figure 5.7. **Structural comparison of the Ad16 and Ad11 fiber knobs.**
(A) A ribbon diagram showing two subunits of the Ad16 fiber knob (red) superimposed on the complex of Ad11 fiber knob (green) and SCR1-2 of CD46 (blue). FG, HI and IJ loops of Ad16 are indicated. (B) Structure-based alignment of the amino acids comprising the exposed regions of three surface loops that are likely involved in CD46 binding. The numbers above and below the sequence indicate the position in the intact fiber protein.

5.3.7 Localization of CD46-binding regions in the Ad16 fiber knob

To ascertain the relative contribution of different regions in Ad16 and Ad11 fibers to CD46 interaction, I generated a panel of FK16 and FK11 mutants targeting the HI, FG and IJ loops (Figure 5.8) which, based on the structure model, could impact CD46 binding. Mutations were introduced into the FK16 construct by site directed mutagenesis and the proteins were expressed and purified as previously described. Each of the expressed knobs, with few exceptions, exhibited proper folding and assembly (trimerization) as determined by PAGE electrophoresis.

Fiber Knob type	FG-loop	HI-loop	IJ-loop	expressed	trimerized
FK16	.....NTL.....FITYATETL.....	RRMLASG.....	PE--TT.....	+	+
FK16 R309Q	.....NTL.....FITYATETL.....	QRMLASG.....	PE--TT.....	+	+
FK16 R310N	.....NTL.....FITYATETL.....	RNMLASG.....	PE--TT.....	+	+
FK16 333VQ334	.....NTL.....FITYATETL.....	RRMLASG.....	PEVQTT.....	-	-
FK16 T212M	.....NML.....FITYATETL.....	RRMLASG.....	PE--TT.....	+	+
FK16 T212M, 333VQ334	.....NML.....FITYATETL.....	RRMLASG.....	PEVQTT.....	+	+
FK16 Δ275Y	.....NTL.....FIT-ATETL.....	RRMLASG.....	PE--TT.....	+	+
FK16 Δ276A	.....NTL.....FITY-TETL.....	RRMLASG.....	PE--TT.....	+	+
FK16 Δ275Y/276A	.....NTL.....FIT--TETL.....	RRMLASG.....	PE--TT.....	+	+
FK11	.....NML.....FND--NSRE.....	RRAINDE.....	PEVQTS.....	+	+
FK11 246A247	.....NML.....FNDA-NSRE.....	RRAINDE.....	PEVQTS.....	+	+
FK11 246AA247	.....NML.....FNDAANSRE.....	RRAINDE.....	PEVQTS.....	+	+
FK11 246YA247	.....NML.....FNDYANSRE.....	RRAINDE.....	PEVQTS.....	+	+

Figure 5.8. **Sequences of recombinant fiber knobs containing mutations.** Wild-type and mutant recombinant fiber knob proteins used in the virus binding competition experiments are shown in structure-based alignment. Proper expression and trimerization of fiber knob proteins was verified by semi native gel electrophoresis. Mutated residues are highlighted.

The structural model of the Ad16-CD46 complex suggests that the HI-loop of the fiber knob makes contact with SCR1 and 2 of CD46. The structural features of this receptor-interacting region are highly conserved between Ad11 and Ad16 (Figure 5.9A). The HI-loop of FK11 contains two key arginine residues (R279, R280) that mediate CD46 binding (Persson et al., 2007) and these residues are also conserved in FK16. Arginine 310 (R310) of FK16, corresponding to R280 in FK11, likely makes direct contact with CD46,

possibly forming a salt bridge with glutamic acid 63 (E63). To test this model, I mutated R310 to asparagine, thereby eliminating the positive charge of the side chain. The R310N mutation had a pronounced effect on the ability of FK16 to block virus attachment, essentially eliminating the ability of the fiber knob to compete Ad5.16F virus attachment (Figure 5.9B). The flanking amino acid (R309) in FK16 that corresponds to R279 in FK11 is a residue that has also been identified as critical for CD46 interaction (Gustafsson et al., 2006). R279 does not interact directly with CD46 but is thought to orient the HI and DG loops via association with N247 and R280 (Persson et al., 2007). I therefore substituted R309 in FK16 with a glutamine residue to eliminate the positive charge while retaining the approximate size of the side chain. The R309Q mutation resulted in a substantial loss of CD46 binding as indicated in virus-binding competition assays, although the effect of this particular mutation was somewhat less pronounced than the effect of the R310N mutation. My results demonstrate that the conserved arginine residues in the HI-loop retain their critical function in CD46 binding, suggesting that Ad16 engages the receptor in a fashion similar to that of Ad11.

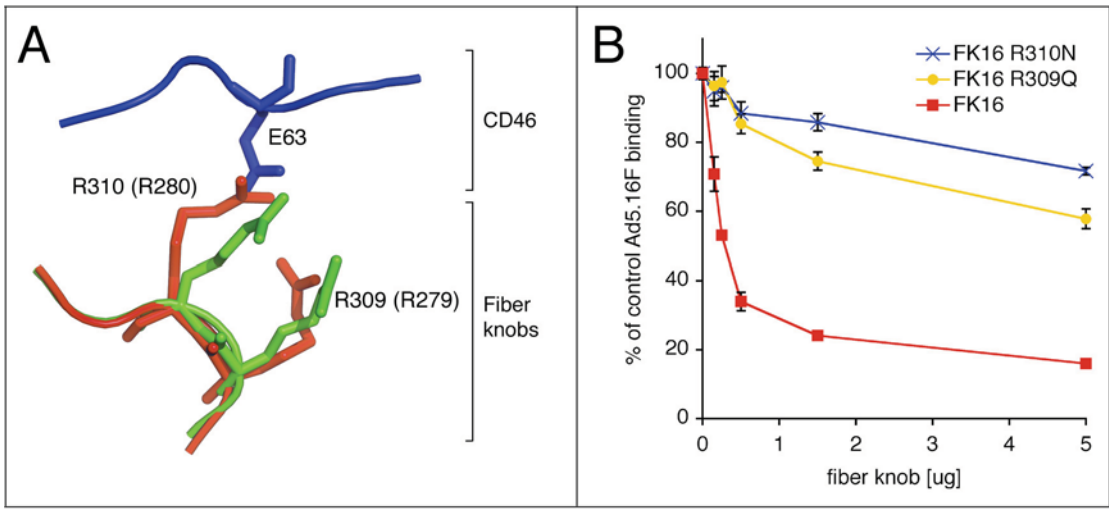

Figure 5.9. **Critical arginine residues in the HI loop are conserved between Ad16 and Ad11 fiber knobs.** (A) Structural comparison of parts of the CD46-binding HI loop of Ad16 (red) and Ad11 (green) in complex with CD46 (blue). E63 of CD46, R309 and R310 of Ad16 and the corresponding arginines of Ad11, R279 and R280

shown as stick representations. (B) Functional analysis of FK16 mutants. CHO cells expressing CD46 were preincubated with varying concentrations of fiber knob mutants targeting the HI loop of FK16 prior to the addition of 30,000 virus particles per cell of Ad5.16F. Mean fluorescence intensity was measured by flow cytometry. Background fluorescence of cells in the absence of virus was subtracted and fluorescence of cells incubated in the presence of virus without preincubation with fiber knob was defined as 100%. Data points represent means of triplicates with standard deviations shown by error bars.

Another CD46 binding region of the fiber knob is comprised of residues in the IJ loop. In Ad11 this loop contains two additional residues relative to that of Ad16, resulting in a longer IJ loop, a situation that could allow greater contact with CD46 based on the structure model (Figure 5.10A). Thus, I investigated whether FK16 binding to CD46 could be enhanced by inserting two residues from FK11 into the IJ loop of FK16. However, a mutant protein with the missing residues valine and glutamine inserted after E333 of FK16 (333VQ334) could not be expressed, suggesting that insertion of these residues in the context of the FK16 interfered with the proper folding and/or trimerization of the molecule. In support of this, I noted that the extended IJ loop of FK11 is likely supported by the large side chain of the buried amino acid, M184. This residue corresponds to T212 with its shorter side chain in FK16. To investigate whether this longer side chain is needed to support the extended IJ loop, I created an additional T212M mutation in FK16. Both constructs, the T212M as well as the combined 333VQ334/T212M mutant could be expressed and retained trimeric organization. Interestingly however, the 333VQ334/T212M mutation did not improve, and actually decreased, the ability to compete virus binding, while the T212M mutation alone inhibited virus attachment to CD46 at levels similar to wild type FK16 (Figure 5.10B). Thus, I conclude that the two extra residues in the IJ loop are not necessary or not beneficial for CD46 association in the context of the Ad16 fiber knob, potentially due to unfavorable interactions with side chains of other residues that are in close proximity.

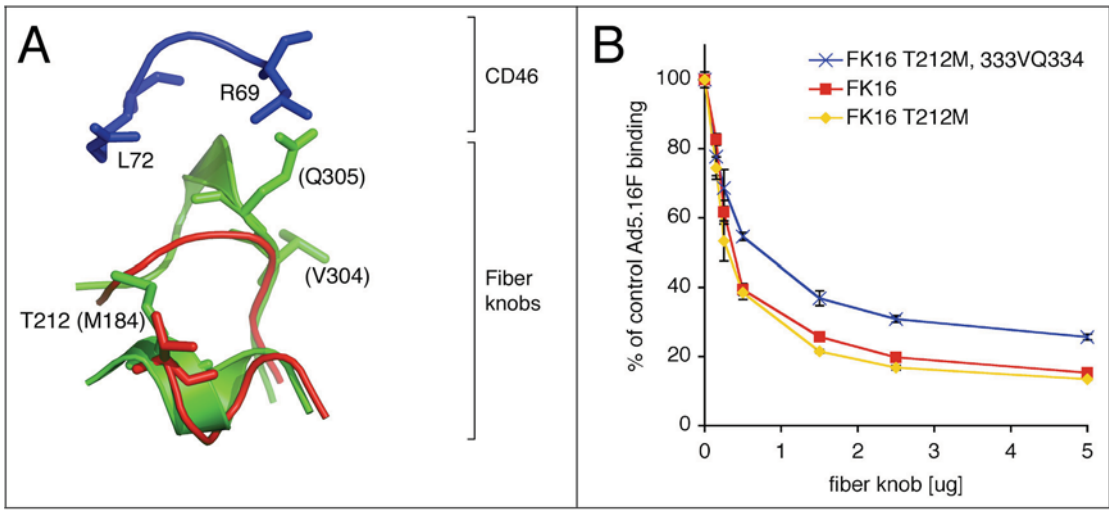

Figure 5.10. **The IJ loop of Ad16 fiber knob is lacking two residues when compared to the corresponding loop of FK11.** (A) Structural comparison of the CD46-binding regions of the IJ loop of Ad16 (red) and Ad11 (green) in complex with CD46 (blue). R69 and L72 of CD46, T212 of Ad16 and V304, Q305 and M184 of Ad11 shown as stick representations. Residues belonging to FK11 in parentheses. (B) Functional analysis of mutants targeting the IJ loop of FK16. Competition assay was performed as described in the legend to Figure 5.9.

One of the most obvious structural differences in the species B Ad fibers is in the FG-loop (Figure 5.11A). Two additional residues in Ad16 result in a longer FG-loop that extends further than the corresponding DG-loop of the Ad11 fiber. The structure model (Figure 5.7A) suggests that this extended loop may need to bend out of the way in order to allow efficient interaction of FK16 with CD46. To investigate the possibility that the longer FG loop of Ad16 fiber interferes with CD46 association, I created two FK16 mutants with either one or two residues removed from the FG-loop. I deleted either Y275 or A276 or both residues since I anticipated that the side chains of these amino acids would not likely be involved in direct critical interactions with CD46. The ΔY275 as well as the ΔA276 mutant each showed a small improvement in CD46 association compared to the wild type FK16. In contrast, the double deletion mutant ΔY275/A276 showed a substantial improvement in CD46 binding as measured in virus competition assays (Figure 5.11B). These findings suggest that the larger FG loop in the FK16 creates steric hindrance

for CD46 association, although the side chains in the extended loop do not appear to contribute to this situation.

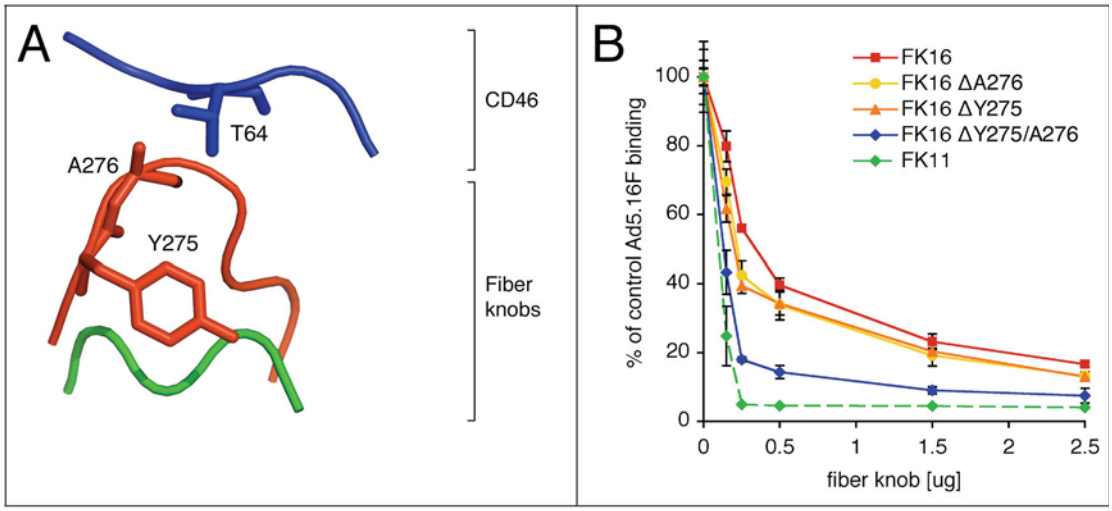

Figure 5.11. **The longer FG loop of Ad16 causes sterical interference with CD46 binding.** (A) Structural comparison of parts of the FG loop of Ad16 (red) and the corresponding DG loop ofAd11 (green) in complex with CD46 (blue). Residues T64 of CD46, Y275 and A276 of Ad16 fiber are shown as stick representations. Side chains of the FK16 FG loop would collide with the CD46 molecule if the loop were positioned as shown in this model. (B) Functional analysis of deletion mutants targeting the FG loop of the Ad16 fiber knob. The competition assay was performed as described in Figure 5.9. The plots are overlaid with a curve (dashed line) showing inhibition by FK11 for comparison.

To investigate further whether the longer FG-loop in Ad16 contributes to a lower CD46 binding efficiency, I next extended the corresponding loop of FK11 in order to resemble that of Ad16 by inserting one or two alanine residues in the DG-loop (246A247 and 246AA247). The insertion of a single alanine resulted in a substantial loss in binding efficiency (Figure 5.12A) and the addition of a second alanine reduced the binding of the Ad11 fiber knob close to the level of FK16. A third mutant consisting of an insertion of a tyrosine and an alanine residue (246YA247) exhibited almost equivalent binding to the 246AA247 mutant, further indicating that length of the loop, rather than composition of the amino acid side chains, modulates CD46 binding. To investigate whether the decreased CD46 binding efficiency on

cells was also reflected in a loss of intrinsic receptor association, I measured the equilibrium dissociation constant (K_D) of the FK11 246AA247 mutant by equilibrium binding analysis (Figure 5.12B). This analysis revealed that the mutant fiber had a substantially reduced binding affinity, K_D of ~377 nM, further indicating that the overall length of the FG loop plays a significant role in regulating the efficiency of CD46 association.

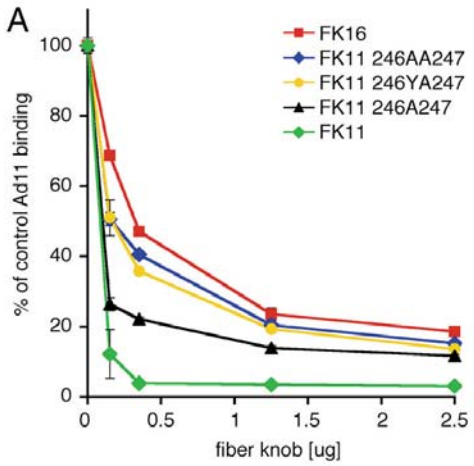

B

Fiber knob	k_a [10^6 $s^{-1}M^{-1}$]	k_d [s^{-1}]	K_D [nM]
FK11	1.865(3)	0.010762(4)	5.769(8)
FK16	1.315(3)	0.575(3)	437(3)
FK11 246AA247	1.16(3)	0.441(3)	379(8)

Figure 5.12. **Effect of mutations in the DG loop on Ad11 binding to CD46.**
(A) Virus-binding competition experiments with insertion mutants targeting the DG loop of Ad11 fiber knob were performed as described in Figure 5.9. Data points represent mean of triplicates with standard deviation shown by error bars. (B) Comparison of the equilibrium dissociation constants (K_D) of Ad11 and Ad16 fiber knob with FK11 246AA247. K_D for FK11 246AA247 was obtained by BIAcore. The level of sCD46 bound to immobilized FK11 246AA247 at equilibrium was measured for varying concentrations of sCD46 and plotted against the concentration of injected sCD46. The equilibrium dissociation constant (K_D) was obtained by nonlinear curve fitting of a 1:1 binding model. Values are shown with the error of the fitting procedure.

5.4 Discussion

My studies described in the previous chapter comparing the CD46 binding efficiency of two species B2 adenoviruses, Ad11 and Ad35, showed that despite subtle structural differences in their CD46 binding sites, both fiber knobs exhibit comparable binding efficiencies (Pache et al., 2008; Persson et al., 2007; Wang et al., 2007). However, it had not been previously determined whether B1 and B2 species utilize CD46 with similar efficiency.

I used surface plasmon resonance (BIAcore) to study the kinetics and affinities of CD46 binding to B1 and B2 adenovirus fiber knobs. The overall affinity of CD46 binding to FK11 measured by BIAcore compared well to that previously reported using isothermal titration calorimetry (ITC) (Persson et al., 2007). The modest difference (5.77 nM vs. ~2 nM) between the two values likely results from the different methods used: ITC detects interactions of two molecules in solution while BIAcore studies are performed on a solid support. The kinetic constants of FK11 determined by BIAcore in my studies are also similar to the published constants of FK35 (K_D of 15.35 nM) (Wang et al., 2007) with a less than three fold difference in overall affinity (K_D). In striking contrast, FK16 exhibited a more than 70 fold lower affinity for soluble CD46 than the FK11. As both, Ad11 and Ad16 are known to use CD46 as receptor, I was surprised to observe such a pronounced difference in CD46 binding. Given the relatively weak intrinsic binding affinity of individual CD46 binding sites on FK16, I wondered whether this might significantly impact virus binding to CD46 on host cells. Fiber-based competition experiments demonstrated that despite the low intrinsic binding affinity for CD46, FK16 was still capable of mediating attachment to CD46 on the cell surface, albeit at a significantly reduced level compared to FK11.

The determination of the FK16 crystal structure allowed me to generate a comparative model of its complex with CD46 to further investigate the underlying structural basis of CD46 binding. While the structure of FK16 is generally very similar to that of other members of species B, distinguishing

features were apparent in the surface loops involved in CD46 binding. In mutagenesis studies, I specifically targeted these loops to shed light on the structure-function relationships between FK11 and FK16. The HI loop is the structurally most conserved of all three loops involved in CD46 binding and has a crucial impact in receptor binding that is retained in FK16. In contrast, the FG and IJ loops show notable structural differences when compared to FK11. Two additional residues extend the FG-loop of FK16 while the IJ-loop lacks two residues present in FK11. I was not able to conclusively determine the impact of the shortened IJ loop in FK16 by mutating it to match that of the Ad11 fiber. I interpret this to mean that either the insertion resulted in additional structural changes by interfering with other residues in the fiber knob or that the elongated IJ loop might not be necessary or beneficial in the context of the Ad16 fiber knob. However, the IJ loop of FK16 is identical to the IJ loop of FK35, the binding efficiency of which closely resembles that of FK11, suggesting that this structural difference is probably not sufficient to explain the striking difference in overall receptor affinities.

The most notable structural difference between the fiber knobs was located in the elongated FG loop of FK16. Interestingly, the protruding loop of FK16 is not shared by any members of B2 adenovirus species. In my studies involving mutants targeting the FG loop of FK16 as well as the corresponding loop of FK11, I demonstrated that the length of the FG loop is a critical structural feature in CD46 binding. In particular, as few as two amino acid residues inserted into the corresponding loop (DG) of FK11 greatly reduced CD46 association, while the absence of these residues in the wild-type fibers of B2 Ad types favored receptor binding. It should be noted, however, that besides the structural differences in the FG loop, other individual residues in the fiber knobs are also likely to significantly influence the binding efficiency of Ad16, as shortening of the FG loop of FK16 to match FK11 did not completely restore optimal CD46 association. This was also reflected by preliminary BIAcore experiments analyzing CD46 binding of the FK16 ΔY275/A276

mutant that showed a substantial improvement in the binding affinity compared to FK16 wild-type, albeit not to the level of FK11.

My findings raise the question of whether other B1 Ads that have been reported to have low or negligible CD46 binding activity might be influenced by their FG loop sequence. The most similar fiber knobs to FK16 are those of Ad3 and Ad7h, based on sequence similarity (Figure 5.13A). Interestingly, there has not been complete agreement on the ability of Ad3 to utilize CD46. While Marttila and colleagues (Marttila et al., 2005) suggested that CD46 is not a receptor for Ad3, other reports have indicated that Ad3 does bind to CD46, albeit at a lower level than certain other serotypes (Fleischli et al., 2005; Sirena et al., 2004). In comparing the sequences of the predicted CD46 binding regions, I noted that the fiber knobs of Ad3 and Ad7h, like Ad16, have an FG loop that is two residues longer than that of species B2 and certain species B1 adenoviruses (Figure 5.13B). A model of the Ad3 crystal structure (Durmort et al., 2001) superimposed onto the Ad11-CD46 SCR1-2 structure shows that the FG loop is indeed extended further than that of B2 adenoviruses and, because of a proline residue close to the apex of the loop, is oriented in a way that binding to CD46 might be even more reduced than that of Ad16 (Figure 5.13C). It is also worth noting that the bend in the FG loop caused by the proline residue likely hinders the side chain of R276 in the Ad3 fiber knob to assume the same orientation as the corresponding R280 in the Ad11 fiber, thereby preventing formation of a critical salt bridge with E63 of CD46. Based on my findings with FK16 and these potential structural similarities with Ad3, I suggest that certain species B1 fibers might share reduced CD46 binding due to a protruding FG loop.

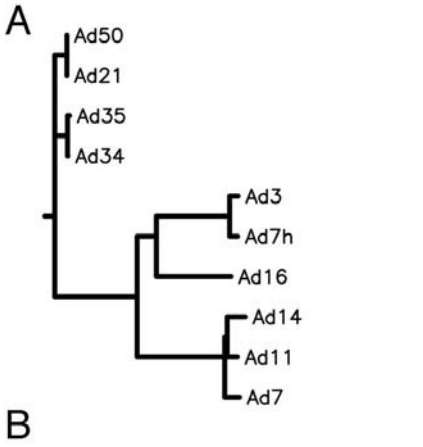

B

Serotype	Apex of FG-loop
Ad16	...YATETLN...
Ad3	...PNAGTDN...
Ad7h	...PNAGTDN...
Ad21	...TTRDS--...
Ad50	...TTRDS--...
Ad34	...TTRDS--...
Ad35	...TTRDS--...
Ad7	...NSREK--...
Ad11p	...NSREK--...
Ad14	...NSREK--...

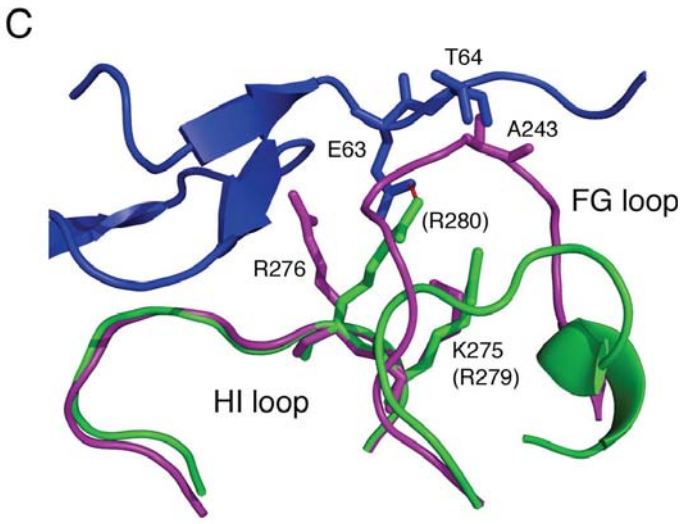

Figure 5.13. **Comparison of species B adenovirus fiber knobs.**
(A) Phylogenetic tree diagram of the amino acid sequence of species B adenovirus fiber knob domains. Sequences were aligned from the TLWT sequence that marks the start of the knob domain to the stop codon. (B) Sequence alignment of the partial FG loop of Ad16 fiber knob (residues 275-281) with the corresponding sequences of other species B Ads. Ad16, Ad3 and Ad7h differ from the other Ad serotypes by having two extra residues in the FG loop. (C) Superimposition of parts of the Ad3 fiber knob structure (PDB-ID 1H7Z) onto the structure of the Ad11-CD46 complex. CD46 is shown in blue, Ad11 in green and Ad3 in purple. The HI and FG loops of Ad3 are indicated. E63 and T64 of CD46, R276 and K275 of Ad3 and the corresponding residues R280 and R279 of Ad11 (in parentheses) are shown as stick representation. Also shown is A243 of Ad3 that collides with T64 of CD46 in the conformation shown. The critical salt bridge between R280 of Ad11 and E63 of CD46 is indicated in red. Note that the Ad3 residue R276 is not optimally positioned to make contact with E63.

One implication of my findings is that the evolutionary pressure that impact sequence variation in external Ad fiber loops (e.g. escaping antibody neutralization) can nonetheless preserve receptor usage due to avidity effects. The fiber knob has been shown to be an important target for the humoral immune response (Krause et al., 2006; Stallwood et al., 2000). During the immune response anti-fiber antibodies appear early, before anti-penton base or anti-hexon antibodies, and are thought to play an important role in the neutralization of adenovirus in combination with anti-penton antibodies. Antibodies against the fiber recognize conformational epitopes on the knob domain of the trimeric fiber protein (Gahery-Segard et al., 1998). Thus, conformational changes caused by variations of exposed surface loops in the fiber knob might be an efficient way for the virus to escape antibody neutralization. In fact, a recent study found that even minor modification of the fiber knob of an Ad5-based vector were sufficient to allow a significant level of escape from preexisting neutralizing antibodies and improved virus transduction *in vivo* (Särkioja et al., 2008). These findings support my implications that structural modifications of a surface loop as accessible as the FG loop in species B Ads could provide the virus a selective advantage by avoiding antibody neutralization, despite a somewhat reduced binding efficiency. Avidity effects provide a relatively large “window” for effective CD46 association on host cells, albeit with distinct efficiencies, thereby allowing a considerable level of sequence variation on exposed loops of the fibers. Given the fact that previous studies indicated that preexisting neutralizing antibodies against epitopes on capsid proteins may negatively impact the expression of transgene products in gene therapy applications (Rosenecker et al., 1996), my results could provide insights for the development of novel gene therapy vectors that preserve receptor binding while evading the host immune response.

6. Overall discussion and future perspectives

Following the discovery that the non CAR-tropic species D adenovirus Ad37 interacts with the integral membrane protein CD46, I investigated the interaction of the Ad37 fiber knob with this receptor. Binding studies showed a weak, albeit significant attachment of a soluble form of CD46 to immobilized Ad37 fiber knob protein. Expression of CD46 on CHO cells that naturally lack this receptor increased virus attachment to the cell surface significantly. However, the level of enhancement was weak compared to that of an Ad5 vector equipped with the fiber knob of species B Ad16 (Ad5.16F). Furthermore, a considerable level of Ad5.37F attachment was observed in the absence of CD46 on the cell surface, indicating that other cell surface molecules besides CD46 play a role in the attachment of this virus. The findings prompted me to investigate whether a previously described interaction with cell surface sialic acid moieties (Arnberg et al., 2000a) influences attachment of the virus to the cell surface. My experiments showed that Ad5.37F bound to and transduced neuraminidase-treated cells with a lower efficiency than untreated cells. Ad5.16F transduction by contrast was not inhibited but rather enhanced, likely due to a reduction of steric or charge-dependent inhibitions as previously suggested (Arcasoy et al., 1997; Arnberg et al., 2000a; Bergelson et al., 1997). However, the effect of neuraminidase treatment on Ad5.37F attachment was less pronounced when CD46 was expressed on the cell surface. This further indicated a role of CD46 in the attachment of Ad37 to the cell surface. The degree to which CD46 and sialic acid contribute to the attachment of Ad37 to the cell surface remains to be investigated though. In this regard, sialic acid interaction with Ad37 has been shown to be of relatively low affinity (Burmeister et al., 2004). Nonetheless, studies of influenza virus hemagglutinin demonstrate that due to avidity effects, the low-affinity binding to sialic acid can be sufficient to mediate virus association to the host cell. However, studies also suggest that in addition to

sialic acid, a separate protein component is likely involved in adenovirus attachment (Burmeister et al., 2004). Whether CD46 alone represents this additional receptor or a separate molecule is involved in the interaction has not been evaluated to date. Nevertheless, the reported co-crystal structure of the Ad11-CD46 complex (Persson et al., 2007) now allows a comparison of the CD46 binding site in species B Ads with the corresponding regions in the Ad37 fiber knob. The structural comparison of the different complex models shows considerable differences between the two fiber knobs. The HI loop of FK37 is shorter that the one of FK11 (Figure 6.1).

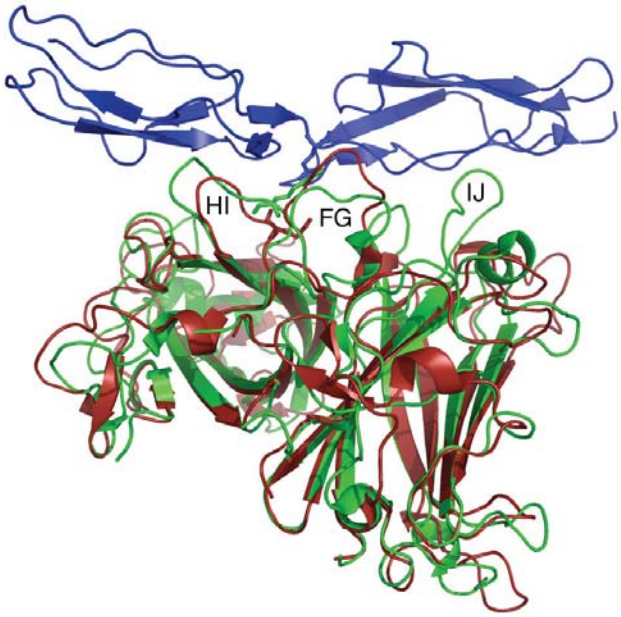

Figure 6.1. **A structural comparison of FK37 with the CD46 binding site of FK11.** The protein structure of two Ad37 fiber knob subunits (dark red) (PDB-ID 1UXE) was superimposed onto the corresponding structure of FK11 (green) in complex with CD46 (blue). Residue R280 in the HI loop of FK11 makes a critical contact with E63 of CD46 (both residues shown as stick representation) while the corresponding Q329 in FK37 cannot make a similar contact. The FG loop of FK37 is longer than the corresponding DG loop of FK11 while its IJ loop is barely visible.

Further, the arginine residue (R280) in the HI loop that forms a critical contact of FK11 with a glutamic acid residue (E63) in CD46 is missing in FK37. Similar to the fiber knobs of Ad16 and Ad3, the FG loop of FK37 is

longer than the corresponding DG loop in FK11 and would pose a steric hindrance for an interaction. Finally, the IJ loop in FK37 is so short that a contact of CD46 with this region of the fiber knob is implausible. Overall, the structural differences of FK37 compared to CD46-binding species B adenoviruses indicate, that an interaction of FK37 with CD46 would likely be mediated by a different binding site. Considering the unresolved role of CD46 in Ad37 infection and the suggested interactions with multiple cell surface molecules, Ad37 did not seem to be a good model for analyzing adenovirus interactions with CD46. Given the fact that species B Ad16 infection showed a clear CD46-dependency in my experiments and other reports (Gaggar et al., 2003), this virus type appeared to represent a more promising model to characterize receptor interaction.

While studying the binding activity of different recombinant fiber knob constructs, I discovered that FK37 significantly enhanced transduction of cells by Ad5 based vectors. The enhancing effect was limited to this particular fiber type since other fiber knobs from species B or C Ads efficiently inhibited CD46- and CAR-mediated transduction, respectively. Further studies indicated that FK37 can bind to the viral capsid in a charge dependent manner and likely functions as an adaptor, mediating attachment of the virus to cell surface sialic acid glycoconjugates. This mechanism might be utilized by Ad37 virus during normal infection. An excess of fiber protein released from Ad37-infected cells together with progeny virions upon cell lysis would enhance virus attachment and thereby infection of cells. An infection enhancing mechanism has also been previously reported for the Ad5 fiber protein (C. J. Cohen et al., 2001; Walters et al., 2002). Excess Ad5 fiber released from cells upon lysis disrupts cell junctions, thus allowing the escape of virions released to the basolateral side of endothelial cells and rendering CAR molecules that are sequestered in tight junctions more accessible to virus attachment. The infection enhancing effect of FK37 was especially pronounced in CD44-positive murine hematopoietic stem cells, a situation

that could have important practical applications. The lab is now testing the routine use of this recombinant fiber knob protein for the transduction of human bone marrow derived progenitor cells (CD44+) cells with adenoviral vectors in gene therapy applications. The Ad5-based vectors used in these trials carrying either CAR-tropic Ad5 fiber or CD46-tropic Ad16 fiber exhibited poor transduction efficiencies in human myeloid progenitor cells. Successful enhancement of virus transduction by FK37 could allow a significant reduction in the number of virus particles needed for such applications.

To gain further insight into the association of species B Ads with CD46, I investigated whether all four receptor isoforms commonly found on human cells could support equivalent levels of virus transduction. The generation of cell lines stably expressing these CD46 isoforms individually allowed me to demonstrate that no obvious isoform-specific differences influenced transduction efficiency. Inhibition of virus transduction by an antibody directed to the N-terminal SCR1 domain of CD46 indicated that the membrane-distal region was the binding site for the Ad fiber knob. By comparing virus transduction of cell lines expressing chimeric forms of CD46, I was able to narrow down the potential binding site to a region comprised of the SCR1 and 2 domains of CD46. My results conflicted with those of a previous study reporting that the binding site for the related species B Ad11 involves the membrane proximal SCR4 domain of CD46 (Segerman et al., 2003b). This earlier finding was based on the observation that an antibody directed to the SCR4 domain of CD46 blocked binding of Ad11 to CD46-expressing CHO cells. However, this antibody inhibited cell attachment of Ad7 as well. Since Ad7 is unlikely to bind to CD46 as indicated by the same group (Gustafsson et al., 2006; Segerman et al., 2003a), I suspect that this antibody produced a non-specific inhibitory effect. My findings that the binding site for species B Ads is comprised of the SCR1 and 2 domains of CD46 were confirmed by the structure determination of the Ad11 fiber knob bound to SCRs 1 and 2 of CD46 (Persson et al., 2007). This structural model provided further insight

into the molecular basis of the association of a species B adenovirus with CD46. However, even within the same Ad species, the fiber knobs of different serotypes show considerable sequence variation. Moreover, species B Ads are further divided into B1 and B2 members. While this division reflects tissue tropism rather than receptor usage, the receptor specificity of individual members of species B, especially of B1 Ads remained unresolved.

In order to determine to what extent CD46 usage is conserved among species B Ads, I initially focused on Ad35, a member of the same subspecies (B2) as Ad11. As part of these studies, I crystallized the Ad35 and Ad16 fiber knob and together with Drs. Vijay Reddy and Sangita Venkataraman, determined their crystal structures. Despite a sequence identity of only 50%, the Ad35 fiber knob showed a strong structural conservation with the Ad11 fiber knob. The most significant structural differences were found within the surface loops that mediate CD46 association. Nevertheless, a comparison of the calculated buried surface areas upon CD46 binding indicated that Ad35FK is likely able to attach to this receptor in a manner comparable to FK11. After confirming CD46-specificity of Ad11 and Ad5.35F attachment, I compared binding of the two fiber knobs to CD46 in competition assays that mimic the binding of adenovirus to cell surface CD46. This assay takes into account potential avidity effects. These studies demonstrated comparable binding efficiencies of Ad11 and Ad35 fiber knobs to CD46-expressing CHO cells. Moreover, the comparison of the kinetic constants I determined for CD46 binding to FK11 with the kinetic data published for the Ad35 fiber knob (Wang et al., 2007) revealed only modest differences in the intrinsic affinity of the binding sites.

My findings could provide valuable information for the development of adenoviral vectors that are being used in clinical gene transfer trials. The majority of these vectors is based on adenovirus type 5 (Ad5), a member of species C that utilizes CAR as its primary receptor (Bergelson et al., 1997). However, a challenge for the use of Ad5-based vectors is the limited

expression of CAR in certain target cell types such as hematopoietic cells (Segerman et al., 2000) or certain malignant tumor isolates (Anders et al., 2003; Fuxe et al., 2003; Hemminki et al., 2003). Moreover, Ad5 based vectors are often prone to neutralization by preexisting anti-capsid antibodies. Considering these obstacles, vectors based on species B may prove to be useful alternatives (Sakurai et al., 2007). In this regard, CD46 is ubiquitously expressed, allowing gene transfer to a broader range of target cells. Further, neutralizing antibodies to species B Ad types are present at lower levels compared to those directed against Ad5 (Vogels et al., 2003). Development of species B based Ad vectors is primarily focused on the serotypes Ad11 and Ad35 (Sakurai et al., 2007). My findings indicate that both viruses could provide suitable alternatives with regards to fiber knob attachment. This presents an opportunity to investigate and compare other properties of these viruses, such as susceptibility to antibody neutralization, to aid in the final selection of suitable Ad vectors.

Next, I sought to investigate whether the level of CD46 binding by species B2 Ads is also conserved among CD46-binding species B1 Ads. I determined the intrinsic binding affinity of CD46 and species B2 Ad11 fiber knob as well as the species B1 Ad16 fiber knob. Surprisingy, BIAcore analysis revealed a more than 70-fold lower binding affinity of FK16. The determined equilibrium dissociation constant (K_D) of 437 nM is among the lowest affinities reported for adenovirus binding to any protein receptor. The low K_D value is caused primarily by a very fast dissociation rate (k_d). To better understand the underlying molecular basis for this pronounced difference in binding affinities, I crystallized the Ad16 fiber knob protein. Subsequent determination of the protein structure allowed the generation of a CD46 binding model by superimposing the FK16 structure onto that of FK11 bound to CD46 SCR1-2. The model revealed a strong structural conservation of the protein structure with only two surface loops, the FG and the IJ loop, showing notable structural differences from FK11. The corresponding loops in FK11

are both directly involved in CD46 binding and therefore the structural differences are likely to impact CD46 binding of FK16. The third loop involved in the receptor interaction, the HI loop, is structurally conserved between both fiber knobs. My experiments confirmed the critical contribution of a conserved salt bridge to the CD46 interaction by the HI loop in both fiber knobs. While the precise effect of the shortened IJ loop in FK16 could not be determined conclusively, targeted mutagenesis studies revealed a significant impact of the extended FG loop on CD46-association by FK16. Due to two extra residues, this loop likely needs to bend out of the way to allow receptor binding. Shortening of this loop by mutagenesis improved Ad16 fiber knob attachment to CD46 on the cell surface significantly, as determined in competition experiments.

Interestingly, two additional members of species B1, Ad3 and Ad7h, share the extended FG loop found in FK16. However, the ability of these Ads to use CD46 as their receptor is controversial in the field. By using the published structure of Ad3FK to generate a model for Ad3FK binding to CD46, I found that the extended FG loop in this fiber knob not only causes a steric hindrance for CD46 association, but due to its shape, likely also impedes the formation of a critical salt bridge between CD46 and the HI loop of the fiber knob (corresponding to R280 and E63 in FK11 and CD46, respectively). To test my hypothesis that the low or absent CD46-binding ability of Ad3FK is at least partially caused by an extended FG loop, future mutagenesis studies could be performed that target this fiber knob region similar to those that I undertook with FK16. These experiments could provide further insight into the receptor usage of Ad3, one of the most commonly isolated species B Ads (Schmitz et al., 1983).

Despite its markedly reduced binding affinity to CD46, the Ad16 fiber knob is still able to mediate efficient attachment to CD46 on cells that allows for internalization of the virus. This is likely due to avidity effects caused by the trimeric conformation of the fiber protein. The crystal structure of the Ad11

fiber knob bound to CD46 SCR1-2 indicated that a fiber knob trimer can bind up to three CD46 molecules, thus increasing stability of the fiber knob attachment to the cell surface significantly. Simultaneous attachment of three CD46 molecules to the fiber protein is mediated by the binding interface on the side of the fiber knob domain. This mode of interaction allows attachment of CD46 molecules to individual binding sites without steric interference. Interestingly, the receptor binding site of CAR-interacting fiber knobs is located in a similar orientation (Figure 6.2). While the fiber knob regions involved in CAR binding are distinct from those mediating CD46 interaction, both binding sites are located at the side of the knob domain. Furthermore, in both cases the receptor-interacting domain is oriented diagonally with respect to the fiber axis. The angled receptor binding orientation might allow for efficient multivalent association with receptor molecules on the cell surface thus increasing virus binding via avidity effects. It is interesting to note that this mechanism might not be simply restricted to adenovirus but also to other unrelated viruses. For example, reovirus, a double-stranded RNA virus, attaches to the cell surface receptor junctional adhesion molecule (JAM) with its σ1 protein (Barton et al., 2001). Although σ1 binds to a distinct receptor, it has a remarkable structural similarity to the adenovirus fiber protein. Interestingly, while a structure for the σ1-JAM complex has not been determined, a JAM binding site was proposed to be located on the side of the C-terminal knob-like domain σ1 (Chappell et al., 2002). This suggests a similar mode of receptor interaction that is conserved among different viruses and at least three different receptors.

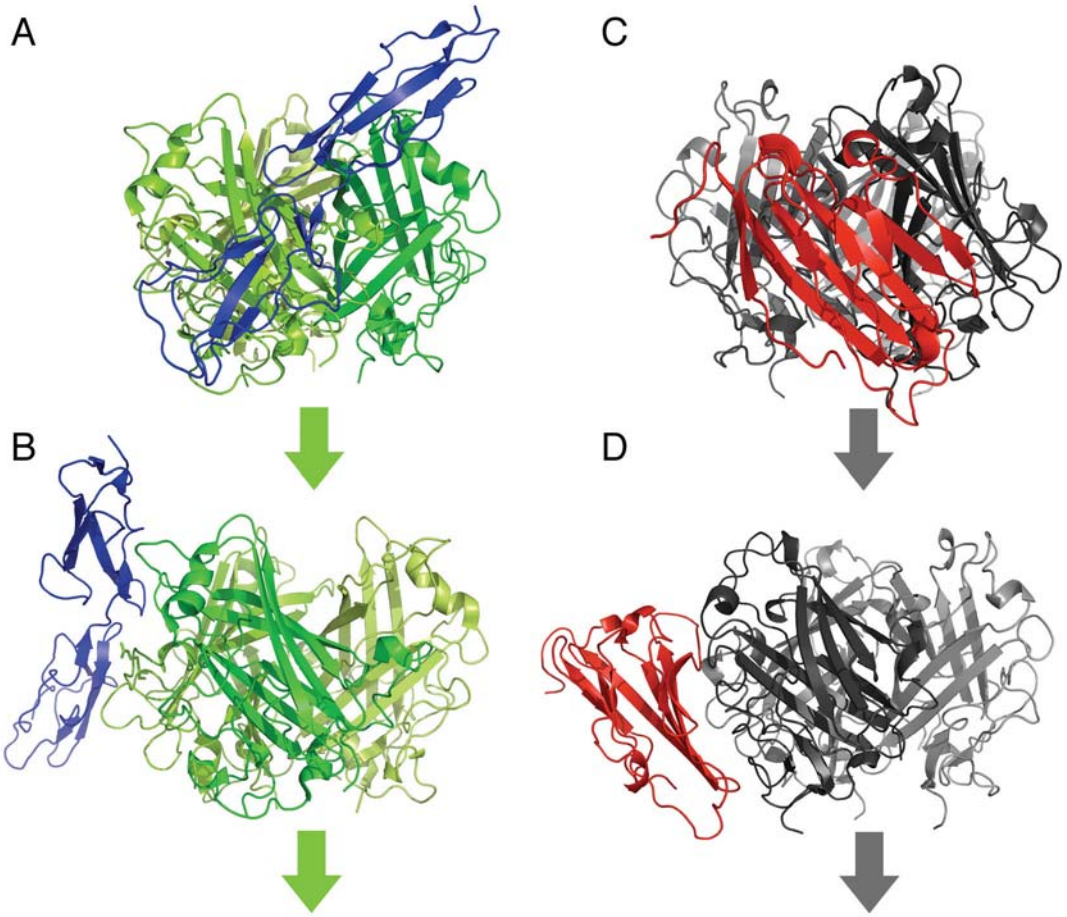

Figure 6.2. **The binding sites for CD46 and CAR are located on the side of the adenovirus fiber knob.** (A, B) Ad11 fiber knob (green) in complex with CD46 SCR1-2 (blue), shown from the side at different viewing angles. The CD46 binding site is stretched diagonally across the side of the fiber knob and encompasses two fiber knob subunits. (C, D) Similar to CD46 attachment to Ad11, the binding site for the CAR D1 domain (red) is located at the side of the Ad12 fiber knob (gray), also in a diagonal orientation. While the binding site is comprised of two fiber knob subunits, the residues critical for binding are contributed by a single subunit. Arrows indicate direction of the fiber shaft. The figures were generated using the program PyMOL (DeLano, 2002) and is based on the crystal structures of the Ad11-CD46 SCR1-2 complex (PDB-ID 2O39) and the Ad12-CAR D1 complex (PDB-ID 1KAC).

The avidity effects likely compensate for a reduced intrinsic binding affinity to a certain degree. While the interaction might be less efficient than that of other Ad fiber knobs, it might be sufficiently strong to enable virus binding to secondary receptors, such as integrins, and allow virus

internalization, which is believed to occur shortly after attachment (Greber et al., 1993). Thus, the avidity effects that strengthen attachment of the fiber knob to the cell surface could allow for a certain amount of sequence diversity (mutation) within the binding site. In my studies presented here, I was able to show that there are not only considerable sequence differences but also structural variations in the fiber knob surface loops among different Ad serotypes, even within the same species. I hypothesized that these structural variations could allow viruses to evade neutralization by preexisting neutralizing antibodies (NAb). In support of this, a recent report demonstrated that even minor modifications within the exposed regions of the fiber knob significantly reduce the level of antibody neutralization by preexisting NAbs *in vivo* (Särkioja et al., 2008). Thus, a small reduction in binding efficiency of the virus might be compensated for by a more effective evasion of neutralizing antibodies.

Differences in receptor affinity resulting from sequence variations in the binding site of the fiber knob domain have previously been reported for CAR-tropic adenoviruses (Howitt et al., 2003; Kirby et al., 2001). However, due to the limited availability of structural data for these fiber knobs, the precise molecular basis for those differences in CAR binding remains to be determined. Nevertheless, it has been suggested that the variations in the fiber knob surface residues likely responsible for those differences in receptor binding efficiency are the result of an antigenic drift due to immunoselective pressure (Howitt et al., 2003). Such sequence variation is a likely cause for an evolution of receptor specificity. While certain species B viruses such as Ads 16, 21, 35 and 50 are thought to use CD46 exclusively as their primary receptor, Ad11 has been reported to use a second, yet to be identified receptor, in addition to CD46. Moreover, Ad serotypes such as 7 and 14 have been suggested to use the newly proposed receptor, designated X, exclusively and lack the ability to bind CD46, despite a strong conservation of the fiber knob sequence (Tuve et al., 2006).

Sequence variations in Ad fibers can give rise to newly emerging Ad subtypes. In May 2006 a virus isolate from a fatal case of adenovirus infection was initially classified as Ad14. However, all samples collected from this and similar cases were distinct from the original strain of this virus and indicated an emerging variant of Ad14. From March to June 2007 a total of 140 reported cases in several states were associated with this new Ad strain that caused severe and sometimes fatal respiratory infections. An unusually high number of these patients were hospitalized (38%), including healthy young adults. An overall mortality rate of 5% was reported (CDC, 2007). The molecular basis for this apparent increased pathogenesis has not been determined. Alternatively, the increased morbidity and mortality could simply be derived from an inadequate immune response or lack of pre-existing antibodies.

The original strain of species B Ad14 (Van Der Veen and Kok, 1957) does not use CD46 efficiently (Tuve et al., 2006). This is likely due to the presence of a glutamine in the HI loop instead of an arginine residue, a mutation that has been shown to abolish CD46-dependent Ad infection in several studies including mine. It is conceivable that a possible gutamine to arginine reversion in the Ad14 mutant could allow the virus to use CD46 in addition to a separate Ad14 receptor. In this case a single point mutation could drastically alter and extend the tropism and infectivity of the virus.

To gain further insight into the cause of the apparent increase in pathogenicity, I suggest the sequencing of the genome of the mutant Ad14 strain, especially of the gene encoding the fiber protein. Should sequencing indeed reveal any mutations in the fiber gene of the emerging Ad14 strain that could possibly affect the CD46 interacting regions, it would be interesting to compare the receptor binding efficiency of the original and the mutant fiber protein in competition assays similar to those described in chapters 4 and 5. These experiments could resolve whether the mutant Ad14 virus gained CD46 binding activity in comparison to the original strain that is thought to

preferably bind to an alternative receptor (Tuve et al., 2006). If mutations are present in the fiber knob that do not affect the CD46 binding ability of the virus, both fiber knobs, the original strain and the mutant Ad, could be assayed for competition of Ad14 infection to reveal whether they bind differently to the newly proposed, yet to be identified receptor. Furthermore, antibody neutralization studies with both Ad14 strains could shed light on the influence of possible mutations on antibody recognition.

Emerging adenoviruses represent a particular problem for the military. Military recruits are at a comparably higher risk of suffering from respiratory infections than the general population, possibly due to significant exposure to stress and overcrowding (G Gray, 1995; G. C. Gray et al., 1999). Adenovirus represents the single largest cause of febrile respiratory infections in the military and is the primary pathogen associated with morbidity among US recruits in training (K. L. Russell et al., 2006b). A study reported that 80% of recruits became infected, 40% ill and about 20% missed one week or more of training due to adenovirus associated illness prior to the introduction of a vaccination program (Ryan et al., 2002). In 1971 the US military implemented a routine vaccination program against the most prevalent serotypes Ad4 and Ad7 which reduced the number of adenovirus-related illnesses by up to 96% (K. L. Russell et al., 2006b). However, production of the vaccine ceased in 1996 and available stocks were depleted by 1999. Subsequently, infection rates have been increasing towards pre-vaccination levels (K. L. Russell et al., 2006a).

Following the first isolation of Ad14 in military recruits in 1957 (Van Der Veen and Kok, 1957), few cases of Ad14-related acute respiratory disease (ARD) have been reported (Lin et al., 2004). Given the fact that Ad14 infections have been extremely rare in the Unites States, seroprevalence of specific antibodies is likely low in the population, suggesting a high susceptibility to this virus (Binn et al., 2007). This could lead to a fast spread and possibly a persistence of Ad14 as a significant cause of ARD. The steady

rise of adenovirus illness among US military recruits since depletion of the vaccine stocks has triggered efforts to restore a systematic vaccination program (K. L. Russell et al., 2006b). Previous studies reported the presence of heterotypic antibodies against species B1 Ad3 and the original strain of species B2 Ad14 following administration of an Ad7 vaccine (Van Der Veen and Prins, 1960). However, it is not known whether the previously used vaccine against species E Ad4 and species B1 Ad7 offers any protection against the emerging strain of mutant Ad14. Further studies of the structural differences among fiber knobs of different species could lead to a better understanding of preexisting antibodies crossblocking adenovirus infection of different serotypes.

Understanding and predicting the adaptive immune response against adenovirus capsids is further important for the development and improvement of Ad vectors for clinical applications. Optimally, the use of adenoviral vectors for vaccine delivery depends on repeated administration of the same vector, which is significantly inhibited by the generation of high titers of antibodies against capsid proteins as a response to vector administration. An important target of these neutralizing antibodies is the fiber knob (Krause et al., 2006; Stallwood et al., 2000). However, even a minor modification of the fiber knob surface can increase the level of escape from preexisting antibodies and improve gene delivery efficacy (Särkioja et al., 2008). Based on my findings that the fiber knob can tolerate a certain level of variation in its surface loops while retaining its receptor binding capability, the use of different fiber proteins or even the generation of new fiber knobs that incorporate modified surface loops could allow the use of different Ad vectors for repeated administration. This could significantly reduce the number of vector particles administered, thus limiting the innate immune response. In this regard, the Ad16 fiber might prove to be an interesting alternative for the predominantly used Ad11 and Ad35 fiber proteins in the development of CD46-specific Ad vectors, despite a comparably lower binding efficiency. Comparing antibody neutralization of

Ad16 with Ad11 and Ad35 in cross-blocking experiments could provide further information not only to better understand the impact of structural differences between fiber proteins but also to assess their suitability for gene delivery applications.

7. Summary

Adenovirus is a major cause of acute respiratory and ocular infections. However, despite their disease association, recombinant forms of this virus are currently being employed for gene transfer applications and vaccine delivery. A large number of the more than 50 identified serotypes of human adenovirus can use the cell surface protein CAR as primary attachment receptor on host cells. Recently, non CAR-using adenoviruses belonging to species B as well as the species D member Ad37 have been found to bind to the integral membrane protein CD46. Upon comparison of their CD46-usage, I found that the species B Ads utilize this primary attachment receptor while Ad37 recognizes CD46 less efficiently and also binds to cells via other host cell molecules, including sialic acid. Unexpectedly, I found that the soluble Ad37 fiber knob actually promoted virus infection through a novel bridging mechanism. Further investigation of the CD46 binding by species B Ads led to the identification of a site comprised of the CD46 domains SCR1 and 2 that mediates attachment of the Ad fiber protein. Structural and functional analysis of the binding site indicated a strong conservation of receptor usage by members of the Ad subspecies B2. However, a detailed kinetic analysis of CD46 binding to the fiber knobs of Ad11 (species B2) and Ad16 (species B1) indicated significant differences in CD46 association. In particular, we observed that Ad16 has a strikingly low binding affinity for CD46 due to an increased dissociation rate. Further structural and functional studies identified an extended surface loop in the Ad16 fiber knob that plays a major role in reduced binding affinity. Nonetheless, avidity effects permit efficient virus attachment and cell entry via CD46. However, the structural variations in the surface loops that regulate receptor affinity might enable this virus to evade preexisting neutralizing antibodies more efficiently. Together, my findings shed further light on CD46 association by distinct adenovirus species and could aid in the selection and development of second generation viral vectors.

8. Zusammenfassung

Adenoviren sind eine häufige Ursache von akuten Infektionen des Respirationstraktes sowie der Augenbindehaut. Trotz der Pathogenität dieses Viruses werden rekombinante Formen zum Gentranfer sowie zur Übertragung von Impfstoffen eingesetzt. Bislang wurden mehr als 50 verschiedene Adenovirustypen identifiziert, von denen die Mehrzahl das Zelloberflächenprotein CAR als primären Rezeptor auf Wirtszellen nutzt. Unlängst wurde festgestellt, daß Adenoviren der Gattung B sowie der zur Gattung D gehörende Adenovirustyp 37, die nicht CAR als Rezeptor nutzen, das integrale Membranprotein CD46 binden können. Durch einen Vergleich der Nutzung von CD46 durch diese Viren konnte ich feststellen, daß Adenoviren der Gattung B dieses Protein als primären Rezeptor nutzen, während Adenovirustyp 37 CD46 mit einem geringeren Wirkungsgrad nutzt und darüberhinaus noch weitere Moleküle an der Zelloberfläche bindet, unter anderem Sialinsäure. Überraschenderweise habe ich entdeckt, daß eine rekombinante Form der Kopfdomäne des Ad37 Fiberproteins die Infektion mit Adenoviren auf eine bisher unbekannte Weise fördert. Durch weitere Untersuchungen der Interaktion mit CD46 konnte ich feststellen, daß die Domänen SCR1 und SCR2 dieses Rezeptors die Bindungsstelle für das Fiberprotein von Adenoviren bilden. Eine Struktur- und Funktionsanalyse der Bindungsstelle deutete auf eine erhebliche Konservierung der Rezeptorinteraktion von Adenoviren der Gattung B2 hin. Eine genaue kinetische Analyse der Interaktion von CD46 mit den Fiberkopfdomänen von Adenoviren der Gattungen B2 (Ad11) und B1 (Ad16) zeigte jedoch deutliche Unterschiede in der Rezeptorbindung auf, wobei insbesondere eine äußerst niedrige Affinität von Ad16 für Cd46 auffiel. Durch weitere Struktur- und Funktionsanalysen konnte eine vorstehende Schlaufe an der Oberfläche des Ad16 Fiberkopfes identifiziert werden, die eine wichtige Ursache für die reduzierte Bindungsaffinität dieses Proteins darstellt. Trotz einer solch

niedrigen Affinität kann der Virus aufgrund von Aviditätseffekten mittels CD46 in Wirtszellen eindringen. Die strukturellen Variationen in den Oberflächenschlaufen des Fiberkopfproteins, die für Unterschiede in der Bindungsaffinität verantwortlich sind, erlauben es dem Virus möglicherweise, neutralisierenden Antikörpern auszuweichen. Meine Forschungsergebnisse geben Aufschluß über die Interaktion von verschiedenen Adenovirustypen mit dem Rezeptor CD46 und können so möglicherweise die Auswahl und Entwicklung von viralen Vektoren der zweiten Generation erleichtern.

References

(CDC), C. f. D. C. a. P. (2007). Acute respiratory disease associated with adenovirus serotype 14--four states, 2006-2007. *MMWR Morb Mortal Wkly Rep* **56**(45)**,** 1181-4.

Abbink, P., Lemckert, A. A., Ewald, B. A., Lynch, D. M., Denholtz, M., Smits, S., Holterman, L., Damen, I., Vogels, R., Thorner, A. R., O'Brien, K. L., Carville, A., Mansfield, K. G., Goudsmit, J., Havenga, M. J., and Barouch, D. H. (2007). Comparative seroprevalence and immunogenicity of six rare serotype recombinant adenovirus vaccine vectors from subgroups B and D. *J Virol* **81**(9)**,** 4654-63.

Adams, E. M., Brown, M. C., Nunge, M., Krych, M., and Atkinson, J. P. (1991). Contribution of the repeating domains of membrane cofactor protein (CD46) of the complement system to ligand binding and cofactor activity. *J Immunol* **147**(9)**,** 3005-11.

Alba, R., Bosch, A., and Chillon, M. (2005). Gutless adenovirus: last-generation adenovirus for gene therapy. *Gene Ther* **12 Suppl 1,** S18-27.

Albinsson, B., and Kidd, A. H. (1999). Adenovirus type 41 lacks an RGD alpha(v)-integrin binding motif on the penton base and undergoes delayed uptake in A549 cells. *Virus Res* **64**(2)**,** 125-36.

Alemany, R., and Curiel, D. T. (2001). CAR-binding ablation does not change biodistribution and toxicity of adenoviral vectors. *Gene Ther* **8**(17)**,** 1347-53.

Amalfitano, A., Hauser, M. A., Hu, H., Serra, D., Begy, C. R., and Chamberlain, J. S. (1998). Production and characterization of improved adenovirus vectors with the E1, E2b, and E3 genes deleted. *J Virol* **72**(2)**,** 926-33.

Anders, M., Christian, C., McMahon, M., McCormick, F., and Korn, W. M. (2003). Inhibition of the Raf/MEK/ERK pathway up-regulates expression of the coxsackievirus and adenovirus receptor in cancer cells. *Cancer Res* **63**(9)**,** 2088-95.

Anderson, C. W. (1990). The proteinase polypeptide of adenovirus serotype 2 virions. *Virology* **177**(1)**,** 259-72.

Arcasoy, S. M., Latoche, J., Gondor, M., Watkins, S. C., Henderson, R. A., Hughey,

R., Finn, O. J., and Pilewski, J. M. (1997). MUC1 and other sialoglycoconjugates inhibit adenovirus-mediated gene transfer to epithelial cells. *Am J Respir Cell Mol Biol* **17**(4)**,** 422-35.

Arnberg, N., Edlund, K., Kidd, A. H., and Wadell, G. (2000a). Adenovirus type 37 uses sialic acid as a cellular receptor. *J Virol* **74**(1)**,** 42-8.

Arnberg, N., Kidd, A. H., Edlund, K., Nilsson, J., Pring-Akerblom, P., and Wadell, G. (2002). Adenovirus type 37 binds to cell surface sialic acid through a charge-dependent interaction. *Virology* **302**(1)**,** 33-43.

Arnberg, N., Kidd, A. H., Edlund, K., Olfat, F., and Wadell, G. (2000b). Initial interactions of subgenus D adenoviruses with A549 cellular receptors: sialic acid versus alpha(v) integrins. *J Virol* **74**(16)**,** 7691-3.

Baker, N. A., Sept, D., Joseph, S., Holst, M. J., and McCammon, J. A. (2001). Electrostatics of nanosystems: application to microtubules and the ribosome. *Proc Natl Acad Sci U S A* **98**(18)**,** 10037-41.

Barton, E. S., Forrest, J. C., Connolly, J. L., Chappell, J. D., Liu, Y., Schnell, F. J., Nusrat, A., Parkos, C. A., and Dermody, T. S. (2001). Junction adhesion molecule is a receptor for reovirus. *Cell* **104**(3)**,** 441-51.

Bayo-Puxan, N., Cascallo, M., Gros, A., Huch, M., Fillat, C., and Alemany, R. (2006). Role of the putative heparan sulfate glycosaminoglycan-binding site of the adenovirus type 5 fiber shaft on liver detargeting and knob-mediated retargeting. *J Gen Virol* **87**(Pt 9)**,** 2487-95.

Beck, K., and Brodsky, B. (1998). Supercoiled protein motifs: the collagen triple-helix and the alpha-helical coiled coil. *J Struct Biol* **122**(1-2)**,** 17-29.

Ben-Israel, H., and Kleinberger, T. (2002). Adenovirus and cell cycle control. *Front Biosci* **7,** d1369-95.

Bergelson, J. M., Cunningham, J. A., Droguett, G., Kurt-Jones, E. A., Krithivas, A., Hong, J. S., Horwitz, M. S., Crowell, R. L., and Finberg, R. W. (1997). Isolation of a common receptor for Coxsackie B viruses and adenoviruses 2 and 5. *Science* **275**(5304)**,** 1320-3.

Berget, S. M., Moore, C., and Sharp, P. A. (1977). Spliced segments at the 5' terminus of adenovirus 2 late mRNA. *Proc Natl Acad Sci U S A* **74**(8)**,** 3171-5.

Berk, A. J. (1986). Adenovirus promoters and E1A transactivation. *Annu Rev Genet*

20, 45-79.

Berkner, K. L., and Sharp, P. A. (1985). Effect of the tripartite leader on synthesis of a non-viral protein in an adenovirus 5 recombinant. *Nucleic Acids Res* **13**(3)**,** 841-57.

Bett, A. J., Prevec, L., and Graham, F. L. (1993). Packaging capacity and stability of human adenovirus type 5 vectors. *J Virol* **67**(10)**,** 5911-21.

Bewley, M. C., Springer, K., Zhang, Y. B., Freimuth, P., and Flanagan, J. M. (1999). Structural analysis of the mechanism of adenovirus binding to its human cellular receptor, CAR. *Science* **286**(5444)**,** 1579-83.

Binn, L. N., Sanchez, J. L., and Gaydos, J. C. (2007). Emergence of adenovirus type 14 in US military recruits--a new challenge. *J Infect Dis* **196**(10)**,** 1436-7.

Bordigoni, P., Carret, A. S., Venard, V., Witz, F., and Le Faou, A. (2001). Treatment of adenovirus infections in patients undergoing allogeneic hematopoietic stem cell transplantation. *Clin Infect Dis* **32**(9)**,** 1290-7.

Bouri, K., Feero, W. G., Myerburg, M. M., Wickham, T. J., Kovesdi, I., Hoffman, E. P., and Clemens, P. R. (1999). Polylysine modification of adenoviral fiber protein enhances muscle cell transduction. *Hum Gene Ther* **10**(10)**,** 1633-40.

Braithwaite, A., Nelson, C., Skulimowski, A., McGovern, J., Pigott, D., and Jenkins, J. (1990). Transactivation of the p53 oncogene by E1a gene products. *Virology* **177**(2)**,** 595-605.

Brunger, A. T., Adams, P. D., Clore, G. M., DeLano, W. L., Gros, P., Grosse-Kunstleve, R. W., Jiang, J. S., Kuszewski, J., Nilges, M., Pannu, N. S., Read, R. J., Rice, L. M., Simonson, T., and Warren, G. L. (1998). Crystallography & NMR system: A new software suite for macromolecular structure determination. *Acta Crystallogr D Biol Crystallogr* **54**(Pt 5)**,** 905-21.

Burmeister, W. P., Guilligay, D., Cusack, S., Wadell, G., and Arnberg, N. (2004). Crystal structure of species D adenovirus fiber knobs and their sialic acid binding sites. *J Virol* **78**(14)**,** 7727-36.

Caillet-Boudin, M. L. (1989). Complementary peptide sequences in partner proteins of the adenovirus capsid. *J Mol Biol* **208**(1)**,** 195-8.

Campos, S. K., and Barry, M. A. (2007). Current advances and future challenges in Adenoviral vector biology and targeting. *Curr Gene Ther* **7**(3)**,** 189-204.

Casasnovas, J. M., Larvie, M., and Stehle, T. (1999). Crystal structure of two CD46

domains reveals an extended measles virus-binding surface. *EMBO J* **18**(11)**,** 2911-22.

Cashman, S. M., Morris, D. J., and Kumar-Singh, R. (2004). Adenovirus type 5 pseudotyped with adenovirus type 37 fiber uses sialic acid as a cellular receptor. *Virology* **324**(1)**,** 129-39.

CCP4 (1994). The CCP4 suite: programs for protein crystallography. *Acta Crystallogr D Biol Crystallogr* **50**(Pt 5)**,** 760-3.

Cepko, C. L., and Sharp, P. A. (1983). Analysis of Ad5 hexon and 100K ts mutants using conformation-specific monoclonal antibodies. *Virology* **129**(1)**,** 137-54.

Chappell, J. D., Prota, A. E., Dermody, T. S., and Stehle, T. (2002). Crystal structure of reovirus attachment protein sigma1 reveals evolutionary relationship to adenovirus fiber. *EMBO J* **21**(1-2)**,** 1-11.

Chatterjee, P. K., Vayda, M. E., and Flint, S. J. (1985). Interactions among the three adenovirus core proteins. *J Virol* **55**(2)**,** 379-86.

Chenna, R., Sugawara, H., Koike, T., Lopez, R., Gibson, T. J., Higgins, D. G., and Thompson, J. D. (2003). Multiple sequence alignment with the Clustal series of programs. *Nucleic Acids Res* **31**(13)**,** 3497-500.

Cheshenko, N., Krougliak, N., Eisensmith, R. C., and Krougliak, V. A. (2001). A novel system for the production of fully deleted adenovirus vectors that does not require helper adenovirus. *Gene Ther* **8**(11)**,** 846-54.

Chiu, C. Y., Mathias, P., Nemerow, G. R., and Stewart, P. L. (1999). Structure of adenovirus complexed with its internalization receptor, alphavbeta5 integrin. *J Virol* **73**(8)**,** 6759-68.

Chiu, C. Y., Wu, E., Brown, S. L., Von Seggern, D. J., Nemerow, G. R., and Stewart, P. L. (2001). Structural analysis of a fiber-pseudotyped adenovirus with ocular tropism suggests differential modes of cell receptor interactions. *J Virol* **75**(11)**,** 5375-80.

Chroboczek, J., Ruigrok, R. W., and Cusack, S. (1995). Adenovirus fiber. *Curr Top Microbiol Immunol* **199 (Pt 1),** 163-200.

Clemens, P. R., Kochanek, S., Sunada, Y., Chan, S., Chen, H. H., Campbell, K. P., and Caskey, C. T. (1996). In vivo muscle gene transfer of full-length dystrophin with an adenoviral vector that lacks all viral genes. *Gene Ther* **3**(11)**,** 965-72.

Cohen, C. J., Shieh, J. T., Pickles, R. J., Okegawa, T., Hsieh, J. T., and Bergelson, J. M. (2001). The coxsackievirus and adenovirus receptor is a transmembrane component of the tight junction. *Proc Natl Acad Sci U S A* **98**(26)**,** 15191-6.

Cohen, G. E. (1997). ALIGN: a program to superimpose protein coordinates, accounting for insertions and deletions. *J Appl Crystallogr* **30,** 1160-1161.

Connelly, S. (1999). Adenoviral vectors for liver-directed gene therapy. *Curr Opin Mol Ther* **1**(5)**,** 565-72.

Coyne, C. B., and Bergelson, J. M. (2005). CAR: a virus receptor within the tight junction. *Adv Drug Deliv Rev* **57**(6)**,** 869-82.

D'Halluin, J. C., Martin, G. R., Torpier, G., and Boulanger, P. A. (1978a). Adenovirus type 2 assembly analyzed by reversible cross-linking of labile intermediates. *J Virol* **26**(2)**,** 357-63.

D'Halluin, J. C., Milleville, M., Boulanger, P. A., and Martin, G. R. (1978b). Temperature-sensitive mutant of adenovirus type 2 blocked in virion assembly: accumulation of light intermediate particles. *J Virol* **26**(2)**,** 344-56.

Dales, S., and Chardonnet, Y. (1973). Early events in the interaction of adenoviruses with HeLa cells. IV. Association with microtubules and the nuclear pore complex during vectorial movement of the inoculum. *Virology* **56**(2)**,** 465-83.

Davison, A. J., Benko, M., and Harrach, B. (2003). Genetic content and evolution of adenoviruses. *J Gen Virol* **84**(Pt 11)**,** 2895-908.

Dechecchi, M. C., Melotti, P., Bonizzato, A., Santacatterina, M., Chilosi, M., and Cabrini, G. (2001). Heparan sulfate glycosaminoglycans are receptors sufficient to mediate the initial binding of adenovirus types 2 and 5. *J Virol* **75**(18)**,** 8772-80.

Dechecchi, M. C., Tamanini, A., Bonizzato, A., and Cabrini, G. (2000). Heparan sulfate glycosaminoglycans are involved in adenovirus type 5 and 2-host cell interactions. *Virology* **268**(2)**,** 382-90.

Defer, C., Belin, M. T., Caillet-Boudin, M. L., and Boulanger, P. (1990). Human adenovirus-host cell interactions: comparative study with members of subgroups B and C. *J Virol* **64**(8)**,** 3661-73.

DeLano, W. L. (2002). The PyMOL Molecular Graphics System. http://www.pymol.org

Denby, L., Work, L. M., Graham, D., Hsu, C., von Seggern, D. J., Nicklin, S. A., and Baker, A. H. (2004). Adenoviral serotype 5 vectors pseudotyped with fibers from subgroup D show modified tropism in vitro and in vivo. *Hum Gene Ther* **15**(11)**,** 1054-64.

Devaux, C., Caillet-Boudin, M. L., Jacrot, B., and Boulanger, P. (1987). Crystallization, enzymatic cleavage, and the polarity of the adenovirus type 2 fiber. *Virology* **161**(1)**,** 121-8.

Dmitriev, I., Krasnykh, V., Miller, C. R., Wang, M., Kashentseva, E., Mikheeva, G., Belousova, N., and Curiel, D. T. (1998). An adenovirus vector with genetically modified fibers demonstrates expanded tropism via utilization of a coxsackievirus and adenovirus receptor-independent cell entry mechanism. *J Virol* **72**(12)**,** 9706-13.

Dolinsky, T. J., Nielsen, J. E., McCammon, J. A., and Baker, N. A. (2004). PDB2PQR: an automated pipeline for the setup of Poisson-Boltzmann electrostatics calculations. *Nucleic Acids Res* **32**(Web Server issue)**,** W665-7.

Dorig, R. E., Marcil, A., Chopra, A., and Richardson, C. D. (1993). The human CD46 molecule is a receptor for measles virus (Edmonston strain). *Cell* **75**(2)**,** 295-305.

Dormitzer, P. R., Sun, Z. Y., Blixt, O., Paulson, J. C., Wagner, G., and Harrison, S. C. (2002). Specificity and affinity of sialic acid binding by the rhesus rotavirus VP8* core. *J Virol* **76**(20)**,** 10512-7.

Durmort, C., Stehlin, C., Schoehn, G., Mitraki, A., Drouet, E., Cusack, S., and Burmeister, W. P. (2001). Structure of the fiber head of Ad3, a non-CAR-binding serotype of adenovirus. *Virology* **285**(2)**,** 302-12.

Edvardsson, B., Everitt, E., Jornvall, H., Prage, L., and Philipson, L. (1976). Intermediates in adenovirus assembly. *J Virol* **19**(2)**,** 533-47.

Fabry, C. M., Rosa-Calatrava, M., Conway, J. F., Zubieta, C., Cusack, S., Ruigrok, R. W., and Schoehn, G. (2005). A quasi-atomic model of human adenovirus type 5 capsid. *EMBO J* **24**(9)**,** 1645-54.

Fanning, A. S., Mitic, L. L., and Anderson, J. M. (1999). Transmembrane proteins in the tight junction barrier. *J Am Soc Nephrol* **10**(6)**,** 1337-45.

PHYLIP (Phylogeny Inference Package) version 3.6: Distributed by the author. Department of Genome Sciences, University of Washington, Seattle

Fleischli, C., Verhaagh, S., Havenga, M., Sirena, D., Schaffner, W., Cattaneo, R., Greber, U. F., and Hemmi, S. (2005). The distal short consensus repeats 1 and 2 of the membrane cofactor protein CD46 and their distance from the cell membrane determine productive entry of species B adenovirus serotype 35. *J Virol* **79**(15)**,** 10013-22.

Ford, E., Nelson, K. E., and Warren, D. (1987). Epidemiology of epidemic keratoconjunctivitis. *Epidemiol Rev* **9,** 244-61.

Freimuth, P., Springer, K., Berard, C., Hainfeld, J., Bewley, M., and Flanagan, J. (1999). Coxsackievirus and adenovirus receptor amino-terminal immunoglobulin V-related domain binds adenovirus type 2 and fiber knob from adenovirus type 12. *J Virol* **73**(2)**,** 1392-8.

Fuhlbrigge, R. C., Fine, S. M., Unanue, E. R., and Chaplin, D. D. (1988). Expression of membrane interleukin 1 by fibroblasts transfected with murine pro-interleukin 1 alpha cDNA. *Proc Natl Acad Sci U S A* **85**(15)**,** 5649-53.

Fuxe, J., Liu, L., Malin, S., Philipson, L., Collins, V. P., and Pettersson, R. F. (2003). Expression of the coxsackie and adenovirus receptor in human astrocytic tumors and xenografts. *Int J Cancer* **103**(6)**,** 723-9.

Gaggar, A., Shayakhmetov, D. M., and Lieber, A. (2003). CD46 is a cellular receptor for group B adenoviruses. *Nat Med* **9**(11)**,** 1408-12.

Gaggar, A., Shayakhmetov, D. M., Liszewski, M. K., Atkinson, J. P., and Lieber, A. (2005). Localization of regions in CD46 that interact with adenovirus. *J Virol* **79**(12)**,** 7503-13.

Gahery-Segard, H., Farace, F., Godfrin, D., Gaston, J., Lengagne, R., Tursz, T., Boulanger, P., and Guillet, J. G. (1998). Immune response to recombinant capsid proteins of adenovirus in humans: antifiber and anti-penton base antibodies have a synergistic effect on neutralizing activity. *J Virol* **72**(3)**,** 2388-97.

Gambke, C., and Deppert, W. (1983). Specific complex of the late nonstructural 100,000-dalton protein with newly synthesized hexon in adenovirus type 2-infected cells. *Virology* **124**(1)**,** 1-12.

Giannakis, E., Jokiranta, T. S., Ormsby, R. J., Duthy, T. G., Male, D. A., Christiansen, D., Fischetti, V. A., Bagley, C., Loveland, B. E., and Gordon, D. L. (2002). Identification of the streptococcal M protein binding site on

membrane cofactor protein (CD46). *J Immunol* **168**(9)**,** 4585-92.

Gorziglia, M. I., Kadan, M. J., Yei, S., Lim, J., Lee, G. M., Luthra, R., and Trapnell, B. C. (1996). Elimination of both E1 and E2 from adenovirus vectors further improves prospects for in vivo human gene therapy. *J Virol* **70**(6)**,** 4173-8.

Graham, F. L., Smiley, J., Russell, W. C., and Nairn, R. (1977). Characteristics of a human cell line transformed by DNA from human adenovirus type 5. *J Gen Virol* **36**(1)**,** 59-74.

Gray, G. (1995). Acute respiratory disease in the military. *Federal Practitioner* **12,** 27-33.

Gray, G. C., Callahan, J. D., Hawksworth, A. W., Fisher, C. A., and Gaydos, J. C. (1999). Respiratory diseases among U.S. military personnel: countering emerging threats. *Emerg Infect Dis* **5**(3)**,** 379-85.

Greber, U. F. (1998). Virus assembly and disassembly: the adenovirus cysteine protease as a trigger factor. *Rev Med Virol* **8**(4)**,** 213-222.

Greber, U. F., Suomalainen, M., Stidwill, R. P., Boucke, K., Ebersold, M. W., and Helenius, A. (1997). The role of the nuclear pore complex in adenovirus DNA entry. *EMBO J* **16**(19)**,** 5998-6007.

Greber, U. F., Willetts, M., Webster, P., and Helenius, A. (1993). Stepwise dismantling of adenovirus 2 during entry into cells. *Cell* **75**(3)**,** 477-86.

Greenstone, H. L., Santoro, F., Lusso, P., and Berger, E. A. (2002). Human Herpesvirus 6 and Measles Virus Employ Distinct CD46 Domains for Receptor Function. *J Biol Chem* **277**(42)**,** 39112-8.

Gunning, P., Leavitt, J., Muscat, G., Ng, S. Y., and Kedes, L. (1987). A human beta-actin expression vector system directs high-level accumulation of antisense transcripts. *Proc Natl Acad Sci U S A* **84**(14)**,** 4831-5.

Gustafsson, D. J., Segerman, A., Lindman, K., Mei, Y. F., and Wadell, G. (2006). The Arg279Gln [corrected] substitution in the adenovirus type 11p (Ad11p) fiber knob abolishes EDTA-resistant binding to A549 and CHO-CD46 cells, converting the phenotype to that of Ad7p. *J Virol* **80**(4)**,** 1897-905.

Havenga, M. J., Lemckert, A. A., Ophorst, O. J., van Meijer, M., Germeraad, W. T., Grimbergen, J., van Den Doel, M. A., Vogels, R., van Deutekom, J., Janson, A. A., de Bruijn, J. D., Uytdehaag, F., Quax, P. H., Logtenberg, T., Mehtali, M., and Bout, A. (2002). Exploiting the natural diversity in adenovirus tropism

for therapy and prevention of disease. *J Virol* **76**(9)**,** 4612-20.

Hemminki, A., Kanerva, A., Liu, B., Wang, M., Alvarez, R. D., Siegal, G. P., and Curiel, D. T. (2003). Modulation of coxsackie-adenovirus receptor expression for increased adenoviral transgene expression. *Cancer Res* **63**(4)**,** 847-53.

Hidaka, C., Milano, E., Leopold, P. L., Bergelson, J. M., Hackett, N. R., Finberg, R. W., Wickham, T. J., Kovesdi, I., Roelvink, P., and Crystal, R. G. (1999). CAR-dependent and CAR-independent pathways of adenovirus vector-mediated gene transfer and expression in human fibroblasts. *J Clin Invest* **103**(4)**,** 579-87.

Hong, J. S., and Engler, J. A. (1991). The amino terminus of the adenovirus fiber protein encodes the nuclear localization signal. *Virology* **185**(2)**,** 758-67.

Hong, J. S., and Engler, J. A. (1996). Domains required for assembly of adenovirus type 2 fiber trimers. *J Virol* **70**(10)**,** 7071-8.

Hourcade, D., Holers, V. M., and Atkinson, J. P. (1989). The regulators of complement activation (RCA) gene cluster. *Adv Immunol* **45,** 381-416.

Howitt, J., Bewley, M. C., Graziano, V., Flanagan, J. M., and Freimuth, P. (2003). Structural basis for variation in adenovirus affinity for the cellular coxsackievirus and adenovirus receptor. *J Biol Chem* **278**(28)**,** 26208-15.

Hsu, C., Boysen, M., Gritton, L. D., Frosst, P. D., Nemerow, G. R., and Von Seggern, D. J. (2005). In vitro dendritic cell infection by pseudotyped adenoviral vectors does not correlate with their in vivo immunogenicity. *Virology* **332**(1)**,** 1-7.

Hsu, E. C., Dorig, R. E., Sarangi, F., Marcil, A., Iorio, C., and Richardson, C. D. (1997). Artificial mutations and natural variations in the CD46 molecules from human and monkey cells define regions important for measles virus binding. *J Virol* **71**(8)**,** 6144-54.

Hu, H., Serra, D., and Amalfitano, A. (1999). Persistence of an [E1-, polymerase-] adenovirus vector despite transduction of a neoantigen into immune-competent mice. *Hum Gene Ther* **10**(3)**,** 355-64.

Huang, S., Reddy, V., Dasgupta, N., and Nemerow, G. R. (1999). A single amino acid in the adenovirus type 37 fiber confers binding to human conjunctival cells. *J Virol* **73**(4)**,** 2798-802.

Iacobelli-Martinez, M., and Nemerow, G. R. (2007). Preferential activation of Toll-like receptor nine by CD46-utilizing adenoviruses. *J Virol* **81**(3)**,** 1305-12.

Iacobelli-Martinez, M., Nepomuceno, R. R., Connolly, J., and Nemerow, G. R. (2005). CD46-utilizing adenoviruses inhibit C/EBPbeta-dependent expression of proinflammatory cytokines. *J Virol* **79**(17)**,** 11259-68.

Johnstone, R. W., Loveland, B. E., and McKenzie, I. F. (1993). Identification and quantification of complement regulator CD46 on normal human tissues. *Immunology* **79**(3)**,** 341-7.

Jones, T. A., Zou, J. Y., Cowan, S. W., and Kjeldgaard, M. (1991). Improved methods for building protein models in electron density maps and the location of errors in these models. *Acta Crystallogr A* **47 (Pt 2),** 110-9.

Källström, H., Blackmer Gill, D., Albiger, B., Liszewski, M. K., Atkinson, J. P., and Jonsson, A. B. (2001). Attachment of Neisseria gonorrhoeae to the cellular pilus receptor CD46: identification of domains important for bacterial adherence. *Cell Microbiol* **3**(3)**,** 133-43.

Källström, H., Liszewski, M. K., Atkinson, J. P., and Jonsson, A. B. (1997). Membrane cofactor protein (MCP or CD46) is a cellular pilus receptor for pathogenic Neisseria. *Mol Microbiol* **25**(4)**,** 639-47.

Kalyuzhniy, O., Di Paolo, N. C., Silvestry, M., Hofherr, S. E., Barry, M. A., Stewart, P. L., and Shayakhmetov, D. M. (2008). Adenovirus serotype 5 hexon is critical for virus infection of hepatocytes in vivo. *Proc Natl Acad Sci U S A* **105**(14)**,** 5483-8.

Karp, C. L., Wysocka, M., Wahl, L. M., Ahearn, J. M., Cuomo, P. J., Sherry, B., Trinchieri, G., and Griffin, D. E. (1996). Mechanism of suppression of cell-mediated immunity by measles virus. *Science* **273**(5272)**,** 228-31.

Kasher, M. S., Wakulchik, M., Cook, J. A., and Smith, M. C. (1993). One-step purification of recombinant human papillomavirus type 16 E7 oncoprotein and its binding to the retinoblastoma gene product. *Biotechniques* **14**(4)**,** 630-41.

Kelkar, S. A., Pfister, K. K., Crystal, R. G., and Leopold, P. L. (2004). Cytoplasmic dynein mediates adenovirus binding to microtubules. *J Virol* **78**(18)**,** 10122-32.

Kirby, I., Davison, E., Beavil, A. J., Soh, C. P., Wickham, T. J., Roelvink, P. W., Kovesdi, I., Sutton, B. J., and Santis, G. (2000). Identification of contact residues and definition of the CAR-binding site of adenovirus type 5 fiber protein. *J Virol* **74**(6)**,** 2804-13.

Kirby, I., Lord, R., Davison, E., Wickham, T. J., Roelvink, P. W., Kovesdi, I., Sutton, B. J., and Santis, G. (2001). Adenovirus type 9 fiber knob binds to the coxsackie B virus-adenovirus receptor (CAR) with lower affinity than fiber knobs of other CAR-binding adenovirus serotypes. *J Virol* **75**(15)**,** 7210-4.

Kleywegt, G. J., and Jones, T. A. (1994). *In* "From first map to final model" (S. Bailey, R. Hubbard, and D. Waller, Eds.), pp. 59-66, SERC Daresbury Laboratory, Warrington, U.K.

Kohfeldt, E., Maurer, P., Vannahme, C., and Timpl, R. (1997). Properties of the extracellular calcium binding module of the proteoglycan testican. *FEBS Lett* **414**(3)**,** 557-61.

Krause, A., Joh, J. H., Hackett, N. R., Roelvink, P. W., Bruder, J. T., Wickham, T. J., Kovesdi, I., Crystal, R. G., and Worgall, S. (2006). Epitopes expressed in different adenovirus capsid proteins induce different levels of epitope-specific immunity. *J Virol* **80**(11)**,** 5523-30.

Kritz, A. B., Nicol, C. G., Dishart, K. L., Nelson, R., Holbeck, S., Von Seggern, D. J., Work, L. M., McVey, J. H., Nicklin, S. A., and Baker, A. H. (2007). Adenovirus 5 fibers mutated at the putative HSPG-binding site show restricted retargeting with targeting peptides in the HI loop. *Mol Ther* **15**(4)**,** 741-9.

Kubo, S., Saeki, Y., Chiocca, E. A., and Mitani, K. (2003). An HSV amplicon-based helper system for helper-dependent adenoviral vectors. *Biochem Biophys Res Commun* **307**(4)**,** 826-30.

Kwong, P. D., Wyatt, R., Robinson, J., Sweet, R. W., Sodroski, J., and Hendrickson, W. A. (1998). Structure of an HIV gp120 envelope glycoprotein in complex with the CD4 receptor and a neutralizing human antibody. *Nature* **393**(6686)**,** 648-59.

Lehmberg, E., Traina, J. A., Chakel, J. A., Chang, R. J., Parkman, M., McCaman, M. T., Murakami, P. K., Lahidji, V., Nelson, J. W., Hancock, W. S., Nestaas, E., and Pungor, E., Jr. (1999). Reversed-phase high-performance liquid chromatographic assay for the adenovirus type 5 proteome. *J Chromatogr B Biomed Sci Appl* **732**(2)**,** 411-23.

Leight, E. R., and Sugden, B. (2000). EBNA-1: a protein pivotal to latent infection by Epstein-Barr virus. *Rev Med Virol* **10**(2)**,** 83-100.

Li, E., Stupack, D., Bokoch, G. M., and Nemerow, G. R. (1998a). Adenovirus

endocytosis requires actin cytoskeleton reorganization mediated by Rho family GTPases. *J Virol* **72**(11)**,** 8806-12.

Li, E., Stupack, D., Klemke, R., Cheresh, D. A., and Nemerow, G. R. (1998b). Adenovirus endocytosis via alpha(v) integrins requires phosphoinositide-3-OH kinase. *J Virol* **72**(3)**,** 2055-61.

Li, J., Lad, S., Yang, G., Luo, Y., Iacobelli-Martinez, M., Primus, F. J., Reisfeld, R. A., and Li, E. (2006). Adenovirus fiber shaft contains a trimerization element that supports peptide fusion for targeted gene delivery. *J Virol* **80**(24)**,** 12324-31.

Li, Q. G., Lindman, K., and Wadell, G. (1997). Hydropathic characteristics of adenovirus hexons. *Arch Virol* **142**(7)**,** 1307-22.

Lin, K. H., Lin, Y. C., Chen, H. L., Ke, G. M., Chiang, C. J., Hwang, K. P., Chu, P. Y., Lin, J. H., Liu, D. P., and Chen, H. Y. (2004). A two decade survey of respiratory adenovirus in Taiwan: the reemergence of adenovirus types 7 and 4. *J Med Virol* **73**(2)**,** 274-9.

Liszewski, M. K., and Atkinson, J. P. (1996). Membrane cofactor protein (MCP; CD46). Isoforms differ in protection against the classical pathway of complement. *J Immunol* **156**(11)**,** 4415-21.

Liszewski, M. K., Leung, M. K., and Atkinson, J. P. (1998). Membrane cofactor protein: importance of N- and O-glycosylation for complement regulatory function. *J Immunol* **161**(7)**,** 3711-8.

Liszewski, M. K., Post, T. W., and Atkinson, J. P. (1991). Membrane cofactor protein (MCP or CD46): newest member of the regulators of complement activation gene cluster. *Annu Rev Immunol* **9,** 431-55.

Liszewski, M. K., Tedja, I., and Atkinson, J. P. (1994). Membrane cofactor protein (CD46) of complement. Processing differences related to alternatively spliced cytoplasmic domains. *J Biol Chem* **269**(14)**,** 10776-9.

Lochmuller, H., Jani, A., Huard, J., Prescott, S., Simoneau, M., Massie, B., Karpati, G., and Acsadi, G. (1994). Emergence of early region 1-containing replication-competent adenovirus in stocks of replication-defective adenovirus recombinants (delta E1 + delta E3) during multiple passages in 293 cells. *Hum Gene Ther* **5**(12)**,** 1485-91.

Logan, J., and Shenk, T. (1984). Adenovirus tripartite leader sequence enhances translation of mRNAs late after infection. *Proc Natl Acad Sci U S A* **81**(12)**,**

3655-9.

Lonberg-Holm, K., Crowell, R. L., and Philipson, L. (1976). Unrelated animal viruses share receptors. *Nature* **259**(5545)**,** 679-81.

Lortat-Jacob, H., Chouin, E., Cusack, S., and van Raaij, M. J. (2001). Kinetic analysis of adenovirus fiber binding to its receptor reveals an avidity mechanism for trimeric receptor-ligand interactions. *J Biol Chem* **276**(12)**,** 9009-15.

Lowe, S. W., and Ruley, H. E. (1993). Stabilization of the p53 tumor suppressor is induced by adenovirus 5 E1A and accompanies apoptosis. *Genes Dev* **7**(4)**,** 535-45.

Lublin, D. M., and Atkinson, J. P. (1989). Decay-accelerating factor: biochemistry, molecular biology, and function. *Annu Rev Immunol* **7,** 35-58.

Lukacik, P., Roversi, P., White, J., Esser, D., Smith, G. P., Billington, J., Williams, P. A., Rudd, P. M., Wormald, M. R., Harvey, D. J., Crispin, M. D., Radcliffe, C. M., Dwek, R. A., Evans, D. J., Morgan, B. P., Smith, R. A., and Lea, S. M. (2004). Complement regulation at the molecular level: the structure of decay-accelerating factor. *Proc Natl Acad Sci U S A* **101**(5)**,** 1279-84.

Lukashok, S. A., and Horwitz, M. S. (1998). New perspectives in adenoviruses. *Curr Clin Top Infect Dis* **18,** 286-305.

Lusky, M., Christ, M., Rittner, K., Dieterle, A., Dreyer, D., Mourot, B., Schultz, H., Stoeckel, F., Pavirani, A., and Mehtali, M. (1998). In vitro and in vivo biology of recombinant adenovirus vectors with E1, E1/E2A, or E1/E4 deleted. *J Virol* **72**(3)**,** 2022-32.

Lutz, P., and Kedinger, C. (1996). Properties of the adenovirus IVa2 gene product, an effector of late-phase-dependent activation of the major late promoter. *J Virol* **70**(3)**,** 1396-405.

Lutz, P., Rosa-Calatrava, M., and Kedinger, C. (1997). The product of the adenovirus intermediate gene IX is a transcriptional activator. *J Virol* **71**(7)**,** 5102-9.

Maione, D., Della Rocca, C., Giannetti, P., D'Arrigo, R., Liberatoscioli, L., Franlin, L. L., Sandig, V., Ciliberto, G., La Monica, N., and Savino, R. (2001). An improved helper-dependent adenoviral vector allows persistent gene expression after intramuscular delivery and overcomes preexisting immunity to adenovirus. *Proc Natl Acad Sci U S A* **98**(11)**,** 5986-91.

Maisner, A., Alvarez, J., Liszewski, M. K., Atkinson, D. J., Atkinson, J. P., and Herrler, G. (1996). The N-glycan of the SCR 2 region is essential for membrane cofactor protein (CD46) to function as a measles virus receptor. *J Virol* **70**(8)**,** 4973-7.

Manchester, M., Gairin, J. E., Patterson, J. B., Alvarez, J., Liszewski, M. K., Eto, D. S., Atkinson, J. P., and Oldstone, M. B. (1997). Measles virus recognizes its receptor, CD46, via two distinct binding domains within SCR1-2. *Virology* **233**(1)**,** 174-84.

Manchester, M., Naniche, D., and Stehle, T. (2000). CD46 as a measles receptor: form follows function. *Virology* **274**(1)**,** 5-10.

Manchester, M., Valsamakis, A., Kaufman, R., Liszewski, M. K., Alvarez, J., Atkinson, J. P., Lublin, D. M., and Oldstone, M. B. (1995). Measles virus and C3 binding sites are distinct on membrane cofactor protein (CD46). *Proc Natl Acad Sci U S A* **92**(6)**,** 2303-7.

Marie, J. C., Astier, A. L., Rivailler, P., Rabourdin-Combe, C., Wild, T. F., and Horvat, B. (2002). Linking innate and acquired immunity: divergent role of CD46 cytoplasmic domains in T cell induced inflammation. *Nat Immunol* **3**(7)**,** 659-66.

Marttila, M., Persson, D., Gustafsson, D., Liszewski, M. K., Atkinson, J. P., Wadell, G., and Arnberg, N. (2005). CD46 is a cellular receptor for all species B adenoviruses except types 3 and 7. *J Virol* **79**(22)**,** 14429-36.

Matthews, B. W. (1968). Solvent content of protein crystals. *J Mol Biol* **33**(2)**,** 491-7.

Matthews, D. A., and Russell, W. C. (1998). Adenovirus core protein V is delivered by the invading virus to the nucleus of the infected cell and later in infection is associated with nucleoli. *J Gen Virol* **79 (Pt 7),** 1671-5.

Maurer, K., Krey, T., Moennig, V., Thiel, H. J., and Rumenapf, T. (2004). CD46 is a cellular receptor for bovine viral diarrhea virus. *J Virol* **78**(4)**,** 1792-9.

Moore, J. P., Klasse, P. J., Dolan, M. J., and Ahuja, S. K. (2008). AIDS/HIV. A STEP into darkness or light? *Science* **320**(5877)**,** 753-5.

Morelock, M. M., Ingraham, R. H., Betageri, R., and Jakes, S. (1995). Determination of receptor-ligand kinetic and equilibrium binding constants using surface plasmon resonance: application to the lck SH2 domain and phosphotyrosyl peptides. *J Med Chem* **38**(8)**,** 1309-18.

Morton, T. A., and Myszka, D. G. (1998). Kinetic analysis of macromolecular interactions using surface plasmon resonance biosensors. *Methods Enzymol* **295,** 268-94.

Murakami, S., Sakurai, F., Kawabata, K., Okada, N., Fujita, T., Yamamoto, A., Hayakawa, T., and Mizuguchi, H. (2007). Interaction of penton base Arg-Gly-Asp motifs with integrins is crucial for adenovirus serotype 35 vector transduction in human hematopoietic cells. *Gene Ther* **14**(21)**,** 1525-33.

Muruve, D. A., Cotter, M. J., Zaiss, A. K., White, L. R., Liu, Q., Chan, T., Clark, S. A., Ross, P. J., Meulenbroek, R. A., Maelandsmo, G. M., and Parks, R. J. (2004). Helper-dependent adenovirus vectors elicit intact innate but attenuated adaptive host immune responses in vivo. *J Virol* **78**(11)**,** 5966-72.

Myszka, D. G. (1999). Improving biosensor analysis. *J Mol Recognit* **12**(5)**,** 279-84.

Nakano, M. Y., Boucke, K., Suomalainen, M., Stidwill, R. P., and Greber, U. F. (2000). The first step of adenovirus type 2 disassembly occurs at the cell surface, independently of endocytosis and escape to the cytosol. *J Virol* **74**(15)**,** 7085-95.

Nepomuceno, R. R., Pache, L., and Nemerow, G. R. (2007). Enhancement of gene transfer to human myeloid cells by adenovirus-fiber complexes. *Mol Ther* **15**(3)**,** 571-8.

Ng, P., Beauchamp, C., Evelegh, C., Parks, R., and Graham, F. L. (2001). Development of a FLP/frt system for generating helper-dependent adenoviral vectors. *Mol Ther* **3**(5 Pt 1)**,** 809-15.

Nicklin, S. A., Wu, E., Nemerow, G. R., and Baker, A. H. (2005). The influence of adenovirus fiber structure and function on vector development for gene therapy. *Mol Ther* **12**(3)**,** 384-93.

Oosterom-Dragon, E. A., and Ginsberg, H. S. (1981). Characterization of two temperature-sensitive mutants of type 5 adenovirus with mutations in the 100,000-dalton protein gene. *J Virol* **40**(2)**,** 491-500.

Otwinowski, Z., and Minor, W. (1997). Processing X-ray diffraction data collected in oscillation mode. *In* "Methods in Enzymology" (C. W. J. Carter, and R. M. Sweet, Eds.), Vol. 276, pp. 307-326. Academic Press, San Diego.

Pache, L., Venkataraman, S., Nemerow, G. R., and Reddy, V. S. (2008). Conservation of fiber structure and CD46 usage by subgroup B2

adenoviruses. *Virology*.

Palmer, D., and Ng, P. (2003). Improved system for helper-dependent adenoviral vector production. *Mol Ther* **8**(5)**,** 846-52.

Palmer, D. J., and Ng, P. (2005). Helper-dependent adenoviral vectors for gene therapy. *Hum Gene Ther* **16**(1)**,** 1-16.

Parker, A. L., Waddington, S. N., Nicol, C. G., Shayakhmetov, D. M., Buckley, S. M., Denby, L., Kemball-Cook, G., Ni, S., Lieber, A., McVey, J. H., Nicklin, S. A., and Baker, A. H. (2006). Multiple vitamin K-dependent coagulation zymogens promote adenovirus-mediated gene delivery to hepatocytes. *Blood* **108**(8)**,** 2554-61.

Parks, R. J., Chen, L., Anton, M., Sankar, U., Rudnicki, M. A., and Graham, F. L. (1996). A helper-dependent adenovirus vector system: removal of helper virus by Cre-mediated excision of the viral packaging signal. *Proc Natl Acad Sci U S A* **93**(24)**,** 13565-70.

Parks, R. J., and Graham, F. L. (1997). A helper-dependent system for adenovirus vector production helps define a lower limit for efficient DNA packaging. *J Virol* **71**(4)**,** 3293-8.

Persson, B. D., Reiter, D. M., Marttila, M., Mei, Y. F., Casasnovas, J. M., Arnberg, N., and Stehle, T. (2007). Adenovirus type 11 binding alters the conformation of its receptor CD46. *Nat Struct Mol Biol* **14**(2)**,** 164-6.

Post, T. W., Liszewski, M. K., Adams, E. M., Tedja, I., Miller, E. A., and Atkinson, J. P. (1991). Membrane cofactor protein of the complement system: alternative splicing of serine/threonine/proline-rich exons and cytoplasmic tails produces multiple isoforms that correlate with protein phenotype. *J Exp Med* **174**(1)**,** 93-102.

Qi, R., Fetzner, S., and Oakley, A. J. (2007). Crystallization and diffraction data of 1H-3-hydroxy-4-oxoquinoline 2,4-dioxygenase: a cofactor-free oxygenase of the alpha/beta-hydrolase family. *Acta Crystallogr Sect F Struct Biol Cryst Commun* **63**(Pt 5)**,** 378-81.

Querido, E., Blanchette, P., Yan, Q., Kamura, T., Morrison, M., Boivin, D., Kaelin, W. G., Conaway, R. C., Conaway, J. W., and Branton, P. E. (2001). Degradation of p53 by adenovirus E4orf6 and E1B55K proteins occurs via a novel mechanism involving a Cullin-containing complex. *Genes Dev* **15**(23)**,** 3104-

17.

Rahman, A., Tsai, V., Goudreau, A., Shinoda, J. Y., Wen, S. F., Ramachandra, M., Ralston, R., Maneval, D., LaFace, D., and Shabram, P. (2001). Specific depletion of human anti-adenovirus antibodies facilitates transduction in an in vivo model for systemic gene therapy. *Mol Ther* **3**(5 Pt 1)**,** 768-78.

Rao, L., Debbas, M., Sabbatini, P., Hockenbery, D., Korsmeyer, S., and White, E. (1992). The adenovirus E1A proteins induce apoptosis, which is inhibited by the E1B 19-kDa and Bcl-2 proteins. *Proc Natl Acad Sci U S A* **89**(16)**,** 7742-6.

Raschperger, E., Thyberg, J., Pettersson, S., Philipson, L., Fuxe, J., and Pettersson, R. F. (2006). The coxsackie- and adenovirus receptor (CAR) is an in vivo marker for epithelial tight junctions, with a potential role in regulating permeability and tissue homeostasis. *Exp Cell Res* **312**(9)**,** 1566-80.

Read, R. J. (2001). Pushing the boundaries of molecular replacement with maximum likelihood. *Acta Crystallogr D Biol Crystallogr* **57**(Pt 10)**,** 1373-82.

Reddy, P. S., Sakhuja, K., Ganesh, S., Yang, L., Kayda, D., Brann, T., Pattison, S., Golightly, D., Idamakanti, N., Pinkstaff, A., Kaloss, M., Barjot, C., Chamberlain, J. S., Kaleko, M., and Connelly, S. (2002). Sustained human factor VIII expression in hemophilia A mice following systemic delivery of a gutless adenoviral vector. *Mol Ther* **5**(1)**,** 63-73.

Rezcallah, M. S., Hodges, K., Gill, D. B., Atkinson, J. P., Wang, B., and Cleary, P. P. (2005). Engagement of CD46 and alpha5beta1 integrin by group A streptococci is required for efficient invasion of epithelial cells. *Cell Microbiol* **7**(5)**,** 645-53.

Riley-Vargas, R. C., Gill, D. B., Kemper, C., Liszewski, M. K., and Atkinson, J. P. (2004). CD46: expanding beyond complement regulation. *Trends Immunol* **25**(9)**,** 496-503.

Ritter, M. R., Banin, E., Moreno, S. K., Aguilar, E., Dorrell, M. I., and Friedlander, M. (2006). Myeloid progenitors differentiate into microglia and promote vascular repair in a model of ischemic retinopathy. *J Clin Invest* **116**(12)**,** 3266-76.

Roberts, D. M., Nanda, A., Havenga, M. J., Abbink, P., Lynch, D. M., Ewald, B. A., Liu, J., Thorner, A. R., Swanson, P. E., Gorgone, D. A., Lifton, M. A., Lemckert, A. A., Holterman, L., Chen, B., Dilraj, A., Carville, A., Mansfield, K. G., Goudsmit, J., and Barouch, D. H. (2006). Hexon-chimaeric adenovirus

serotype 5 vectors circumvent pre-existing anti-vector immunity. *Nature* **441**(7090)**,** 239-43.

Roelvink, P. W., Lizonova, A., Lee, J. G., Li, Y., Bergelson, J. M., Finberg, R. W., Brough, D. E., Kovesdi, I., and Wickham, T. J. (1998). The coxsackievirus-adenovirus receptor protein can function as a cellular attachment protein for adenovirus serotypes from subgroups A, C, D, E, and F. *J Virol* **72**(10)**,** 7909-15.

Roelvink, P. W., Mi Lee, G., Einfeld, D. A., Kovesdi, I., and Wickham, T. J. (1999). Identification of a conserved receptor-binding site on the fiber proteins of CAR-recognizing adenoviridae. *Science* **286**(5444)**,** 1568-71.

Rosenecker, J., Harms, K. H., Bertele, R. M., Pohl-Koppe, A., v Mutius, E., Adam, D., and Nicolai, T. (1996). Adenovirus infection in cystic fibrosis patients: implications for the use of adenoviral vectors for gene transfer. *Infection* **24**(1)**,** 5-8.

Ruigrok, R. W., Barge, A., Albiges-Rizo, C., and Dayan, S. (1990). Structure of adenovirus fibre. II. Morphology of single fibres. *J Mol Biol* **215**(4)**,** 589-96.

Russell, K. L., Broderick, M. P., Franklin, S. E., Blyn, L. B., Freed, N. E., Moradi, E., Ecker, D. J., Kammerer, P. E., Osuna, M. A., Kajon, A. E., Morn, C. B., and Ryan, M. A. (2006a). Transmission dynamics and prospective environmental sampling of adenovirus in a military recruit setting. *J Infect Dis* **194**(7)**,** 877-85.

Russell, K. L., Hawksworth, A. W., Ryan, M. A., Strickler, J., Irvine, M., Hansen, C. J., Gray, G. C., and Gaydos, J. C. (2006b). Vaccine-preventable adenoviral respiratory illness in US military recruits, 1999-2004. *Vaccine* **24**(15)**,** 2835-42.

Russell, S. (2004). CD46: a complement regulator and pathogen receptor that mediates links between innate and acquired immune function. *Tissue Antigens* **64**(2)**,** 111-8.

Russell, S. M., Sparrow, R. L., McKenzie, I. F., and Purcell, D. F. (1992). Tissue-specific and allelic expression of the complement regulator CD46 is controlled by alternative splicing. *Eur J Immunol* **22**(6)**,** 1513-8.

Ryan, M. A., Gray, G. C., Smith, B., McKeehan, J. A., Hawksworth, A. W., and Malasig, M. D. (2002). Large epidemic of respiratory illness due to adenovirus

types 7 and 3 in healthy young adults. *Clin Infect Dis* **34**(5)**,** 577-82.

Saban, S. D., Silvestry, M., Nemerow, G. R., and Stewart, P. L. (2006). Visualization of alpha-helices in a 6-angstrom resolution cryoelectron microscopy structure of adenovirus allows refinement of capsid protein assignments. *J Virol* **80**(24)**,** 12049-59.

Sakurai, F., Kawabata, K., and Mizuguchi, H. (2007). Adenovirus vectors composed of subgroup B adenoviruses. *Curr Gene Ther* **7**(4)**,** 229-38.

Sakurai, F., Murakami, S., Kawabata, K., Okada, N., Yamamoto, A., Seya, T., Hayakawa, T., and Mizuguchi, H. (2006). The short consensus repeats 1 and 2, not the cytoplasmic domain, of human CD46 are crucial for infection of subgroup B adenovirus serotype 35. *J Control Release* **113**(3)**,** 271-8.

Salzwedel, K., and Berger, E. A. (2000). Cooperative subunit interactions within the oligomeric envelope glycoprotein of HIV-1: functional complementation of specific defects in gp120 and gp41. *Proc Natl Acad Sci U S A* **97**(23)**,** 12794-9.

Sandig, V., Youil, R., Bett, A. J., Franlin, L. L., Oshima, M., Maione, D., Wang, F., Metzker, M. L., Savino, R., and Caskey, C. T. (2000). Optimization of the helper-dependent adenovirus system for production and potency in vivo. *Proc Natl Acad Sci U S A* **97**(3)**,** 1002-7.

Santoro, F., Kennedy, P. E., Locatelli, G., Malnati, M. S., Berger, E. A., and Lusso, P. (1999). CD46 is a cellular receptor for human herpesvirus 6. *Cell* **99**(7)**,** 817-27.

Sarkioja, M., Pesonen, S., Raki, M., Hakkarainen, T., Salo, J., Ahonen, M. T., Kanerva, A., and Hemminki, A. (2008). Changing the adenovirus fiber for retaining gene delivery efficacy in the presence of neutralizing antibodies. *Gene Ther* **15**(12)**,** 921-9.

Särkioja, M., Pesonen, S., Raki, M., Hakkarainen, T., Salo, J., Ahonen, M. T., Kanerva, A., and Hemminki, A. (2008). Changing the adenovirus fiber for retaining gene delivery efficacy in the presence of neutralizing antibodies. *Gene Ther* **15**(12)**,** 921-9.

Sarnow, P., Ho, Y. S., Williams, J., and Levine, A. J. (1982). Adenovirus E1b-58kd tumor antigen and SV40 large tumor antigen are physically associated with the same 54 kd cellular protein in transformed cells. *Cell* **28**(2)**,** 387-94.

Sauter, N. K., Bednarski, M. D., Wurzburg, B. A., Hanson, J. E., Whitesides, G. M., Skehel, J. J., and Wiley, D. C. (1989). Hemagglutinins from two influenza virus variants bind to sialic acid derivatives with millimolar dissociation constants: a 500-MHz proton nuclear magnetic resonance study. *Biochemistry* **28**(21)**,** 8388-96.

Schmitz, H., Wigand, R., and Heinrich, W. (1983). Worldwide epidemiology of human adenovirus infections. *Am J Epidemiol* **117**(4)**,** 455-66.

Segerman, A., Arnberg, N., Erikson, A., Lindman, K., and Wadell, G. (2003a). There are two different species B adenovirus receptors: sBAR, common to species B1 and B2 adenoviruses, and sB2AR, exclusively used by species B2 adenoviruses. *J Virol* **77**(2)**,** 1157-62.

Segerman, A., Atkinson, J. P., Marttila, M., Dennerquist, V., Wadell, G., and Arnberg, N. (2003b). Adenovirus type 11 uses CD46 as a cellular receptor. *J Virol* **77**(17)**,** 9183-91.

Segerman, A., Mei, Y. F., and Wadell, G. (2000). Adenovirus types 11p and 35p show high binding efficiencies for committed hematopoietic cell lines and are infective to these cell lines. *J Virol* **74**(3)**,** 1457-1467.

Seiradake, E., Lortat-Jacob, H., Billet, O., Kremer, E. J., and Cusack, S. (2006). Structural and mutational analysis of human Ad37 and canine adenovirus 2 fiber heads in complex with the D1 domain of coxsackie and adenovirus receptor. *J Biol Chem* **281**(44)**,** 33704-16.

Shayakhmetov, D. M., Eberly, A. M., Li, Z. Y., and Lieber, A. (2005a). Deletion of penton RGD motifs affects the efficiency of both the internalization and the endosome escape of viral particles containing adenovirus serotype 5 or 35 fiber knobs. *J Virol* **79**(2)**,** 1053-61.

Shayakhmetov, D. M., Gaggar, A., Ni, S., Li, Z. Y., and Lieber, A. (2005b). Adenovirus binding to blood factors results in liver cell infection and hepatotoxicity. *J Virol* **79**(12)**,** 7478-91.

Shayakhmetov, D. M., and Lieber, A. (2000). Dependence of adenovirus infectivity on length of the fiber shaft domain. *J Virol* **74**(22)**,** 10274-86.

Shenk, T. (1996). Adenoviridae: The viruses and their replication. *In* "Virology" (B. N. Fields, D. M. Knipe, P. M. Howley, and R. M. Chancock, Eds.), pp. 2111-2148. Lippincott-Raven Publishers, Philadelphia, PA.

Short, J. J., Pereboev, A. V., Kawakami, Y., Vasu, C., Holterman, M. J., and Curiel, D. T. (2004). Adenovirus serotype 3 utilizes CD80 (B7.1) and CD86 (B7.2) as cellular attachment receptors. *Virology* **322**(2)**,** 349-59.

Short, J. J., Vasu, C., Holterman, M. J., Curiel, D. T., and Pereboev, A. (2006). Members of adenovirus species B utilize CD80 and CD86 as cellular attachment receptors. *Virus Res* **122**(1-2)**,** 144-53.

Shtrichman, R., Sharf, R., Barr, H., Dobner, T., and Kleinberger, T. (1999). Induction of apoptosis by adenovirus E4orf4 protein is specific to transformed cells and requires an interaction with protein phosphatase 2A. *Proc Natl Acad Sci U S A* **96**(18)**,** 10080-5.

Sirena, D., Lilienfeld, B., Eisenhut, M., Kalin, S., Boucke, K., Beerli, R. R., Vogt, L., Ruedl, C., Bachmann, M. F., Greber, U. F., and Hemmi, S. (2004). The human membrane cofactor CD46 is a receptor for species B adenovirus serotype 3. *J Virol* **78**(9)**,** 4454-62.

Smith, A., Santoro, F., Di Lullo, G., Dagna, L., Verani, A., and Lusso, P. (2003a). Selective suppression of IL-12 production by human herpesvirus 6. *Blood* **102**(8)**,** 2877-84.

Smith, T. A., Idamakanti, N., Marshall-Neff, J., Rollence, M. L., Wright, P., Kaloss, M., King, L., Mech, C., Dinges, L., Iverson, W. O., Sherer, A. D., Markovits, J. E., Lyons, R. M., Kaleko, M., and Stevenson, S. C. (2003b). Receptor interactions involved in adenoviral-mediated gene delivery after systemic administration in non-human primates. *Hum Gene Ther* **14**(17)**,** 1595-604.

Smith, T. A., Idamakanti, N., Rollence, M. L., Marshall-Neff, J., Kim, J., Mulgrew, K., Nemerow, G. R., Kaleko, M., and Stevenson, S. C. (2003c). Adenovirus serotype 5 fiber shaft influences in vivo gene transfer in mice. *Hum Gene Ther* **14**(8)**,** 777-87.

Spiller, O. B., Goodfellow, I. G., Evans, D. J., Almond, J. W., and Morgan, B. P. (2000). Echoviruses and coxsackie B viruses that use human decay-accelerating factor (DAF) as a receptor do not bind the rodent analogues of DAF. *J Infect Dis* **181**(1)**,** 340-3.

Stallwood, Y., Fisher, K. D., Gallimore, P. H., and Mautner, V. (2000). Neutralisation of adenovirus infectivity by ascitic fluid from ovarian cancer patients. *Gene Ther* **7**(8)**,** 637-43.

Steinbacher, S., Seckler, R., Miller, S., Steipe, B., Huber, R., and Reinemer, P. (1994). Crystal structure of P22 tailspike protein: interdigitated subunits in a thermostable trimer. *Science* **265**(5170)**,** 383-6.

Stevens, R. C. (2000). Design of high-throughput methods of protein production for structural biology. *Structure* **8**(9)**,** R177-85.

Stevenson, B. R., and Keon, B. H. (1998). The tight junction: morphology to molecules. *Annu Rev Cell Dev Biol* **14,** 89-109.

Stevenson, S. C., Rollence, M., White, B., Weaver, L., and McClelland, A. (1995). Human adenovirus serotypes 3 and 5 bind to two different cellular receptors via the fiber head domain. *J Virol* **69**(5)**,** 2850-7.

Stewart, P. L., and Nemerow, G. R. (2007). Cell integrins: commonly used receptors for diverse viral pathogens. *Trends Microbiol* **15**(11)**,** 500-7.

Storoni, L. C., McCoy, A. J., and Read, R. J. (2004). Likelihood-enhanced fast rotation functions. *Acta Crystallogr D Biol Crystallogr* **60**(Pt 3)**,** 432-8.

Sumida, S. M., Truitt, D. M., Lemckert, A. A., Vogels, R., Custers, J. H., Addo, M. M., Lockman, S., Peter, T., Peyerl, F. W., Kishko, M. G., Jackson, S. S., Gorgone, D. A., Lifton, M. A., Essex, M., Walker, B. D., Goudsmit, J., Havenga, M. J., and Barouch, D. H. (2005). Neutralizing antibodies to adenovirus serotype 5 vaccine vectors are directed primarily against the adenovirus hexon protein. *J Immunol* **174**(11)**,** 7179-85.

Tollefson, A. E., Ryerse, J. S., Scaria, A., Hermiston, T. W., and Wold, W. S. (1996a). The E3-11.6-kDa adenovirus death protein (ADP) is required for efficient cell death: characterization of cells infected with adp mutants. *Virology* **220**(1)**,** 152-62.

Tollefson, A. E., Scaria, A., Hermiston, T. W., Ryerse, J. S., Wold, L. J., and Wold, W. S. (1996b). The adenovirus death protein (E3-11.6K) is required at very late stages of infection for efficient cell lysis and release of adenovirus from infected cells. *J Virol* **70**(4)**,** 2296-306.

Tomko, R. P., Xu, R., and Philipson, L. (1997). HCAR and MCAR: the human and mouse cellular receptors for subgroup C adenoviruses and group B coxsackieviruses. *Proc Natl Acad Sci U S A* **94**(7)**,** 3352-6.

Trotman, L. C., Mosberger, N., Fornerod, M., Stidwill, R. P., and Greber, U. F. (2001). Import of adenovirus DNA involves the nuclear pore complex receptor

CAN/Nup214 and histone H1. *Nat Cell Biol* **3**(12)**,** 1092-100.

Tuve, S., Wang, H., Ware, C., Liu, Y., Gaggar, A., Bernt, K., Shayakhmetov, D., Li, Z., Strauss, R., Stone, D., and Lieber, A. (2006). A new group B adenovirus receptor is expressed at high levels on human stem and tumor cells. *J Virol* **80**(24)**,** 12109-20.

Van Der Veen, J., and Kok, G. (1957). Isolation and typing of adenoviruses recovered from military recruits with acute respiratory disease in The Netherlands. *Am J Hyg* **65**(2)**,** 119-29.

Van Der Veen, J., and Prins, A. (1960). Studies of the significance of the recall phenomenon in the antibody response to adenovirus vaccine and infection. *J Immunol* **84,** 562-8.

van Raaij, M. J., Chouin, E., van der Zandt, H., Bergelson, J. M., and Cusack, S. (2000). Dimeric structure of the coxsackievirus and adenovirus receptor D1 domain at 1.7 A resolution. *Structure* **8**(11)**,** 1147-55.

van Raaij, M. J., Mitraki, A., Lavigne, G., and Cusack, S. (1999). A triple beta-spiral in the adenovirus fibre shaft reveals a new structural motif for a fibrous protein. *Nature* **401**(6756)**,** 935-8.

Vogels, R., Zuijdgeest, D., van Rijnsoever, R., Hartkoorn, E., Damen, I., de Bethune, M. P., Kostense, S., Penders, G., Helmus, N., Koudstaal, W., Cecchini, M., Wetterwald, A., Sprangers, M., Lemckert, A., Ophorst, O., Koel, B., van Meerendonk, M., Quax, P., Panitti, L., Grimbergen, J., Bout, A., Goudsmit, J., and Havenga, M. (2003). Replication-deficient human adenovirus type 35 vectors for gene transfer and vaccination: efficient human cell infection and bypass of preexisting adenovirus immunity. *J Virol* **77**(15)**,** 8263-71.

Waddington, S. N., McVey, J. H., Bhella, D., Parker, A. L., Barker, K., Atoda, H., Pink, R., Buckley, S. M., Greig, J. A., Denby, L., Custers, J., Morita, T., Francischetti, I. M., Monteiro, R. Q., Barouch, D. H., van Rooijen, N., Napoli, C., Havenga, M. J., Nicklin, S. A., and Baker, A. H. (2008). Adenovirus serotype 5 hexon mediates liver gene transfer. *Cell* **132**(3)**,** 397-409.

Walters, R. W., Freimuth, P., Moninger, T. O., Ganske, I., Zabner, J., and Welsh, M. J. (2002). Adenovirus fiber disrupts CAR-mediated intercellular adhesion allowing virus escape. *Cell* **110**(6)**,** 789-99.

Wang, H., Liaw, Y. C., Stone, D., Kalyuzhniy, O., Amiraslanov, I., Tuve, S., Verlinde,

C. L., Shayakhmetov, D., Stehle, T., Roffler, S., and Lieber, A. (2007). Identification of CD46 binding sites within the adenovirus serotype 35 fiber knob. *J Virol* **81**(23)**,** 12785-92.

Webster, A., Hay, R. T., and Kemp, G. (1993). The adenovirus protease is activated by a virus-coded disulphide-linked peptide. *Cell* **72**(1)**,** 97-104.

Wickham, T. J., Mathias, P., Cheresh, D. A., and Nemerow, G. R. (1993). Integrins alpha v beta 3 and alpha v beta 5 promote adenovirus internalization but not virus attachment. *Cell* **73**(2)**,** 309-19.

Wickham, T. J., Tzeng, E., Shears, L. L., 2nd, Roelvink, P. W., Li, Y., Lee, G. M., Brough, D. E., Lizonova, A., and Kovesdi, I. (1997). Increased in vitro and in vivo gene transfer by adenovirus vectors containing chimeric fiber proteins. *J Virol* **71**(11)**,** 8221-9.

Wiethoff, C. M., Wodrich, H., Gerace, L., and Nemerow, G. R. (2005). Adenovirus protein VI mediates membrane disruption following capsid disassembly. *J Virol* **79**(4)**,** 1992-2000.

Wilson, A. J. C. (1942). Determination of absolute from relative X-ray data intensities. *Nature* **150,** 151-152.

Wodrich, H., Cassany, A., D'Angelo, M. A., Guan, T., Nemerow, G., and Gerace, L. (2006). Adenovirus core protein pVII is translocated into the nucleus by multiple import receptor pathways. *J Virol* **80**(19)**,** 9608-18.

Wodrich, H., Guan, T., Cingolani, G., Von Seggern, D., Nemerow, G., and Gerace, L. (2003). Switch from capsid protein import to adenovirus assembly by cleavage of nuclear transport signals. *EMBO J* **22**(23)**,** 6245-55.

Wu, E., Fernandez, J., Fleck, S. K., Von Seggern, D. J., Huang, S., and Nemerow, G. R. (2001). A 50-kDa membrane protein mediates sialic acid-independent binding and infection of conjunctival cells by adenovirus type 37. *Virology* **279**(1)**,** 78-89.

Wu, E., and Nemerow, G. R. (2004). Virus yoga: the role of flexibility in virus host cell recognition. *Trends Microbiol* **12**(4)**,** 162-9.

Wu, E., Pache, L., Von Seggern, D. J., Mullen, T. M., Mikyas, Y., Stewart, P. L., and Nemerow, G. R. (2003). Flexibility of the adenovirus fiber is required for efficient receptor interaction. *J Virol* **77**(13)**,** 7225-35.

Wu, E., Trauger, S. A., Pache, L., Mullen, T. M., von Seggern, D. J., Siuzdak, G.,

and Nemerow, G. R. (2004). Membrane cofactor protein is a receptor for adenoviruses associated with epidemic keratoconjunctivitis. *J Virol* **78**(8)**,** 3897-905.

Xia, D., Henry, L. J., Gerard, R. D., and Deisenhofer, J. (1994). Crystal structure of the receptor-binding domain of adenovirus type 5 fiber protein at 1.7 A resolution. *Structure* **2**(12)**,** 1259-70.

Yang, Y., Nunes, F. A., Berencsi, K., Furth, E. E., Gonczol, E., and Wilson, J. M. (1994a). Cellular immunity to viral antigens limits E1-deleted adenoviruses for gene therapy. *Proc Natl Acad Sci U S A* **91**(10)**,** 4407-11.

Yang, Y., Nunes, F. A., Berencsi, K., Gonczol, E., Engelhardt, J. F., and Wilson, J. M. (1994b). Inactivation of E2a in recombinant adenoviruses improves the prospect for gene therapy in cystic fibrosis. *Nat Genet* **7**(3)**,** 362-9.

Yoder, M. D., Keen, N. T., and Jurnak, F. (1993). New domain motif: the structure of pectate lyase C, a secreted plant virulence factor. *Science* **260**(5113)**,** 1503-7.

Zhang, W., and Imperiale, M. J. (2003). Requirement of the adenovirus IVa2 protein for virus assembly. *J Virol* **77**(6)**,** 3586-94.

Zhang, Y., and Skolnick, J. (2005). TM-align: a protein structure alignment algorithm based on the TM-score. *Nucleic Acids Res* **33**(7)**,** 2302-9.

Zheng, L., Baumann, U., and Reymond, J. L. (2004). An efficient one-step site-directed and site-saturation mutagenesis protocol. *Nucleic Acids Res* **32**(14)**,** e115.

Zubieta, C., Schoehn, G., Chroboczek, J., and Cusack, S. (2005). The structure of the human adenovirus 2 penton. *Mol Cell* **17**(1)**,** 121-35.

Abbreviations

6x His tag – hexahistidine tag

aa – amino acids

ABTS – 2,2'-azino-bis(3-ethylbenzthiazoline-6-sulphonic acid)

Ad – adenovirus

APS – Advanced Photon Source

bp – base pairs

BSA – bovine serum albumin

CAR – coxsackievirus and adenovirus receptor

CD46 – membrane cofactor protein (MCP)

CD55 – decay acceleration factor (DAF)

cDNA – complementary deoxyribonucleic acid

CHO – Chinese hamster ovary cells

Ci – Curie

cpm – counts per minute

CryoEM – cryo electron microscopy

CYT – cytoplasmic tail domain of CD46

Da – Dalton

DAF – decay acceleration factor (CD55)

DMEM – Dulbecco’s modified Eagle's minimal essential medium

DNA – deoxyribonucleic acid

E. coli – *Escherichia coli*

EBNA – Epstein-Barr virus nuclear antigen

EDC – 1-ethyl 3-(3-dimethylaminopropyl)-carbodiimide hydrochloride

EDTA – ethylene diamine tetraacetic acid

EKC – epidemic keratoconjuctivitis

ELISA – enzyme-linked immunosorbent assay

FACS – fluorescence-activated cell sorting

FCS – fetal calf serum

FK – fiber knob

FPLC – fast protein liquid chromatography

FX – coagulation factor X

GFP – green fluorescent protein

GPI – glycosyl-phosphatidylinositol

HDAd – helper-dependent adenovirus vector

HEK – human embryonic kidney

HEPES – N-2-hydroxylpiperazine-N'-2-ethanesulfonic acid

HHV – human herpesvirus

HS-GAG – heparan sulfate glycosaminoglycan

HVR – hyper variable region

IFN-γ – interferon gamma

IFN-1 – type I interferon

IMAC – immobilized metal ion affinity chromatography

IPTG – isopropyl β-D-thiogalactopyranoside

JAM – junctional adhesion molecule

k_a – association rate constant

kb – kilobasepairs

k_d – dissociation rate constant

K_D – equilibrium dissociation constant

LB – lysogeny broth (also: Luria-Bertani broth)

MES – 2-(N-morpholino)ethanesulfonic acid

mHSC – murine hematopoietic stem cells

MLP – major late promoter

MLTU – major late transcription unit

MOI – multiplicity of infection

mRNA – messenger ribonucleic acid

MV – measles virus

NAb – neutralizing antibody

NHS – *N*-hydroxysuccinimide

NLS – nuclear localization signal

NPC – nuclear pore complex

PAGE – polyacrylamide gel electrophoresis

PBS – phosphate-buffered saline

PCR – polymerase chain reaction

PE – phycoerythrin

pI – isoelectric point

pII, pIIIa etc. – adenovirus protein II, IIIa etc.

PI3K – phosphatidylinositol-3-OH kinase

RCA – regulators of complement activation

rcf – relative centrifugal force

RGD – Arg-Gly-Asp

RMSD – root mean square deviation

RNA – ribonucleic acid

rpm – revolutions per minute

RPMI – Rosewell Park Memorial Institute medium

RU – resonance unit

SA – sialic acid

sCD46 – soluble CD46, consisting of the entire extracellular domain of the C-isoform of CD46

SCR – short consensus repeat

SDS – sodium dodecyl sulfate

SPR – surface plasmon resonance

STP – serine, threonine, proline rich domain of CD46

TBS – Tris-buffered saline

TLR9 – Toll-like receptor 9

TP – adenovirus terminal protein

TPL – tripartite leader

Tris – tris(hydroxymethyl)aminomethane

List of publications

Pache, L., Venkataraman, S., Reddy, V. S., and Nemerow, G. R. (2008). Structural Variations in Species B Adenovirus Fibers Impact CD46 Association. *J Virol*. [Epub ahead of print Jun 4, 2008]

Pache, L., Venkataraman, S., Nemerow, G. R., and Reddy, V. S. (2008). Conservation of fiber structure and CD46 usage by subgroup B2 adenoviruses. *Virology* **375**(2)**,** 573-9.

Nepomuceno, R. R., **Pache, L.**, and Nemerow, G. R. (2007). Enhancement of gene transfer to human myeloid cells by adenovirus-fiber complexes. *Mol Ther* **15**(3)**,** 571-8.

Wu, E., Trauger, S. A., **Pache, L.**, Mullen, T. M., von Seggern, D. J., Siuzdak, G., and Nemerow, G. R. (2004). Membrane cofactor protein is a receptor for adenoviruses associated with epidemic keratoconjunctivitis. *J Virol* **78**(8)**,** 3897-905.

Hiermit versichere ich, die vorliegende Arbeit selbständig verfaßt und alle verwendeten Hilfsmittel sowie Kollaborationen entsprechend gekennzeichnet zu haben.